



UNIVERSIDADE ESTADUAL DE CAMPINAS

Faculdade de Engenharia Química

ALESSANDRA SUZIN BERTAN

MICROFILTRAÇÃO DE MICELAS A PARTIR DA FERMENTAÇÃO DE
Streptomyces tsukubaensis PARA A PRODUÇÃO DE TACROLIMO

MICROFILTRATION OF MICELLES FROM FERMENTATION OF
Streptomyces tsukubaensis FOR THE PRODUCTION OF TACROLIMUS

CAMPINAS

2021

ALESSANDRA SUZIN BERTAN

MICROFILTRATION OF MICELLES FROM FERMENTATION OF
Streptomyces tsukubaensis FOR THE PRODUCTION OF TACROLIMUS

MICROFILTRAÇÃO DE MICELAS A PARTIR DA FERMENTAÇÃO DE
Streptomyces tsukubaensis PARA A PRODUÇÃO DE TACROLIMO

Dissertação apresentada à Faculdade de Engenharia Química da Universidade Estadual de Campinas como parte dos requisitos exigidos para a obtenção do título de Mestra, em Engenharia Química.

Dissertation presented to the School of Chemical Engineering of the University of Campinas in partial fulfillment of the requirements for the degree of Master in Chemical Engineering.

Advisor: Professor Marco Aurélio Cremasco

THIS EXAMPLE CORRESPONDS TO THE FINAL VERSION OF THE DISSERTATION DEFENDED BY ENG. ALESSANDRA SUZIN BERTAN AND ORIENTED BY PROF. MARCO AURÉLIO CREMASCO.

CAMPINAS

2021

Ficha catalográfica
Universidade Estadual de Campinas
Biblioteca da Área de Engenharia e Arquitetura
Rose Meire da Silva - CRB 8/5974

B461m Bertan, Alessandra Suzin, 1995-
Microfiltration of micelles from fermentation of *Streptomyces tsukubaensis* for the production of tacrolimus / Alessandra Suzin Bertan. – Campinas, SP : [s.n.], 2021.

Orientador: Marco Aurélio Cremasco.
Dissertação (mestrado) – Universidade Estadual de Campinas, Faculdade de Engenharia Química.

1. Tacrolimo. 2. Microfiltração. 3. Fermentação. 4. Esperança. 5. Fármacos.
I. Cremasco, Marco Aurélio, 1962-. II. Universidade Estadual de Campinas. Faculdade de Engenharia Química. III. Título.

Informações para Biblioteca Digital

Título em outro idioma: Microfiltração de micelas a partir da fermentação de *Streptomyces tsukubaensis* para a produção do tacrolimo

Palavras-chave em inglês:

Tacrolimus
Microfiltration
Fermentation
Hope
Drug

Área de concentração: Engenharia Química

Titulação: Mestra em Engenharia Química

Banca examinadora:

Marco Aurélio Cremasco [Orientador]

Guilherme José de Castilho

Maria Carolina Sérgi Gomes

Data de defesa: 27-01-2021

Programa de Pós-Graduação: Engenharia Química

Folha de Aprovação de Defesa de Dissertação defendida por Alessandra Suzin Bertan e aprovada em 27 de janeiro de 2021 pela banca examinadora constituída pelos professores doutores:

Prof. Dr. Marco Aurélio Cremasco

Instituição: Universidade Estadual de Campinas (UNICAMP)

Prof. Dr. Guilherme José de Castilho

Instituição: Universidade Estadual de Campinas (UNICAMP)

Prof^a . Dr^a . Maria Carolina Sérgi Gomes

Instituição: Universidade Tecnológica Federal do Paraná (UTFPR)

A Ata de Defesa com as respectivas assinaturas dos membros encontra-se no SIGA e na Secretaria de Pós Graduação da Faculdade de Engenharia Química da UNICAMP.

ACKNOWLEDGMENT

I thank and dedicate this Dissertation to:

My family, especially my mother Sandra, my father Idacir, my brother Lucas, my grandmother Maria, and my grandfather Dorvalino who have always supported and encouraged my studies;

My friends and colleagues, who have always been rooting for me;

My advisor, professor Marco, for offering the opportunities to my academic, personal, and research growth;

The State University of Campinas, for all the essential support;

This work was carried out with support from the Conselho Nacional de Desenvolvimento Científico e Tecnológico (CNPq) [Process 130989/2019-3];

Professor Telma and her entire LABBPOR team, for technical support;

Levi, for his teachings and patience in helping me;

Fabiane for always helping;

My laboratory colleagues Luciana and Séforah, for all their help and learning;

All other people who directly or indirectly contributed to the success of this work;

And God, who always chooses special people to walk along in my path.

Hope wins uncertainty

RESUMO

Tacrolimo é um fármaco recomendado como imunossupressor para terapia de transplante renal e hepático, tratamento de doenças autoimunes, artrite reumatóide e líquen plano, bem como no tratamento de asma brônquica, distúrbios dermatológicos como vitiligo, psoríase, dermatite atópica, doenças oculares, como uveíte e no tratamento de pacientes com nefropatia membranosa idiopática. Esta Dissertação visa aprimorar o processo de recuperação do tacrolimo por meio do desenvolvimento de uma coluna pressurizada destinada à microfiltração de caldo fermentado, de forma que as micelas presentes no caldo sejam retidas com pelo menos 95 % de rejeição. Na presente Dissertação foi proposto e montado um sistema de microfiltração em coluna pressurizada de caldo proveniente de fermentação via *Streptomyces tsukubaensis*, o qual contém tacrolimo. Foram realizados testes de fermentação utilizando-se óleo de coco e glicose enquanto fontes de carbono, obtendo-se a produção específica do fármaco iguais a 1,88 mg/g e 1,69 mg/g, respectivamente. Além de identificar e quantificar o fármaco, foi possível quantificar a biomassa, açúcares e proteínas advindos da fermentação. Tendo em vista a necessidade de se avaliar o desempenho do sistema proposto, endereçado à remoção de micelas, desenvolveu-se a técnica alternativa que associa a contagem de partículas pela câmara de Neubauer com a técnica de espectroscopia, possibilitando associar número de partículas à absorvância. Realizou-se, em complemento, estudo sobre a reologia do caldo cru fermentado com acetona submetido à microfiltração, verificando-se comportamento não-newtoniano, de natureza pseudoplástica, de maneira expressiva para temperaturas superiores a 30 °C. No que se refere ao desempenho da microfiltração, avaliou-se o desempenho de duas membranas, 0,22 µm e 3,00 µm de diâmetro médio de poros, submetidas a pressões de operação de 1 bar e 2 bar. Verificou-se que uma simples batelada de microfiltração não foi o bastante para atingir a remoção de 95 %. Assim, estabeleceu-se a estratégia de múltiplas passagens do permeado pelo filtro, obtendo-se a remoção pretendida em 6 passagens, sendo que a rejeição máxima obtida de micela foi de 97 %, alcançada em dez passagens do permeado pelo filtro. Tal desempenho foi alcançado pela membrana de 3,00 µm, utilizando-se pressão de operação de 1 bar. Observou-se que o fluxo volumétrico do permeado diminui com o aumento do número de passagens até manter-se constante. Esse comportamento é observado com a resistência total do meio filtrante, que permanece constante após um determinado passo, mas, antes, a resistência total aumenta com o número de passagens. Ressalte-se que, dado a abrangência da aplicação do tacrolimo e a sua distribuição pelo Sistema Único de Saúde (SUS), contextualizou-se a dimensão de sua produção para a sociedade, ressaltando a importância da esperança enquanto elemento essencial no projeto químico de obtenção do fármaco, concluindo-se que é possível fazer ciência e desenvolver tecnologia inovadora com forte compromisso social.

Palavras-chave: Tacrolimo, Microfiltração, Fermentação, Esperança.

ABSTRACT

Tacrolimus is a drug recommended as immunosuppressant for kidney and liver transplant therapy, treatment of autoimmune diseases, rheumatoid arthritis and lichen planus, as well as in the treatment of bronchial asthma, dermatological disorders such as vitiligo, psoriasis, atopic dermatitis, eye diseases such as uveitis and in the treatment of patients with idiopathic membranous nephropathy. This Dissertation aims to improve the tacrolimus recovery process through the development of a pressurized column for fermented broth microfiltration from fermentation via *Streptomyces tsukubaensis*, which contains tacrolimus, so that the micelles present in the broth are retained with 95 % rejection at least. Fermentation runs were carried out using coconut oil and glucose as carbon sources, obtaining the specific production of the drug equal to 1.88 mg/g and 1.69 mg/g, respectively. In addition to identifying and quantifying the drug, it was possible to quantify the biomass, sugars, and proteins from fermentation. In view of the need to evaluate the performance of the proposed system, addressed to the removal of micelles, an alternative technique was developed that associates the particle counting by the Neubauer chamber with the spectroscopy technique, making it possible to associate the number of particles with the absorbance. In addition, a study was carried out on the rheology of raw broth fermented with acetone submitted to microfiltration, verifying non-Newtonian behavior, of a pseudoplastic nature, significantly for temperatures above 30 °C. Regarding the performance of microfiltration, the performance of two membranes, 0.22 µm and 3.00 µm of average pore diameter, were subjected to operating pressures of 1 bar and 2 bar. It was found that a simple batch of microfiltration was not enough to achieve 95 % removal. Thus, the strategy of multiple steps of the permeate through the filter was established, obtaining the desired removal in 6 passages, and the maximum rejection obtained from the micelle was 97%, achieved in ten steps. This performance was achieved with 3.00 µm membrane, using 1 bar operating pressure. It was observed that the permeate volumetric flow decreases with the increase in the steps number until it remains constant. This behavior is observed with the total resistance of the filter medium, which remains constant after a certain step, but, before, the total resistance increases with the steps number. It should be noted that, given the scope of the application of tacrolimus and its distribution by the Brazilian Unified Health System (SUS), the dimension of its production for society was contextualized, emphasizing the importance of hope as essential element in the chemical project of obtaining of the drug, concluding that it is possible to do science and develop innovative technology with a strong social commitment.

Keywords: Tacrolimus, Microfiltration, Fermentation, Hope.

LIST OF FIGURES

Figure 1.1 – Structural formula of tacrolimus and applications.....	17
Figure 1.2 – Flowchart characteristic of a chemical design.....	19
Figure 2.1 – Transplants performed at Hospital das Clínicas of Unicamp.....	23
Figure 2.2 – Organ and tissue transplants 2020 in Brazil.....	23
Figure 2.3 – Structural formula of tacrolimus.....	25
Figure 2.4 – Schematic representation of pre-inoculation (a) inoculation (b) and fermentation (c).....	26
Figure 2.5 – Operational filtration classification.....	32
Figure 2.6 – Filtration representation.....	32
Figure 2.7 – Obtaining $\langle\alpha\rangle$ and R_M for constant pressure filtration.....	35
Figure 2.8 – Distribution of pore sizes, pressure used in MSP.....	38
Figure 2.9 – Filtration modes: <i>dead-end</i> and <i>cross-flow</i>	39
Figure 2.10 – Differential for <i>dead-end</i> contact, and transmembrane pressure for <i>cross-flow</i>	40
Figure 2.11 – (a) In mode <i>dead-end</i> the permeate flow decreases with time due to the effect of fouling on the membrane (b) Initial particle deposition and concentration polarization followed by cake layer formation.....	41
Figure 2.12 – V versus t with β that represents the volumetric flow.....	42
Figure 2.13 – Synthetic membrane morphology.....	43
Figure 2.14 – Filtration system.....	45
Figure 2.15 – Representation of the pressurized filtration module.....	45
Figure 3.1 – Apparatus used in the fermentation process.....	50
Figure 3.2 – Counting chamber Fuchs Rosenthal grid optic.....	52
Figure 3.3 – AR 1500 rheometer ex.	52
Figure 3.4 – Pycnometer.....	53
Figure 3.5 – Simplified scheme of the pressurized filter system.....	55
Figure 3.6 – Details of the filter used in microfiltration process.....	56
Figure 3.7 – Parts of the filtration system.....	57
Figure 3.8 – Procedure applied to carry out filtration in a pressurized column.....	58
Figure 3.9 – Drying oven utilized by biomass contend.....	60
Figure 3.10 – Fermentation sample by <i>S. tsukubaensis</i> for the production of tacrolimus..	61
Figure 3.11 – Tacrolimus calibration curve.....	62
Figure 3.12 – Protein calibration curve.....	63
Figure 3.13 – Calibration curve for reducing sugars.....	64
Figure 4.1 – Tacrolimus production for 168 h using coconut oil as carbon source.....	69
Figure 4.2 – Tacrolimus production for 168 h using glucose as carbon source.....	69
Figure 4.3 – Proteins concentration along the fermentation process using glucose and coconut oil as carbon source.....	71
Figure 4.4 – Fermentable sugars concentration along the fermentation process using glucose and coconut oil as carbon source.....	72
Figure 4.5 – Determination of micelles concentration from absorbance.....	73
Figure 4.6 – Observation of micelles in the optical microscope (a) fermented broth: 4 x objective; (b) fermented broth:10 x objective; (c) fermented broth diluted 50 times: 4 x objective; (d) fermented broth diluted 50 times: 10 x objective.....	74
Figure 4.7 – Micelles from fermented broth with a micrometric dimension of 3 μm and a magnification of 5000 x.....	75

Figure 4.8 – Micelles from fermented broth with micrometric dimension of 1 μm and magnification of 10000 x.....	75
Figure 4.9 – Scheme of the proposed alternative technique.....	76
Figure 4.10 – Rheological curves of diluted fermented broth.....	77
Figure 4.11 – Microfiltration with water to obtain the specific resistance of filter components: (a) 1 bar; (b) 2 bar.....	81
Figure 4.12 – Microfiltration with water to obtain the specific resistance of filter medium and membrane: (a) 0.22 μm ; (b) 3.00 μm	83
Figure 4.13 – Membrane appearance at 2 bar: (a) original membrane; (b) folded membrane; (c) partially destroyed membrane	84
Figure 4.14 – Single microfiltration test: 3.00 μm and 1 bar	84
Figure 4.15 – Preliminary study of microfiltration test – 0.22 μm and 1 bar: (a) Step #1 ($R^2 = 0.99993$); (b) Step #2 ($R^2 = 0.99995$); (c) Step #3 ($R^2 = 0.99999$); (d) Step #4 ($R^2 = 0.99965$)	86
Figure 4.16 – Microfiltration in multiple steps: 0.22 μm and 1 bar.....	88
Figure 4.17 – Microfiltration in multiple steps: 0.22 μm and 2 bar.....	89
Figure 4.18 – Microfiltration in multiple steps: 3.00 μm and 1 bar.....	90
Figure 4.19 – Microfiltration in multiple steps: 3.00 μm and 2 bar.....	91
Figure 4.20 – Influence of multiple microfiltration in volumetric flow: (a) 1 bar; (b) 2 bar.....	92
Figure 4.21 – Influence of multiple microfiltration in volumetric flow:(a) 0.22 μm ; (b) 3.00 μm	92
Figure 4.22 – Influence of multiple microfiltration in step time: (a) 1 bar; (b) 2 bar.....	93
Figure 4.23 – Influence of multiple microfiltration in step time: (a) 0.22 μm ; (b) 3.00 μm	94
Figure 4.24 – Influence of multiple microfiltration in micelles rejection: (a) 1 bar; (b) 2 bar.....	95
Figure 4.25 – Influence of multiple microfiltration in micelles rejection: (a) 0.22 μm ; (b) 3.00 μm	95
Figure 4.26 – Biomass of the fermentation broth.....	96
Figure 4.27 – Calibration curve for mass of biomass.....	97
Figure 4.28 – Influence of multiple microfiltration in total resistance: (a)1 bar; (b) 2 bar.....	98
Figure 4.29 – Influence of multiple microfiltration in total resistance: (a) 0.22 μm ; (b) 3.00 μm	99
Figure 4.30 – Membrane 0.22 μm folding verified after the multiple steps microfiltration.....	99
Figure 4.31 – Diversified results from tacrolimus processing at LPTM/DEPro/FEQ/UNICAMP.....	101
Figure 4.32 – Repercussion of tacrolimus production at LPTM/DEPro/FEQ/UNICAMP.....	102
Figure 4.33 – The social impact of hope from technological study.....	103
Figure 4.34 – Best work at I Congresso Brasileiro Interdisciplinar de Ciência e Tecnologia.....	104
Figure 5.1 – (a) raw broth with acetone; (b) permeated from step 10 of the microfiltration conducted on the column pressurized at 1 bar with 3.00 μm membrane... ..	105
Figure 5.2 – LPTM laboratory symbol.....	108
Figure 6.1 – Number of publications/years used in the Dissertation. The authors highlighted are central in this work.....	119
Figure B.1 – Hemodialysis procedure.....	124
Figure B.2 – Perpendicular feeding.....	126

LIST OF TABLES

Table 2.1 – Same strain of <i>Streptomyces tsukubaensis</i>	27
Table 2.2 – Mutants strain of <i>Streptomyces tsukubaensis</i>	28
Table 2.3 – Relationship between land mass and diatom and volume of fermented broth.....	30
Table 2.4 – Examples of application of MSP	37
Table 2.5 – Species retained in the OI, NF, UF and MF processes.....	38
Table 2.6 – Non-Newtonian rheological models.....	46
Table 3.1 – Composition of *GYM culture medium for the bacterium <i>Streptomyces tsukubaensis</i>	49
Table 3.2 – The composition of the medium used in pre-inoculation and inoculation.....	50
Table 3.3 – Composition of the medium used in fermentation.....	50
Table 3.4 – Compounds used for the preparation of the SN-I reagent.....	51
Table 3.5 – Compounds used for the preparation of SN-II reagent.....	51
Table 3.6 – Technical information of the filter medium.....	55
Table 3.7 – Filter characteristics.....	57
Table 4.1 – Rheological parameters at 20 °C.....	77
Table 4.2 – Rheological parameters at 25 °C.....	77
Table 4.3 – Rheological parameters at 30 °C.....	77
Table 4.4 – Rheological parameters at 40 °C.....	78
Table 4.5 – Rheological parameters at 50 °C.....	78
Table 4.6 – Coefficients of Equation 4.3 for $RP = \tau_0$ (Pa)	79
Table 4.7 – Coefficients of Equation 4.3 for $RP = K$ (Pa.s ^m)	79
Table 4.8 – Coefficients of Equation 4.3 for $RP = n$ or m (-).....	79
Table 4.9 – Absolute mean deviation of rheological models analysed in this work (%)...	79
Table 4.10 – Specific resistance of filter components.....	82
Table 4.11 – Specific resistance of filter medium and membrane.....	83
Table 4.12 – Rejection results of single microfiltration test: 3.00 µm and 1 bar.....	85
Table 4.13 – Rejection results of multiple microfiltration tests: 0.22 µm and 1 bar.....	85
Table A.1 – Duplicate test 0.22 µm and pressure 1 bar.....	121
Table A.2 – Duplicate test 0.22 µm and pressure 2 bar	121
Table A.3 – Duplicate test 3.00 µm and pressure 1 bar.....	121
Table A.4 – Duplicate test 3.00 µm and pressure 2 bar.....	122
Table B.1 – Diffusion coefficient of NaCl at 25 °C in aqueous solution for different molalities.....	125
Table B.2 – Evaluation of permeate flow in different particulate media	126

LIST OF SYMBOLS

Area	Specific filtration area	L^2
c_0	Initial concentration	$M.L^{-1}$
c_f	Concentration at column outlet	$M.L^{-1}$
D_V	Viscous diffusion coefficient	$L^2.T^{-1}$
$D_{v,ef}$	Diffusivity capillary	$L^2.T^{-1}$
D	Column diameter	L
j_m	Permeate mass flow	$M.T^{-1}$
k	Parameter associated with fluid consistency	-
k	Permeability	L^2
k_P	Adsorption equilibrium constant	-
L	Column length	L
m	Fluid behavior index	-
m_l	Mass of liquid	M
m_p	Mass of solid in the cake; biomass in feed solution at each step	M
n	Coefficient associated with the residual shear effect	(-)
N_p	Number of particles (micelles number/cm ³)	L^{-3}
N_{pF}	Micelle concentration in feed (micelles number/cm ³)	L^{-3}
N_{pP}	Micelle concentration in permeate (micelles number/cm ³)	L^{-3}
N_{pR}	Number of particles in the retentate (micelles number/cm ³)	L^{-3}
N_T	Number of particles in the feed solution (micelles number/cm ³)	L^{-3}
p	Pressure	$M.L^{-1}.T^{-2}$
P_{abs}	Absolute pressure	$M.L^{-1}.T^{-2}$
p_F	Feed pressure; operational pressure	$M.L^{-1}.T^{-2}$
p_P	Pressure in the permeate outlet	$M.L^{-1}.T^{-2}$
p_R	Pressure in the retentate outlet	$M.L^{-1}.T^{-2}$
p_{TR}	Transmembrane pressure	$M.L^{-1}.T^{-2}$
r	Rotation	T^{-1}
R	Rejection	(%)
R_c	Associated characteristics resistance	$L^2.M^{-1}$
R_f	Intrinsic resistance of the membrane	$L^2.M^{-1}$
R_G	Resistance resulting from fouling effects	$L^2.M^{-1}$
R_M	Resistance of the filter medium	$L^2.M^{-1}$
R_P	Resistance due to polarization	$L^2.M^{-1}$
R_s	Resistance due to the membrane support	$L^2.M^{-1}$

R_T	Total resistance	$L^2.M^{-1}$
s_p	Absolute mass fraction of solids	-
t	Time; filtration time	T
T	Temperature	t
V	Filtrate or permeate volume	L^3
V_1	Volume of the liquid phase	L^3
$V_{micelle}$	Micelles volume	L^3
V_p	Volume of particulate	L^3
$V_{solution}$	Volume of solution	L^3
Q	Volumetric flow rate	$L^3.T^{-1}$

Greek letters

$\langle \alpha \rangle$	Average resistivity of the cake	$L.M^{-1}$
β	Angular inclination; Volumetric flow	$L^3.T^{-1}$
γ	Capture factor	-
γ	Fluid deformation rate	T^{-1}
Δp	Differential pressure	$M.L^{-1}.T^{-2}$
ϵ_p	Void fraction of particulate phase	-
$\epsilon_{p,filtered}$	Volumetric fraction of particulate phase in the permeate	-
ϵ_{pt}	Volumetric fraction of particulate phase in the cake	-
η	Dynamic viscosity	$M.L^{-1}.T^{-1}$
η_0	Pre-exponential dynamic viscosity	$M.L^{-1}.T^{-1}$
ρ	Density	$M.L^{-3}$
ρ_p	Density of biomass	$M.L^{-3}$
τ	Shear stress	$M.L^{-1}.T^{-2}$
τ_0	Yield stress	$M.L^{-1}.T^{-2}$
ϕ	Volumetric fraction of solids	-
ν	Dynamic viscosity	$M.L^{-1}.t^{-1}$
σ_p	Pore diameter	M

SUMMARY

1. INTRODUCTION	16
1.1. Contextualization and motivation for this work.....	16
1.2. Chemical design	19
1.3. Objective	20
1.4. Specific objectives	20
2. BIBLIOGRAPHIC REVIEW	22
2.1. Presentation of the problem	22
2.2. Tacrolimus and its obtaining.....	24
2.3. Determination of concentration of the micelles from fermentation broth	30
2.4. Filtration	31
2.5. Simplified filtration theory	33
2.6. Membrane separation process (MSP)	36
2.7. Microfiltration (MF)	38
2.8. Membrane morphology	43
2.9. Microfiltration systems	44
2.10. Essential properties for the evaluation of microfiltration.....	46
3. MATERIALS AND METHODS	48
3.1. Materials	49
3.1.1. <i>Streptomyces tsukubaensis</i> bacteria strain	49
3.1.2. Petri dish culture medium	49
3.1.3. Pre-inoculation, inoculation and fermentation	49
3.1.4. Apparatus used for fermentation	50
3.1.5. Chromatography	51
3.1.6. Protein quantification	51
3.1.7. Quantification of reducing sugars	51
3.1.8. Determination of micelle concentration	51
3.1.9. Rheology	52
3.1.10. Determination of density	53
3.2 Methods	53
3.2.1. Preparation of culture medium	53
3.2.2. Preparation of pre-inoculum and inoculum	53

3.2.3. Fermentation	54
3.2.4. Pressurized column microfiltration method	54
a) Description of microfiltration system	55
b) Pressurized column assembly	57
c) Air supply	58
d) Bifiltration of water	59
e) Membrane compaction	59
f) Sample microfiltration	59
g) Drying of biomass	60
3.2.5. Quantification of tacrolimus and its specific production	61
3.2.6. Protein quantification	62
3.2.7. Quantification of fermentable sugars	63
3.2.8. Determination of micelle concentration	64
3.2.9. Rheology	66
3.2.10. Density	67
4 RESULTS AND DISCUSSION	68
4.1. Tacrolimus, biomass and specific production	68
4.2. Fermentable sugars and proteins	70
4.3. Determination of micelles concentration	72
4.4. Rheology	76
4.5. Microfiltration	80
4.5.1. Specific resistance of filter components	80
4.5.2. Microfiltration process.....	84
4.5.3. Single step	84
4.5.4. Multiple steps: preliminary study	85
4.5.5. Microfiltration in multiple steps	87
4.6. Tacrolimus and hope in the scientific and social context	99
5 CONCLUSION AND SUGGESTIONS	105
6 REFERENCES	109
APPENDIX A	120
APPENDIX B	123

CHAPTER 1

1. INTRODUCTION

1.1. Contextualization and motivation for this work

The coronavirus pandemic changed our lives, particularly that population on the waiting list for a transplanted organ, whose perspective is full of hope. When kidney disease is detected, the patient hopes for a quick cure but suffers when knows his life will be governed by dialysis. During dialysis, the patient hopes to find a compatible organ. When finds a compative organ and performs the surgery, he has the hope that his organism will accept the new organ and starts administering immunosuppressants that, when adapting the organism to the graft, reduces his immunity and exposes him to the most diverse types of infection, such as Covid-19. In addition, the patient has the hope of having the immunosuppressant at his disposal, so that he begins to sow the hope of living. This reflection clearly points to an important social issue to be resolved, which necessarily involves investments in research and development and innovation in the production of tacrolimus. This compound is recommended as an immunosuppressive drug for the therapy of kidney and liver transplantation treatment. In addition, tacrolimus, as pointed in Figure 1.1, is recommended for the treatment of autoimmune diseases, rheumatoid arthritis, and lichen planus (KOVARIK *et al.*, 2003; SÁNCHEZ *et al.*, 2004), as well as in bronchial asthma treatments, dermatological disorders as vitiligo, psoriasis, atopic dermatitis (DÄHNHARDT *et al.*, 2019), eye diseases like uveitis (HOGAN *et al.*, 2007; ERDINEST *et al.*, 2019) and in the treatment patients with idiopathic membranous nephropathy (IMN) (CUI *et al.*, 2017).

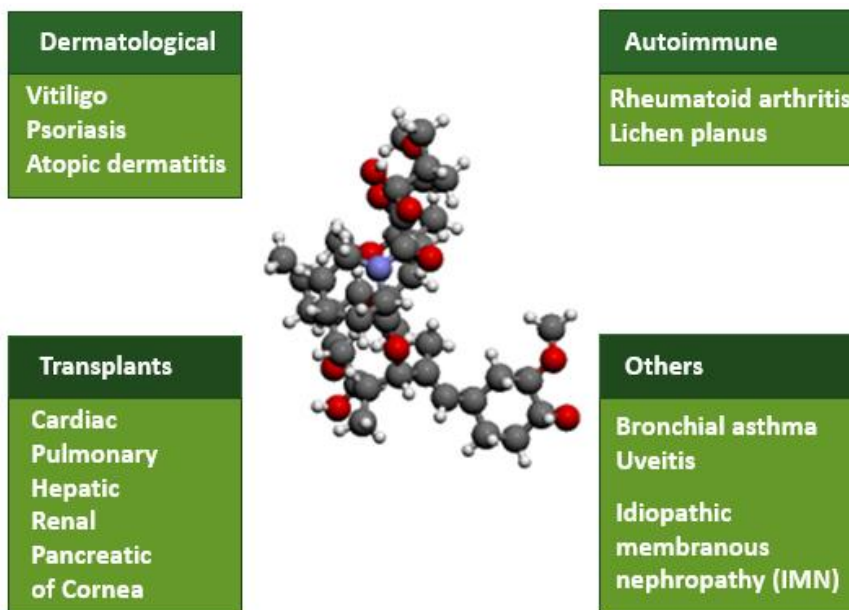


Figure 1.1 - Structural formula of tacrolimus and applications (Author, 2021)

Tacrolimus, known as FK506 and fujimycin, is a macrolide lactone with molar mass 804.018 g/mol and empirical formula $C_{44}H_{69}NO_{12}$, characterized by being a highly hydrophobic substance, can be obtained via fermentation by several species of *Streptomyces* genus, usually, *Streptomyces tsukubaensis*. This bacterium presents shape cylindrical, 0.5 – 0.7 mm in diameter and 0.7 – 0.8 mm in length (MURAMATSU and NAGAI, 2013), and it was found in the Tsukuba's soil, northern Japan (MOREIRA, 2008). The improving FK506 production can be done by a mutant of *Streptomyces tsukubaensis* (SINGH *et al.*, 2017) or from different nutrient media for ordinary *Streptomyces tsukubaensis* bacteria (KINO *et al.*, 1987; CHEN *et al.*, 2012; WANG *et al.*, 2017; SILVA *et al.*, 2019; MOREIRA *et al.*, 2020).

In Brazil, since the promulgation of the 1988 Federal Constitution, the right to health is universal, including comprehensive therapeutic and pharmaceutical assistance. Brazil has the largest public transplantation system in the world, with the Unified Health System (SUS) responsible for financing 96 % of all procedures related to the transplantation process (OLIVEIRA *et al.*, 2019). However, in view of the covid-19 pandemic, there is a totally new situation in people's lives and a profound impact on the current generation. Mankind has a historic moment of extreme exceptionality, whose greatest recommendation is isolation, understanding that this isolation is not a personal choice, but a social necessity. Ordinary situations and demands could be assessed, circumvented, digested in such a way as to proceed

with daily activities. It is not the case, because one lives in a universe that approaches science fiction, apocalyptic, but deeply real. Prudence and common sense are needed, with science and technology as determining allies, especially for the population considered at risk, such as those who need transplants and those who have already had the transplant. The pandemic, since it was enacted in March 2020, by World Health Organization (WHO), has greatly affected the 45,636 people on the waiting list for organ transplants in Brazil. In the case of kidney transplants, which represents 67 % of the total number of surgical interventions, there were, in early March 2019, 510 transplant surgeries, whose number was reduced to 477 in the same period of 2020 (MELO, 2020). Among the reasons that caused this decrease in surgeries, is the new treatment routine, since patients are extremely vulnerable to organ rejection, considering the suppressed immunity due to the use of medications, making people susceptible to infections by viruses, fungi, and bacteria. Also, the hospitalization itself can expose patients, as happened, at the end of May 2020, in the kidney transplant sector at the Hospital das Clínicas de São Paulo, where work was stopped at the end of April after the verification that most patients were infected by the new coronavirus, whose central suspicion was that patients were being accidentally infected by health professionals (SOBRINHO, 2020).

In 2017, several media reported the lack of tacrolimus in various Brazilian states, including São Paulo state, where 40 % of transplanted people live. In the same year, there was a court decision ending the Productive Development Partnership that produced and supplied the drug to the Ministry of Health (FERRARI, 2018). According to an article published by *Jornal Extra Classe* in July 2019, in the Rio Grande do Sul state, approximately 6,000 transplant recipients still suffered from the uncertainty of the supply of the immunosuppressant. Likewise, it happened in the Minas Gerais state, where *Jornal Hoje em Dia* reported that the wait for receiving the drug reached more than 6 months (JORNAL HOJE EM DIA, 2019).

About the national production of tacrolimus, Libbs Farmacêutica and Fiocruz, through the Fiocruz Institute of Pharmaceutical Technology (Farmanguinhos) signed, in August 2010, a technology transfer contract for the production of the drug. It was estimated that such an agreement would generate savings of more than R\$ 240 million for public coffers, in addition to strengthening the Industrial Economic Complex of Health in Brazil and partnerships for product development. In March 2012, the first batch of the drug was produced. The history of the lack of the drug persists, because in 2019 news about the

problem continued. This news points to a productive issue to be resolved and that necessarily involves investment in research and development and innovation.

1.2. Chemical design

A complete chemical design includes a critical review of the idea. There is a need for a process or product, selection of an appropriate process, process optimization, equipment design, description of the optimal operation, an economic forecast of its profitability, and the concern for the well being of the environment that surrounds it.

The purely technical aspects of a design usually involve several standard engineering disciplines (SHERWOOD, 1972). A design for obtaining the specific immunosuppressive drug from fermentation, for example, requires knowledge of biology, chemistry, thermodynamics, mass transfer, and unit operations, to culminate in a typical chemical engineering design, Figure 1.2.

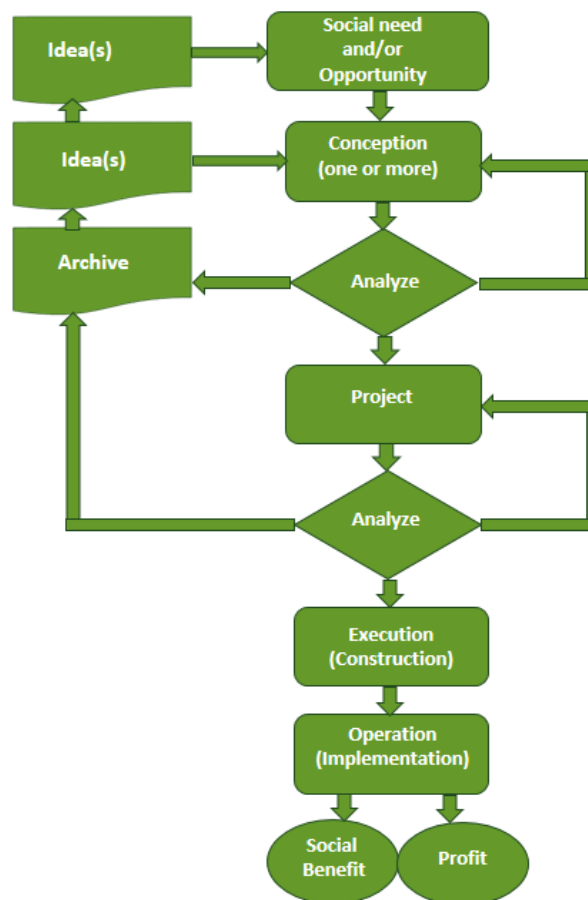


Figure 1.2 - Flowchart characteristic of a chemical design (adapted from SHERWOOD, 1972)

The design ideation begins when someone detects a social need and/or economic opportunity. In the case of immunosuppressants, social need is urgent. For the chemical industry, in turn, this category of the drug can become an economic opportunity. In this context, it is important to remember that Brazil ranks among the ten world powers in the chemical sector, standing behind China, the United States, Japan, Germany, and South Korea. On the other hand, Brazil presents a worrying record in its trade balance, with explosive growth in the deficit from US\$ 1.5 billion in 1991 to over US\$ 32 billion in 2019. According to Vieira (2006), the added value of Brazilian exports is mainly concentrated in products of low technological intensity, such as cellulose, textiles, leather, and exports with a high degree of technology in the products account for less than 10 % of its total. Among the products that involve a high degree of technology, there are drugs. Products derived from tacrolimus produced by *Astellas Pharma Inc.* are the Prograf®, Advagraf®, Graceptor®, Astagraf XL®, Prograf XL®, and Protopic®. In 2016, US\$ 1.841 billion of these drugs were marketed worldwide, representing 15.4 % of the global immunosuppressive market (FERRARI, 2018).

When directing efforts, investments in research, development of immunosuppressant, including innovation in their processing, the result, in addition to bringing financial benefits to the industry, has an impact on the trade balance, reducing their deficit and, mainly, favors the social demand.

1.3. Objective

The central objective of the work is to study microfiltration in a pressurized column to separate the biomass contained in the fermented broth from fermentation via *Streptomyces tsukubaensis* for the production of tacrolimus.

1.4. Specific objectives

- Develop a pressurized column for microfiltration of the broth fermented from fermentation via *Streptomyces tsukubaensis*.
- To study fermentation with coconut oil as an alternative to the traditional source of carbon glucose, and subsequently, to identify and quantify tacrolimus, biomass, sugars, and proteins.

- Obtain the concentration of biomass in the broth by micelles counting, through the development of a technique for the concentration of micelles in the fermented broth.
- Study the rheology of fermented broth by evaluating rheological models associated with fermented broth.
- Evaluate the influences of volumetric flow and operating time in microfiltration performance.
- Obtain a biomass rejection in microfiltration of at least 95 %, considering this parameter while efficiency of the process.
- To evaluate the different resistances involved in the filtration, such as the perforated plate, the stainless-steel screen, and the commercial membranes.
- Contextualize the importance of hope as essential element in chemical design to obtain tacrolimus. Once the health is intrinsically associate with Human Rights.

CHAPTER 2

2. BIBLIOGRAPHIC REVIEW

Chapter 2 presents information on the problem of the lack of tacrolimus in recent years, added this year to the covid-19 disease pandemic, the general characteristics of the drug, a brief presentation on the fermentation process, and the means of cultivation applied and the processing for the production of the FK506. The filtration process, in particular, microfiltration, which is the subject addressed in this dissertation, the filter media (membranes) and their respective porosities, pore diameter, manufacturing material, and the resistance are presented during this membrane separation process. Also, the relationship between the classic approach to filtration and that found in mass diffusion of the Hagen-Poiseuille flow or capillary model is established.

2.1 Presentation of the problem

In 2002, clinical protocols and therapeutic guidelines were established for the use of exceptional and high-cost drugs in the SUS, including those used in kidney transplantation (GUERRA JR, 2015). Clinical protocols recommend, for maintenance in kidney transplantation, the adoption of the tacrolimus/azathioprine/corticosteroids. According to the Brazilian Transplant Registry (RBT) of the Brazilian Organ Transplant Association (ABTO), Brazil's transplant system is well consolidated and regulated. It is necessary to point out that, in the Campinas city at Hospital das Clínicas da Unicamp (HC-Unicamp), more than 7,000 transplants were performed between 1984 and 2017. In Figure 2.1, the transplants performed at HC-Unicamp from 2008 to 2017 are shown.

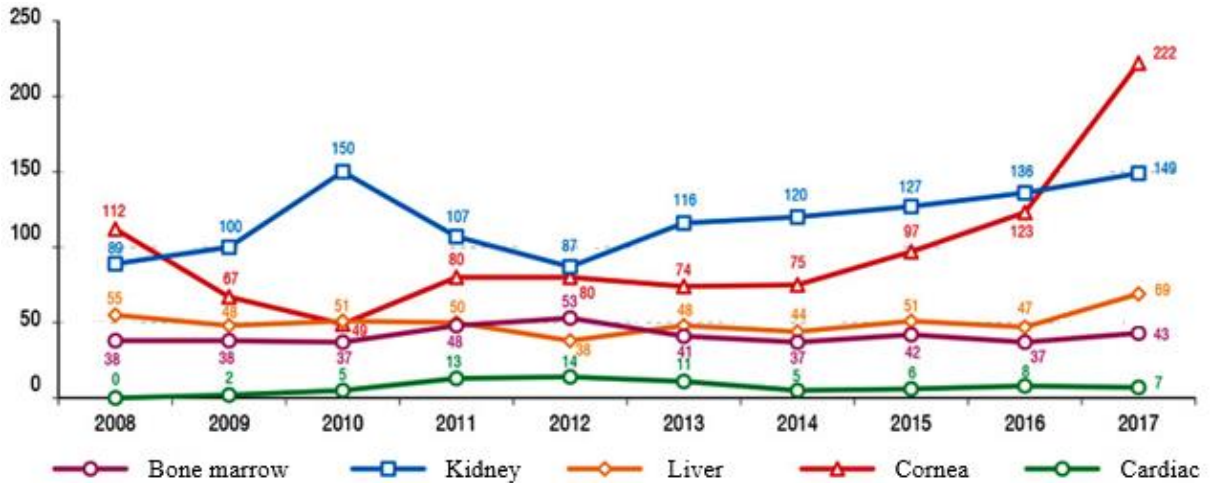


Figure 2.1 - Transplants performed at Hospital das Clínicas of Unicamp (Adapted from MORETTI, 2018)

Despite the promising scenario that presented itself until then, between April and June 2020, with the effect of the covid-19 pandemic, Brazil performed less than half of the organ and tissue transplants at the beginning of the year. With the 61 % decrease in procedures, 44.5 % of the deaths of patients registered on the waiting list between the two periods increased across the country (FREIRE, 2020), as shown in Figure 2.2, a drop-in donation and transplants never seen before. The pandemic caused a decrease in admission patients on the waiting list, as well as the disposal of infected organs.

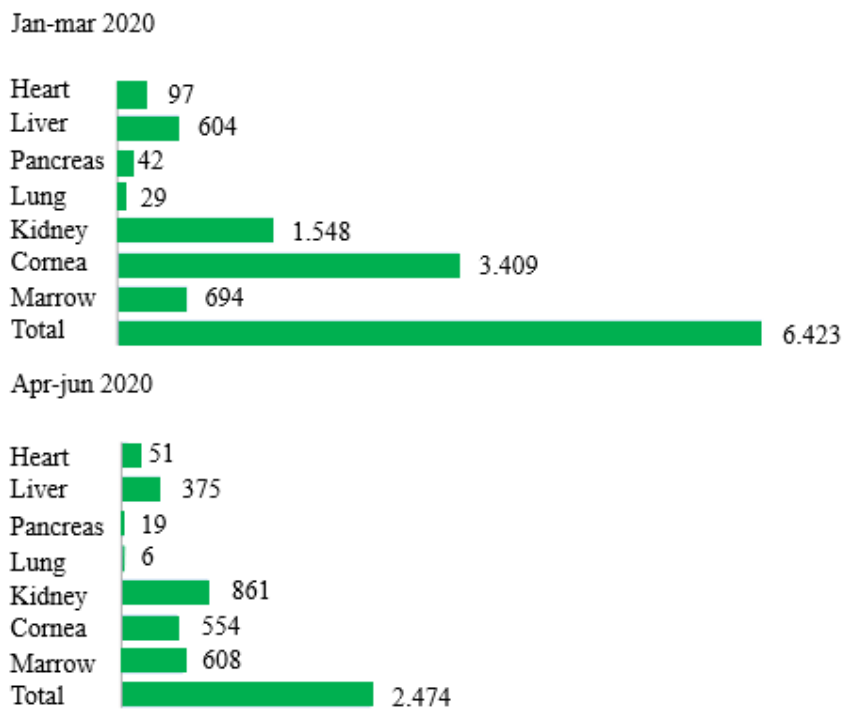


Figure 2.2 - Organ and tissue transplants 2020 in Brazil (Adapted from FREIRE, 2020)

According to the National Commission for the Incorporation of Technologies, tacrolimus is the most recommended drug for therapy in the treatment of kidney and liver transplantation, and cyclosporine is indicated when there is a contraindication to tacrolimus (FERRARI, 2018). With the exception of corneal transplantation, all other transplants are based on a calcineurin inhibitor, such as tacrolimus and cyclosporine. In corneal transplantation immunosuppression therapy, other methods are used to induce T lymphocyte apoptosis, such as the use of methylprednisone pulse therapy (COSTA *et al.*, 2008). However, there are studies showing that tacrolimus drops associated with topical prednisone increase donated corneal survival in high-risk patients (DHALIWAL *et al.*, 2008). It should be added that tacrolimus was recommended as a rescue therapy for use in patients undergoing lung transplantation, undergoing maintenance treatment, resistant or intolerant to cyclosporine, according to criteria that should be established in the Clinical Protocol and Therapeutic Guidelines of the Ministry of Health (CONITEC, 2015a). In pancreatic transplant therapy, tacrolimus decreases the occurrence and severity of refractory rejection episodes and adverse events. In the case of therapeutic treatments with reduced dose tacrolimus and sirolimus, 2 to 5 % of repetitive toxic episodes of severe refractory rejection can be rescued (CONITEC, 2016a). Tacrolimus is consolidated in liver transplant therapy. However, CONITEC proposes the combined use of tacrolimus and everolimus, as it would result in savings of up to R\$ 73 million in the period from 2015 to 2019 (CONITEC, 2015b; CONITEC, 2016b).

2.2 Tacrolimus and its obtaining

Tacrolimus (Figure 2.3) can be obtained via fermentation by several species of the genus *Streptomyces* in an aqueous nutrient medium, containing sources of carbon and nitrogen (Table 2.1), preferably under anaerobic conditions.

Initially, a Petri dish is prepared to sample of bacteria. After bacterial growth, part of the substrate and colonies are transferred to the inoculation medium. After inoculation, an aliquot is taken to the fermentation medium (Figure 2.4). Fermentation takes place under certain conditions of pH, temperature, agitation, and time. Some media used for fermentation destined to obtain tacrolimus are shown in Table 2.1.

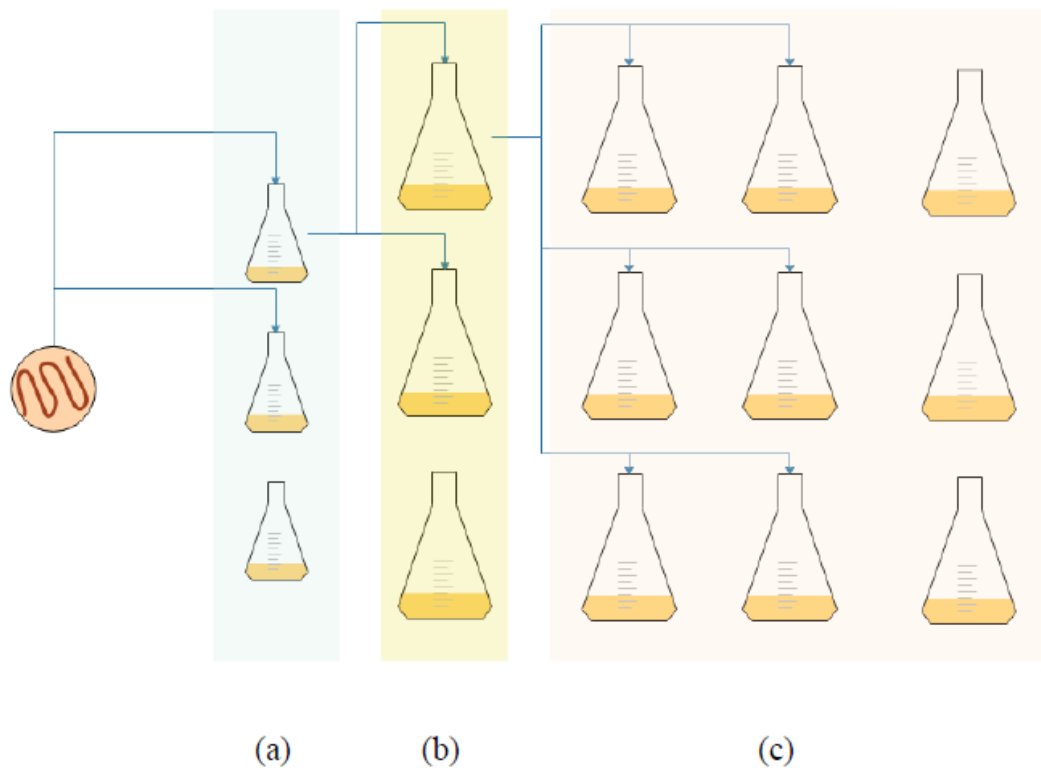


Figure 2.4 - Schematic representation of pre-inoculation (a) inoculation (b) and fermentation (c) (Adapted from MOREIRA, 2018).

Table 2.1 – Same strain of *Streptomyces tsukubaensis* (Author, 2021)

Authors	Strain	Operational conditions	Carbon source	Nitrogen source	Phosphate source	Micronutrients	Amino acids and proteins	Production tac	Specific production
Kino <i>et al.</i> (1987)	<i>Streptomyces tsukubaensis</i> No. 9993	² T = 30 °C, t = 2d, r = 300 rpm, pH = 6.5 ³ T = 30°C, t = 4 d, r = 170 rpm, pH = 6.8	² Glycerol, corn starch, glucose, corn steep liquor ³ Soluble starch, corn steep liquor, yeast extract	² Seed meal, corn steep liquor ³ Corn steep liquor	² Seed meal (with smaller amounts of phosphorus)			13.6	not specified
Okuhara <i>et al.</i> (1990)	<i>Streptomyces tsukubaensis</i> No. 9993	¹ T = 30 °C, t =21d, pH=7.5 ² T = 30°C, t = 4d, pH = 7.0, r = 130 rpm ³ T = 30°C, t = 4d (with aeration), r = 250 rpm, pH = 6.8	^{1,2} Sacarose, sodium nitrate, dipotassium phosphate, magnesium sulfate, thiamine hydrochloride, ferrous sulfate, yeast-mal extract, glycerin, glucose, cottonseed meal, corn steep liquor ³ Glycerin, soluble starch, glucose, cottonseed meal, corn steep liquor, peanut powder, gluten meal, Adekanol (defoamin agent)	^{2,3} Dried yeast		^{2,3} CaCO ₃ ³ MgSO ₄ .H ₂ O, KH ₂ PO ₄ , K ₂ HPO ₄ , CoCl ₂ .H ₂ O	³ Soy peptone	14-23	not specified
Turlo <i>et al.</i> (2012)	<i>Streptomyces tsukubaensis</i>	¹ T = 30°, t = 7 d, r = 110 rpm, pH =7.2 ³ T = 30°C, t = 10 d, r = 110 rpm	² Glucose, maltose, malt extract, yeast extract ³ Maltose, corn steep liquor	³ Corn steep, liquor, soy peptone	³ KH ₂ PO ₄ , K ₂ HPO ₄	³ MgSO ₄ , KH ₂ PO ₄ , K ₂ HPO ₄ , CaCO ₃	² Soy peptone ³ Picolinic acid	32.5	≅ 10.0
Moreira (2018)	<i>Streptomyces tsukubaensis</i>	¹ T = 28 °C, t = 5-7d, pH = 7.2, ² T = 28 °C, r = 110 rpm, ³ T = 28 °C, t = 10 d, r = 130 rpm; pH = 7.2	² Malt extract, glucose, maltose, yeast extract ³ Maltose, corn steep liquor	³ Soy peptone, corn steep liquor	³ KH ₂ PO ₄ , K ₂ HPO ₄	³ MgSO ₄ .7H ₂ O, KH ₂ PO ₄ , K ₂ HPO ₄ , CaCO ₃	³ Soy peptone	≅ 75	10.47
Ferrari (2018)	<i>Streptomyces tsukubaensis</i>	¹ T = 28 °C, t = 10 d, pH = 7.2 ² T = 28 °C, t = 24h, r = 130 rpm ³ T=28 °C, t = 7 d, r = 130 rpm pH = 7.2	² Maltose, glucose, yeast extract, malt extract ³ Corn steep liquor, Brazil nut oil	³ Corn steep liquor, soy peptone	³ KH ₂ PO ₄ , K ₂ HPO ₄	³ CaCO ₃ , KH ₂ PO ₄ , K ₂ HPO ₄ , MgSO ₄ .7H ₂ O	³ Picolinic acid, soy peptone	47.4	8,97 ± 1,12
Silva (2019)	<i>Streptomyces tsukubaensis</i>	¹ T = 28 °C, t = 10 d, pH = 7.2 ² T = 28 °C, t = 24h, r = 130 rpm ³ T=28 °C, t = 7 d, r = 130 rpm, pH = 7.2	¹ Glucose, yeast extract, malt extract ² Malt extract, yeast extract, glucose, maltose ³ Corn steep liquor, Brazil nut oil			^{1,3} CaCO ₃ ³ MgSO ₄ .7H ₂ O, KH ₂ PO ₄ , K ₂ HPO ₄	³ Soy peptone	41.67	1.68

¹ Pre inoculation ² Inoculation ³ Fermentation

Table 2.2 – Mutants strain of *Streptomyces tsukubaensis* (Author, 2021)

Authors	Strain	Operational conditions	Carbon source	Nitrogen source	Phosphate source	Micronutrients	Amino acids and proteins	Production tac	Specific production
Mishra and Verma (2012)	<i>Streptomyces sp.</i>	² T = 28 °C, t = 24 h, r = 120 rpm, pH = 7.0 ³ T = 28 °C, t = 9 d, r = 200 rpm, pH = 7.0	^{2,3} Soy oil, soybean meal	^{2,3} (NH ₄) ₂ SO ₄		^{2,3} CaCO ₃	³ L-lysine	135.6	10.67
Dumont <i>et al.</i> (1992)	<i>Streptomyces sp. (MA 6858) ATCC n. 55098</i>	¹ T = 27 °C -28 °C, t = 2 d, pH = 7.0 ² T = 26-32 °C, t = 4 - 7 d, r = 220 rpm ³ T=25 °C - 35°C, t = 4 -7 d, pH = 6.8 – 7.3	² KNO ₃ , Glucose, MgSO ₄ .7H ₂ O, ZnSO ₄ .7H ₂ O, CaCl ₂ .2H ₂ O, FeSO ₄ .7.H ₂ O, Dextrose, Asparagine, MnSO ₄ .4H ₂ O, CuCl ₂ .2H ₂ O ³ Soluble starch, glucose, distillers solubles	³ Dried yeast, corn steep liquor	¹ KH ₂ PO ₄	³ CaCO ₃ , CoCl ₂ .H ₂ O		10 – 37.8	not specified
Vaid (2007)	<i>Streptomyces sp. (Strains PSCS) FERM B027; MA 6858, ATCC n. 55098; Mutant P5C3</i>	¹ T = 25 °C, t = 7 d, pH = 7,0 ² T = 26-32 °C, t = 42-48h, r = 240 rpm ³ T=24 °C - 30°C, t = 2 - 7 d, r = 130 rpm, pH = 6,0- 8,5, ph =7,0 preferencialy	¹ Yeast extract, malt extract, glucose, glycerin ² Dextrose, dextrin white, glycerol, cotton seed meal, soya bean meal, soya peptone, KH ₂ PO ₄ , CaCO ₃ ³ Cotton seed oil, ground, oil, soya oil, sunflower oil, sucrose	³ Yeast, extract, meat extract, gluten meal, cotton seed meal, corn steep licor, dried yeast, wheat germ, feather meal, peanut powder, urea, (NH ₄) ₂ SO ₄		² CaCO ₃ ³ MgSO ₄ .7H ₂ O, KH ₂ PO ₄ , K ₂ HPO ₄		150-250	not specified
Chen <i>et al.</i> (2012)	<i>Streptomyces tsukubaensis</i> ZJU01	² T = 28 °C, t = 24 a 28 h, r = 220 rpm, pH = 7,0 ± 0,2 ³ T = 28 °C, r = 220 rpm, pH = 7.0 ± 0,2	² Glycerol, soybean meal, soluble starch ³ Soluble starch, glucose, soybean oil	³ (NH ₄) ₂ SO ₄	³ K ₂ HPO ₄	² CaCO ₃ ³ K ₂ HPO ₄ , NaCl, MgSO ₄ .7H ₂ O, CaCO ₃	³ L – lysine	46.9 ± 2.5	not specified
Huang <i>et al.</i> (2013)	<i>Streptomyces tsukubaensis</i> D852	³ T = 28 °C, t = 6 d, r = 220 rpm, pH = 7.0	³ Starch, yeast extract, soybean meal	³ Soy peptone	³ K ₂ HPO ₄	³ K ₂ HPO ₄ , MgSO ₄ , CaCO ₃	³ Soy peptone, chorismate	177.8 ± 5.7	19.76

¹ Pre inoculation ² Inoculation ³ Fermentation

The first stage of processing to obtain tacrolimus is to take the fermentation broth and submit it to the process of separating the biomass that is composed of micelles. Micelles are composed of hydrophobic and hydrophilic components. The micelles can be spherical, ellipsoid, cylindrical or unilamellar nanodimensional structures (HANAFY *et al.*, 2018). In this case, the micelles are aggregates of molecules present in the fermentation medium, such as proteins, sugars, lipids, microbial biomass etc (SILVA *et al.*, 2019; MOREIRA *et al.*, 2020). In the study of Silva *et al.* (2019), the rate of protein production during the fermentation process via *Streptomyces tsukubaensis* was higher than the rate of consumption. This situation constitutes a problem for the purification of the drug, since the proteins, together with other compounds of the fermented medium, which configure the micelles, can lead to an increase in the number of stages for the recovery and purification of the tacrolimus.

Such separation is usually done by filtration. The filtered solution obtained is subjected to several adsorption steps, whose stationary phases are conventional resins and/or conventional adsorbents, such as silica gel, activated carbon (DUMONT *et al.*, 1992), using elution with conventional solvents, as n-hexane, ethyl acetate (KINO *et al.*, 1987), tetrahydrofuran (THF), acetone, acetonitrile (ACN), ethanol and isopropanol (KERI *et al.*, 2006). Some studies describe important steps in the process of obtaining the drug, aiming at its purification without, however, going into details regarding the biomass filtration step (micelles) (JUNG *et al.*, 2011; GAJZLERSKA *et al.*, 2015). Other studies, after obtaining the fermented broth, mention the quantification of tacrolimus, via liquid chromatography and omitting the removal of micelles (VAID, 2007; MISHRA and VERMA, 2012; TRIPATHI *et al.*, 2014; MO and YANG, 2016). Various works report the use of diatomaceous earth in the filtration of the fermented broth without, however, specifying the type of filter and the physical characteristics of the particulate material (porosity, average particle diameter), except the mass used in relation to the volume of the fermented broth produced, as summarized in Table 2.3. Of the works that did not use the filtration of the fermented broth via diatomaceous earth, we can mention that of Dumont *et al.* (1992), who used sintered glass funnels without, however, detailing the porosity of the filter medium. Moreira (2018), Ferrari (2018), and Silva (2019) obtained tacrolimus on a laboratory scale using vacuum filtration using 3.00 μm filter paper for the average pore diameter without, however, specifying the separation efficiency.

Table 2.3 - Relationship between land mass and diatom and volume of fermented broth (Author, 2021)

Authors	kg of diatomaceous earth / Liter of fermented broth
Kino <i>et al.</i> (1987)	25/1.500
Okuhara <i>et al.</i> (1990)	5/200; 25/1.600
Ueda <i>et al.</i> (1990)	25/1.600
Okuhara <i>et al.</i> (1997)	5/200; 25/1.600
Okuhara <i>et al.</i> (1998)	5/200
Nishiara <i>et al.</i> (2002)	50/3.000
Patil <i>et al.</i> (2009)	Do not mention
Kulkarni <i>et al.</i> (2005)	Do not mention
Choi <i>et al.</i> (2013)	Do not mention

2.3 Determination of concentration of the micelles from fermentation broth

The counting of micelles was performed using an alternative technique, developed during the tests of the present dissertation, to determine the concentration of micelles in terms of number of micelles/sample volume (crude fermented broth and permeate), obtained by the Neubauer chamber, in absorbance function by spectroscopy.

Because of the need to purify the tacrolimus, the first processing step, after fermentation, is associated with the separation of micelles. However, to evaluate the performance of the filter or other equipment intended for separation, it is necessary to know the concentration of micelles in the broth to be subjected to filtration and in the permeate (DORAN, 2013; MAO, 2016).

In case of particulate material suspended in a liquid medium, its concentration can be obtained in the form of the number of particles/sample volume, where this sample is stored in equipment intended for such measurements, like as particle counters KL-04A (ORION Co., LTD), HIAC 9703⁺ (Beckman Coulter) and APSS-2000 (Particle Measuring Systems). Due to the high cost, this equipment is not always available for analysis. The counting chamber (or Neubauer chamber) is a method aimed at obtaining the number of particles/sample volume with proven efficacy, and much lower cost compared to the above counters mentioned (ABSHER, 1973; ZHANG *et al.*, 2019). The great disadvantage of the counting chamber is the time to count and the inherent complexity of the technique, especially when this counting must be done systematically. However, it is not uncommon to find spectrophotometers in laboratories that work with biotechnological processes. Spectroscopy or spectrophotometry is a technique used in the quantification of chemical and biochemical species, based on absorption of electromagnetic

radiation in the visible and ultraviolet regions from species in solution. The attenuation of the incident radiation beam by the spectrophotometer is proportional to the amount of chemical species contained in the sample (GÖRÖG, 2017).

Therefore, it is possible with the alternative technique to obtain the concentration of micelles, in the form of a number of micelles/sample volume, from the construction of a calibration curve (for the spectrophotometer), that presents the relationship between this concentration, from the counting of particles by the Neubauer chamber, and the absorbance, which comes from the spectrophotometer. This Dissertation presents an alternative technique that associates the counting of particles through the Neubauer chamber with the spectroscopy technique, providing a substantial reduction in the analysis time to obtain the concentration of pseudomyces, mainly for samples considerably more diluted than the original sample.

2.4 Filtration

Filtration is a classic unitary operation designed to separate particulate material present in a fluid medium (gas or liquid), with main purposes: the removal of unwanted solids suspended in the fluid and recovering a solid suspended product (SILVESTRE, 2014). According to the Food and Drug Administration (FDA), filtration steps are important in the proper removal of specific microorganisms and contaminants and, therefore, have an essential impact on the smooth running of the entire biopharmaceutical process, on product yield and quality. Biopharmaceutical formulations are quite expensive, which is why the filter must be sized to avoid dead volume (HAINDL *et al.*, 2020). Filtration is found in various industrial processes, for example, those present in water treatment, drug processing, and in the food industry. Such a mechanical separation operation may involve several types of filtering action, associated with the way in which the phases are subject, for example, gravity, centrifugation, the way in which the particulate phase is removed from the equipment, as well as the separation equipment itself, known as a filter (Figure 2.5). The filter, in turn, contains a porous matrix, known as a filter element, which will selectively retain a certain diameter range of the particulate phase present in its original composition. During filtration, the accumulation of the particulate phase may occur in a mixture, in particular, with the liquid phase on the surface of the filter element, called the filtration cake, and the fluid obtained after the operation is called filtrate, as shown in Figure 2.6 (CREMASCO, 2018).

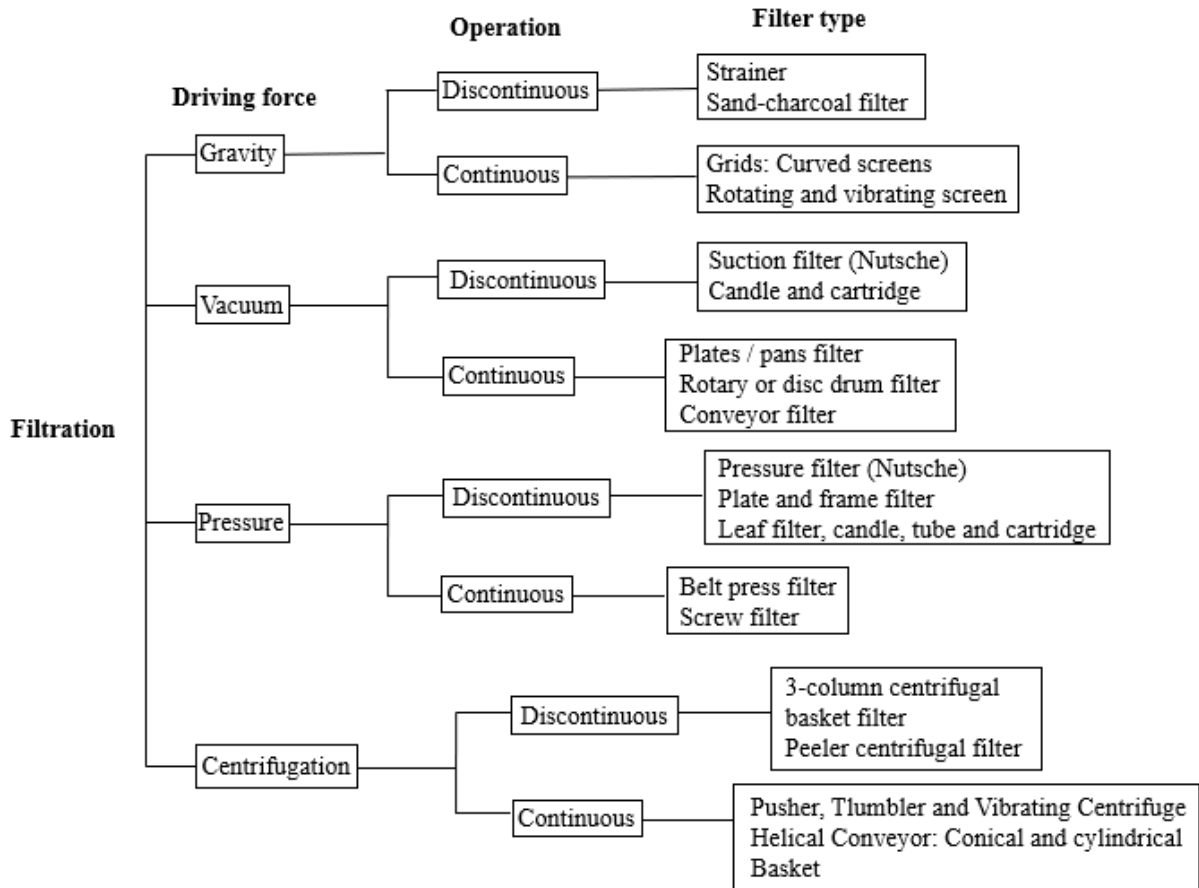


Figure 2.5 - Operational filtration classification (Adapted from RUSHTON *et al.*, 1996)

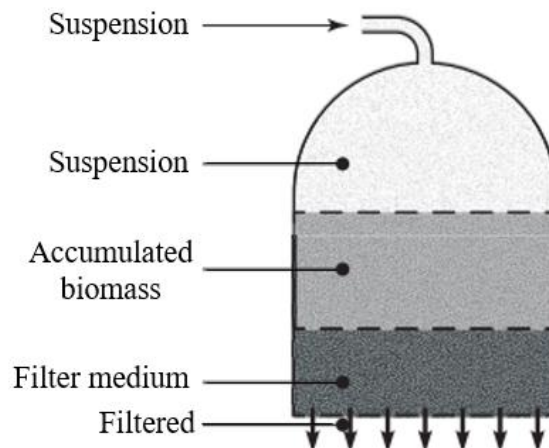


Figure 2.6 - Filtration representation (Adapted from CREMASCO, 2018)

In the fermentation process industry, diatomaceous earth is used as an auxiliary component to the filtration process, as already mentioned in section 2.2, to obtain a higher efficiency value. Although the works indicated in Table 2.3 do not specify the type of filter used to separate the micelles from the fermented broth, it should be noted that regardless of the type of filters that use diatomaceous earth, whether vertical, horizontal, plates and support

plates, are based on a fine-screened filter medium, through which the diatomaceous earth, contained in a given liquid solution, is drained. The filtrate is recirculated to produce a pre-filtration given the formation of layers of particulate material of a smaller diameter on those retained in the filter medium. When it is verified that the filtrate is free of particulate material (diatomaceous earth), the flow of the diatomaceous earth solution is stopped and the filter is fed with the fermented broth, allowing the suspended micelles to also be retained in the interstices between the particles of diatomaceous earth. The filtration is interrupted when the cake formed by the accumulation of layers of particulate material reaches a certain thickness.

2.5 Simplified filtration theory

The filtration process that causes the formation of cake presents a variation in the porosity of the material (particulate phase concentrated in the fluid phase) over the filter medium due to the path taken by the suspension, resulting in a deformable porous medium. The cake is formed over time due to the supersaturation of the filter medium. A theoretical methodology aimed at obtaining the resistance found in microfiltration is that found in the Simplified Theory of Filtration, widely disseminated by Massarani (1997) and used in a filter press, lamellar filter, rotary drum. Such theory allows writing the general filtration equation in the form (CREMASCO, 2018),

$$\frac{dt}{dV} = \frac{\eta}{(\text{Area})(\Delta p)} \left[R_M + \frac{\langle \alpha \rangle}{\text{Area}} \right] \rho s_p \gamma V \quad (2.1)$$

that, for compressible cake, this equation is rewritten as

$$\frac{t}{V} = \frac{\eta}{(\text{Area})(\Delta p)} \left[R_M + \frac{\langle \alpha \rangle}{2(\text{Area})} \right] \rho s_p \gamma V \quad (2.2)$$

with t , filtration time; V , filtrate volume; Area , specific filtration area; Δp , differential pressure; η and ρ , dynamic viscosity and a density of the solution; R_M it is due to the resistance of the filter medium during the operation, the accessories to accommodate the filter medium in the equipment used, as well as that resistance as result of material deposit on the surface and in the pores of the filter element; $\langle \alpha \rangle$, refers to the average resistivity of the cake, which is associated with the accumulation of material on membrane surface, forming a region

whose particulate concentration varies along of its thickness, configuring the cake compressibility; s_p , the absolute mass fraction of solids (mass of particulates in the cake per total mass of liquid), given by

$$s_p = \frac{m_p}{m_\ell} \quad (2.3)$$

and the capture factor, γ , defined by (CREMASCO and WENDRINER, 2017)

$$\gamma = (1 - \varepsilon_{p \text{ filtered}}) + (1 - \varepsilon_{pt}) \frac{V_t}{V} \quad (2.4)$$

$\varepsilon_{p \text{ filtered}}$, ε_{pt} are the volumetric fractions of the particulate phase in the filtrate and in the cake, respectively, whose definition is (CREMASCO, 2018)

$$\varepsilon_p = \frac{V_p}{V_p + V_\ell} \quad (2.5)$$

where V_p and V_ℓ are the volumes of the particulate phase and the liquid phase. When evaluating the volumetric fractions according to the number of particles per volume, considering the linear relationship between them, the capture factor is rewritten according to (CREMASCO and WENDRINER, 2017)

$$\gamma = 1 - \frac{N_p}{N_T} \quad (2.6)$$

N_p refers to the number of particles in the filtrate per volume analyzed and N_T is the number of particles found in the solution per volume analyzed. Cremasco and Wendriner (2015), for example, used the HIAC 9703⁺ particle counter (Beckman Coulter) to assess the concentration of particulate matter suspended in wine. Add that the importance of Equation 2.6 is in the fact that it is directly associated with the rejection, in the case of micelles, in the form

$$(R\%) = 100\gamma \quad (2.7)$$

R_M and $\langle \alpha \rangle$, present in Equation 2.2, depend on the characteristics of the filter medium (such as pore diameter, porosity) and operating pressure, Δp . Such values are obtained through experimental tests, subjecting the membrane to different operating pressure values. For each pressure value, a set of filtration time and filtrate volume values is obtained, allowing the construction of graphs like the one shown in Figure 2.7. For each value of Δp a line will be obtained, in the form t/V vs. V , whose slope, α , will provide $\langle \alpha \rangle$, and the linear coefficient, β , the value of R_M , through, respectively,

$$\langle \alpha \rangle = \alpha \frac{2\Delta p(\text{Area})^2}{\eta \rho s_p \gamma} \quad (2.8)$$

$$R_M = \beta \frac{(\text{Area})(\Delta p)}{\eta} \quad (2.9)$$

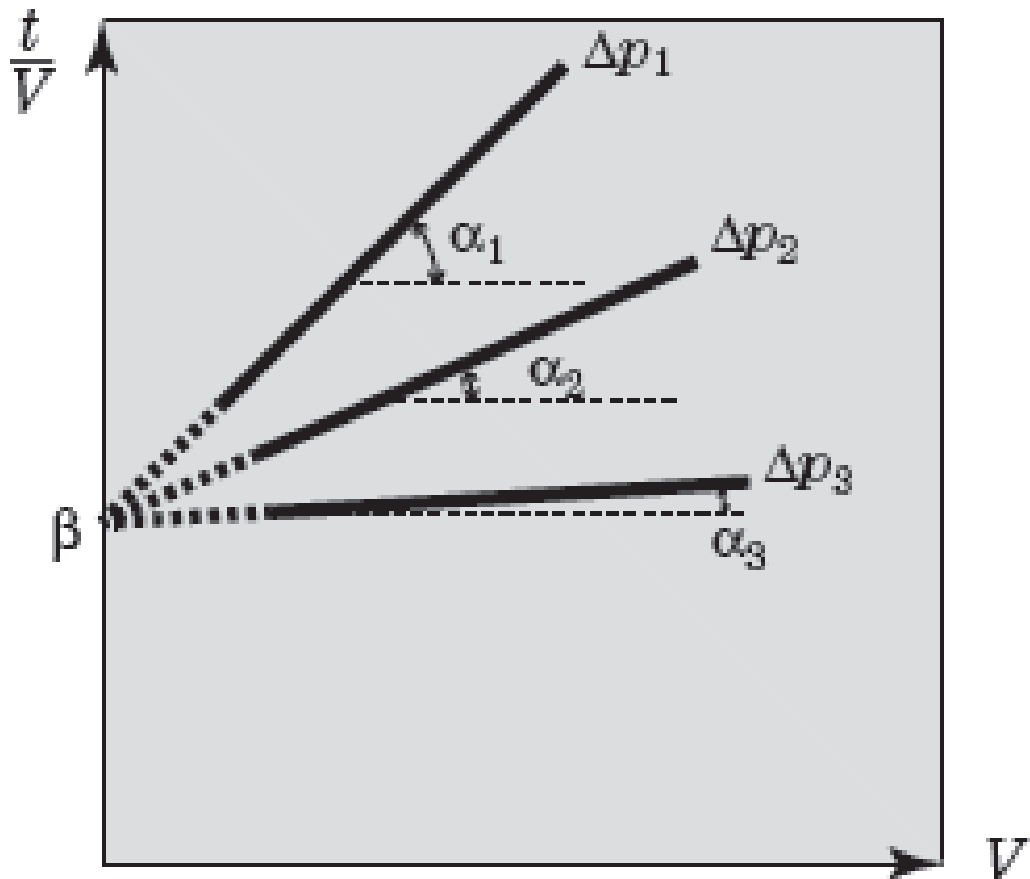


Figure 2.7 – Obtaining $\langle \alpha \rangle$ and R_M for constant pressure filtration (CREMASCO, 2018)

2.6 Membrane separation process (MSP)

Membrane separation process (MSP) is a category of filter media used in processes involving microfiltration, nanofiltration, ultrafiltration, and reverse osmosis (AQUINO, 2011; CREMASCO, 2019). In 1748, there was the first record related to phenomena that occur in membranes with the frenchman called Nollet. Although MSP, as microfiltration has been known and applied on a small scale since 1930, it has not been expanded to an industrial scale, being one of the main factors, the low permeate flows due to the thickness of the membranes. MSP research projects grew significantly in the 1950s when the United States invested in a water desalination project. After the water desalination project, the interest in MSP increased, considering that there was an improvement in the selectivity of the membranes and reduction of resistance concerning the chemical permeating species, making the MSP more competitive than the classic separation processes. Thus, in addition to the classic separation processes such as distillation, filtration, absorption, ion exchange, centrifugation, solvent extraction, crystallization, among others, a new class of processes using synthetic membranes appears at that time, as an attempt to imitate the natural membranes, specifically in terms of selectivity, specificity and permeability with low energy consumption (HABERT *et al.*, 2006).

In this scenario, the water desalination research carried out in the United States in the 1950s, culminated in a discovery by Loeb e Sourirajan (1960-1962) related to membrane preparation, which later resulted in the terms selective layer (or skin) and “support”, which characterize the membranes called anisotropic or asymmetric. With this discovery, these researchers perfected a technique for membrane preparation, demonstrating its economic viability, named years later as immersion-precipitation phase inversion technique. In this preparation of the membrane, it was possible to increase the permeate flow of water, while maintaining high salt retention. The success of the technique was due to the morphology of the membrane since the upper region called "skin" (around 2 % of the total thickness of the membrane), practically has no pores or they are small, configuring the region of the main selectivity. The region below called "support", has progressively larger pores, where it promotes mechanical resistance.

Several studies have been carried out to control and characterize the morphology of the membranes. There are two research segments, the first is to modify the way of preparing the skin and support in the same processing step, and the other to obtain both in different stages, as suggested in the work of Cadotte and Francis (1966),

characterizing the so-called composite membranes. The development of composite membranes provided an advance in the processes of gas permeation (PG) and pervaporation (PV). In the 1980s, the American Monsanto and the German Sulzer Chemtech, Membrane Systems were the pioneers in the industrial application of MSP in gases and liquids, respectively. Currently, classic and MSP processes are combined, since they are more economically advantageous than the use of each technology separately (HABERT *et al.*, 2006).

Linked to commercial success are several advantages of this technology. MSP are used in various sectors of the industry for the fractionation of mixtures, solutions, and suspensions with species of different chemical nature and size. Table 2.4 shows examples of applications of membrane processes.

Table 2.4 - Examples of application of MSP (adapted from HABERT *et al.*, 2006)

Area	Applications
Chemistry	<ul style="list-style-type: none"> - Breaking of the benzene/hexane azeotrope - H₂ recovery - ammonia synthesis - CO₂ / CH₄ fractionation - Air fractionation
Biotechnology and pharmaceuticals	<ul style="list-style-type: none"> - Separation of thermolabile substances - Ethanol dehydration - Enzyme purification - Protein fractionation - Sterilization of fermentation media - Membrane bioreactors
Food & beverage	<ul style="list-style-type: none"> - Concentration of milk - Cheese whey concentration - Concentration of fruit juice - Clarification of wines and beers
Water treatment	<ul style="list-style-type: none"> - Water desalination - Elimination of organic traces - Municipal sewage treatment - Water demineralization for boilers - Ultrapure water for the electronics industry
Treatment of industrial waste	<ul style="list-style-type: none"> - Water / oil separation - Indigo and PVA recovery – Textile - Metal ion recovery – Leather - Protein Recovery – Dairy - Water treatment - Pulp and Paper
Medical	<ul style="list-style-type: none"> - Artificial kidney - Hemodialysis - Artificial lung - Oxygenators - Oxygen - Enriched air - Sterilization of injectable solutions - Controlled dosage of medicines

2.7 Microfiltration (MF)

After fermentation via *Streptomyces tsukubaensis*, this Dissertation carried out the microfiltration process. As previously mentioned, the filter element is an essential component in the filtration operation and its choice depends on the nature of the fluid containing the particulate material to be processed, temperature, among other parameters (AQUINO, 2011). MSP are classified according to the pore size of the membrane, Figure 2.8, and the pressure used, resulting in several applications for each case, as shown in Table 2.5.

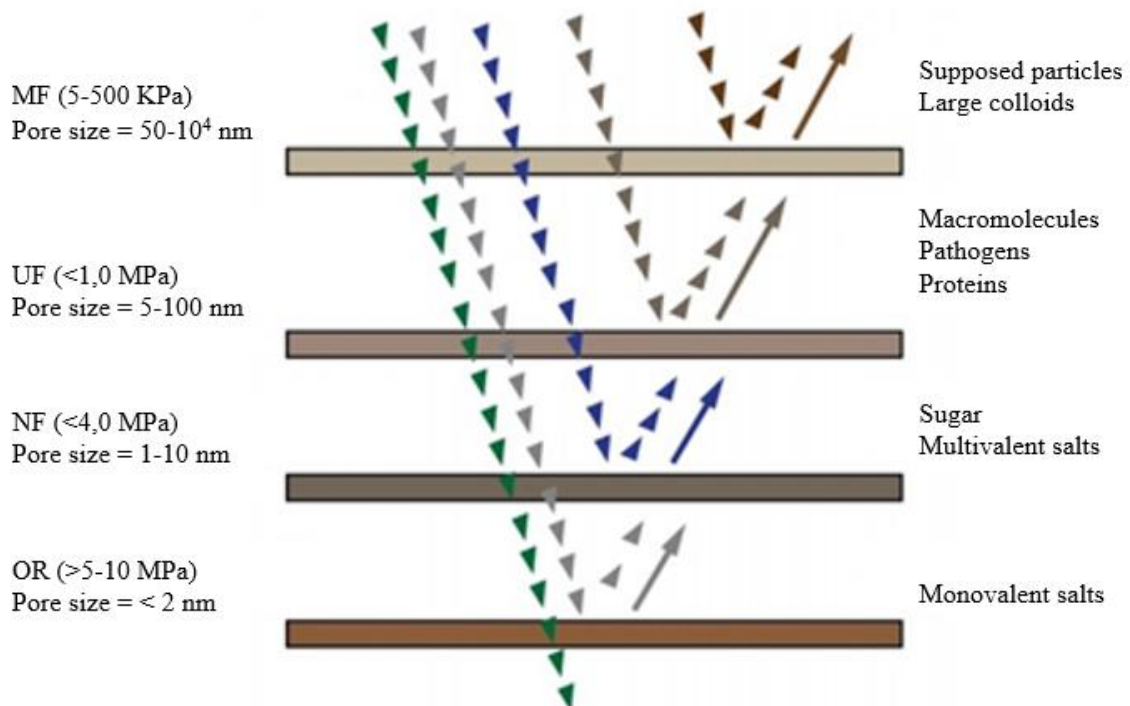


Figure 2.8 - Distribution of pore sizes, pressure used in MSP (Adapted from DUONG and NGUYEN, 2017)

Table 2.5 - Species retained in the OI, NF, UF and MF processes (HABERT *et al.*, 2006)

Species	Molar mass (Da)	Size (nm)	OI*	NF*	UF*	MF*
Yeasts and fungi		10 ³ -10 ⁴				X
Bacterial cells		300-10 ⁴			X	X
Colloids		100-10 ³			X	X
Virus		30-300			X	X
Proteins	10 ⁴ -10 ⁶	2-10			X	
Polysaccharides	10 ³ -10 ⁶	2-10		X	X	
Enzymes	10 ³ -10 ⁶	2-5		X	X	
Simple sugars	200-500	0.8-1.0	X	X		
Organic	100-500	0.4-0.8	X	X		
Inorganic ions	10-100	0.2-0.4	X			

* OI, reverse osmosis; NC, nanofiltration; UF, ultrafiltration; MF, microfiltration.

The microfiltration process (MF) is considered an extension of the classic filtration process, whose main applications are in the purification of biotechnological products, in medicine and in the sterilization of liquids and gases. In the process, the membranes present a pore size between 0.1 to 10 μm , being indicated for the retention of emulsions and suspended materials, with the solvent and soluble substances permeating the membrane (HABERT *et al.*, 2006). The membranes used in MF can retain not only suspended particles and colloids, but also yeasts and fungi, bacterial cells, and viruses (AQUINO, 2011). Thus, MF is normally used to remove particles in suspension of cells in fermentative processes, as well as the food area, as for example, to retain macromolecular solutes, such as those found in the process of producing wine, juices, vegetables, brine, vinegar, gelatin and beer (UMEBARA, 2010). MF can be used also in separation of biochemical and pharmaceutical products (HAINDL *et al.*, 2020; LI *et al.*, 2006; JUANG *et al.*, 2008; JAUREGI, *et al.*, 2013). It should be noted that the pressures used in the MF normally do not exceed 3 bar, considering that the pores of this porous matrix are relatively open. It is worth mentioning that the advantages of microfiltration, under certain conditions, when compared to conventional clarification processes, which include ground and vacuum filtration, reside in the fact that it allows greater yield of the final product (CRISTOFOLI, 2016).

The microfiltration process can be operated in the modes *dead-end* or *cross-flow*, illustrated in Figure 2.9. In *dead-end* (perpendicular microfiltration) the sample fed into the system flows perpendicularly to the membrane surface, permeating the filter element and particulate material (micelles, for example) that are larger than the size of the membrane pores are retained. This filtration mode is recommended as a method to concentrate or separate different components of a food solution or suspension (UMEBARA, 2010). On the operation *cross-flow* (tangential microfiltration) the sample flows along the membrane and only a part of the trapped particles remains on the membrane surface. The permeate passes through the membrane in the direction perpendicular to the direction of flow of the feed. The flow itself exerts a force on the deposited particles in order to drag them from the surface.

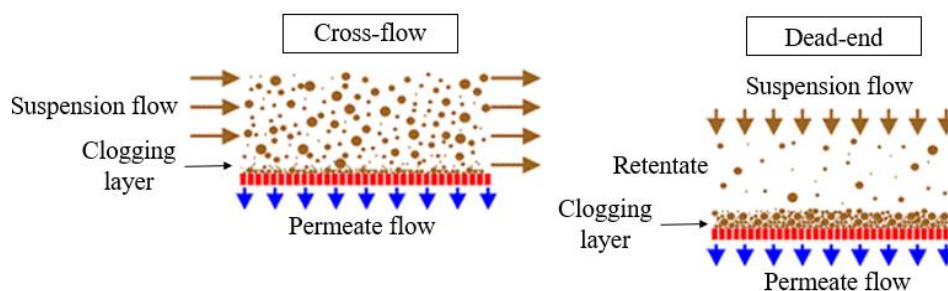


Figure 2.9 – Filtration modes: *dead-end* and *cross-flow* (Adapted from UMEBARA, 2010)

In the case of membranes intended for MF, it is essential to highlight that the size, distribution and shape of the pores are fundamental parameters in the separation process, influencing the mechanisms: exclusion by size; difference in the diffusion coefficient; difference in electrical charge; difference in solubility and difference in adsorption and/or reactivity on surfaces (CRISTOFOLI, 2016). The use of the membrane depends, therefore, on its porous nature, which, in the case of microfiltration, is characterized by presenting, basically, mesopores and macropores and, therefore, the diffusive mechanism is governed by the viscous flow (or capilar diffusion or Poiseuille diffusion), whose driving force is the pressure gradient, presenting an analogy with conventional filtration (CREMASCO, 2018). The permeate mass flow (contaminant-free liquid phase) is described by (SILVA and SCHEER, 2011)

$$j_m = \frac{\Delta p}{\eta R_M} \quad (2.10)$$

where η is the dynamic viscosity of the processed solution; Δp is the pressure differential for dead-end contact (Equation 2.11), and transmembrane pressure for cross-flow contact (Equation 2.12) as shown in Figure 2.10.

$$\Delta p = p_F - p_P \quad (2.11)$$

$$P_{TM} = \frac{1}{2}(P_F + P_R) - P_P \quad (2.12)$$

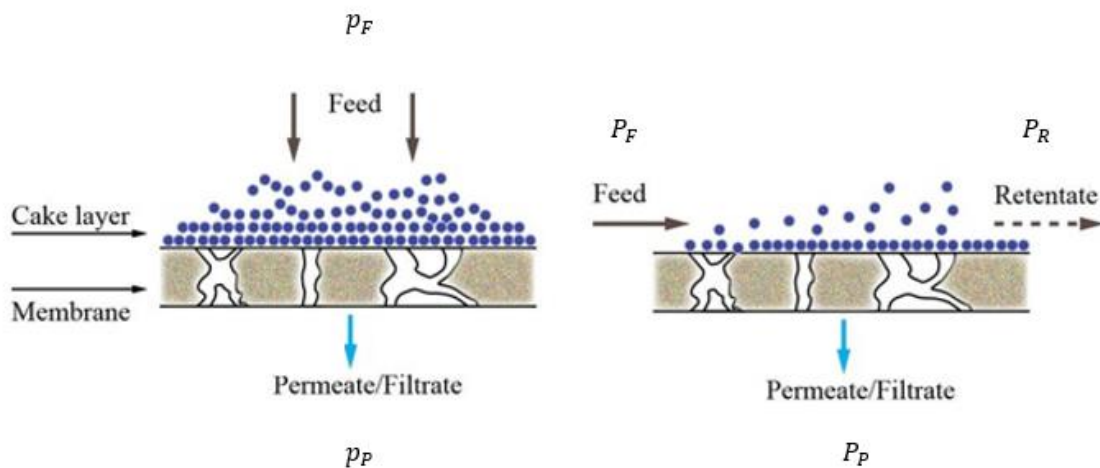


Figure 2.10 - Differential for *dead-end* contact, and transmembrane pressure for *cross-flow* (Adapted from DUONG and NGUYEN, 2017)

The parameter R_M in the Equation 2.10 represent the overall resistance offered by the membrane, and given by

$$R_M = R_f + R_G + R_p + R_s \quad (2.13)$$

R_f is the intrinsic resistance of the membrane. This resistance is obtained from water permeated flow as feed in a new membrane, so that in this way there is no interference from the concentration polarization or the polarized layer, as well as from fouling (CRISTOFOLI, 2016); R_G , refers to the resistance resulting from the fouling effects, which can be defined as the irreversible deposition of retained particles, colloids, emulsions, suspensions, macromolecules, salts etc., on the membrane surface (CREMASCO, 2019), as well as the pore blockage resulting from adsorption, precipitation of substances; R_p , resistance due to polarization as a result of solute concentration (CRISTOFOLI, 2016), and R_s , it concerns the resistance due to the membrane support in the filter (Figure 2.11).

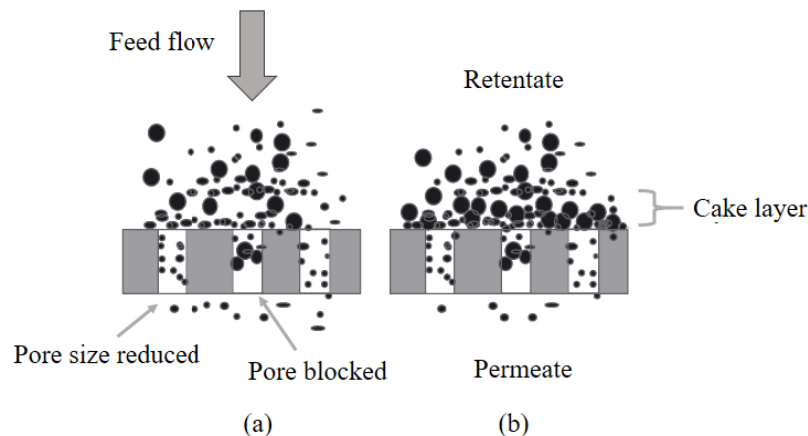


Figure 2.11 – (a) In mode *dead-end* the permeate flow decreases with time due to the effect of fouling on the membrane (b) Initial particle deposition and concentration polarization followed by cake layer formation (HU *et al.*, 2015)

It is important to mention the phenomenon of fouling in the membranes strongly depends on the nature of the solution to be treated, especially when proteins and minerals are present. Micelles, for example, contribute to the formation of deposits on the membrane surface, as well as mineral ions themselves. Fouling, therefore, can occur in several ways: by the deposition of denatured or agglomerated proteins on the membrane surface, or by the adsorption of proteins within the membrane pore structure, making it difficult to remove (ANTUNES, 2014). These effects on the membrane surface as well as

inside the pores are contemplated in terms of R_G and R_p . These resistances, in turn, and mainly that associated with the formation of fouling, turn out to be a limiting factor to the performance of the filter used for microfiltration, in view of decreasing the permeate flow over time. One of the ways to minimize the reduction in the permeate flow is to make the process operate below the critical flow, which is defined as the largest permeate flow in which it is not observed its decreased flow with time. Above this critical flow, irreversible fouling is observed, because in this condition there is a greater drag of the particles that cause the formation of the cake. The limit flow is reached when, as the system pressure increases, the permeate flow ceases to be linear and tends to stabilize. Thus, the permeate flow does not increase with pressure and can no longer be described by the Hagen-Poiseuille model (CRISTOFOLI, 2016). The permeate mass flow can be done also by

$$j_M = \frac{\rho V}{(\text{Area})t} \quad (2.14)$$

where ρ is the density; Area, filtration area, $\text{Area} = 17.30 \times 10^{-4} \text{ m}^2$ in this Dissertation; t , filtration time. The permeate mass flow can be express by differential system pressure by Darcy's law, Equation 2.10, which can be write

$$\frac{\Delta p}{\eta R_c} = \frac{V}{(\text{Area})t} \quad (2.15)$$

R_c is an associated characteristics resistance. Equation 2.15 is put as

$$V = \beta t \quad (2.16)$$

with

$$\beta = \frac{(\text{Area})\Delta p}{\eta R_c} \quad (2.17)$$

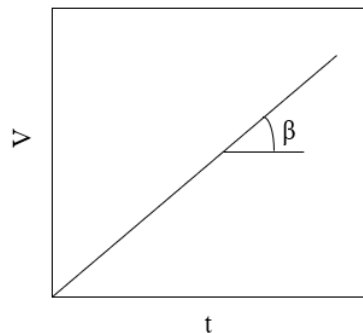


Figure 2.12 – V versus t with β that represents the volumetric flow

It is noticed that β represents the volumetric flow. When someone does a graph V vs t and if it provides a line, there is an angular coefficient equal to β , from which it is possible to obtain the resistance of interest

$$R_c = \frac{(\text{Area})\Delta p}{\eta\beta} \quad (2.18)$$

2.8 Membrane morphology

The morphology of the membrane, the nature of the material and the relationship with the transport properties are important factors for better understanding of the phenomena involved in the separation, as well as making it possible to define the application of the membrane for a separation and its efficiency. According to Habert *et al.* (2006), membranes can be classified according to morphology into symmetrical, asymmetric, porous or dense, as shown Figure 2.13.

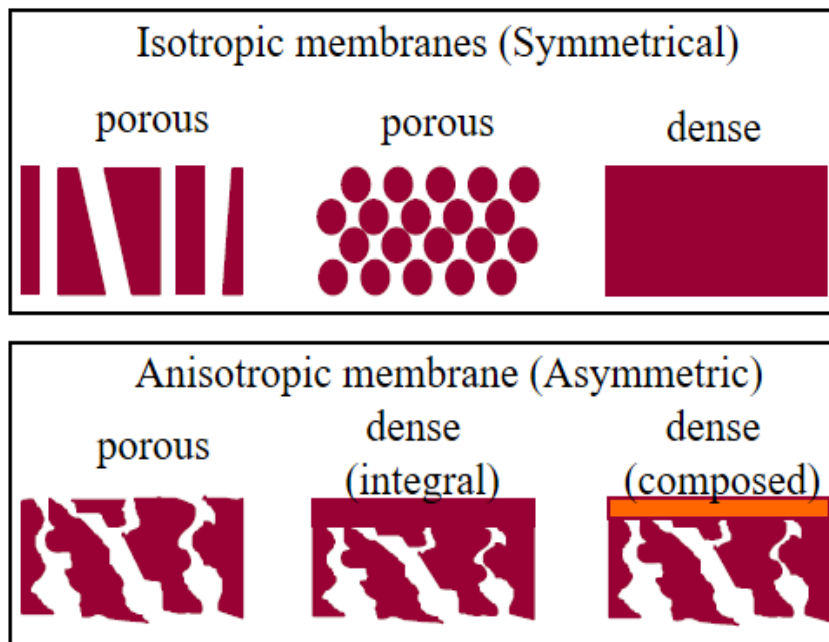


Figure 2.13 – Synthetic membrane morphology (Adapted from HABERT *et al.*, 2006)

- Symmetric: when the properties are the same across the section. Symmetrical membranes can be dense (homogeneous) or porous (heterogeneous), with porous membranes showing uniformity throughout their thickness.
- Asymmetric: there is a density variation along the cross-section of the membrane, being called asymmetric or anisotropic.

- Porous membranes: in porous membranes, the morphological parameters are very relevant, as the distribution of pore size, surface porosity, and thickness, that is, the material from which the membrane is made must affect its selective capacity. It has a casually null, rigid distributed structure with interconnected pores. The pores differ from a conventional filter in that they are extremely small, in the order of 0.01 μm to 10 μm in diameter.
- Dense membranes: for dense membranes, the most significant parameters involve the physical-chemical characteristics, considering the polymer used, the substances to be separated and the thickness of the polymeric film consists of a dense film. The separation of the components of a mixture is directly related to its transport rate in the membrane, which is determined by its diffusion and solubility in the membrane material.

2.9 Microfiltration systems

It is valid to mention that the MF process started in the 1990s, considering the concept of uniform transmembrane pressure (UTP), whose process is based on the recirculation of part of the pressurized (filtered) permeate, to maintain the pressure uniformly over the entire length of the membrane and ensure a constant permeate flow. However, the use of an additional pump system results in high operating costs. For this reason, new systems were developed as alternatives to the use of the UTP system, with less energy consumption and investment savings, without the need for a pump to recirculate the permeate (ANTUNES, 2014). Whatever the system directed to microfiltration, it is essential to maintain the constant operating pressure, which is one of the operational variables as well as the design of fundamental filters for the microfiltration process.

In the specific case of perpendicular or dead-end filtration, the membrane is placed on a support, which is inserted in a chamber to be pressurized. This chamber can have several configurations. As an example, the study of the reduction of turbidity in red wine commercial membranes from 0.18 μm , 1.0 μm , and 1.2 μm , arranged in a metallic envelope and subjected to pressures of 15, 25, and 30 psi. The wine to be treated was placed in a container external to the carcass and injected there due to the pressurization suffered via

compressed air, as shown in Figure 2.14 (CREMASCO and WENDRINER, 2015; CREMASCO e WENDRINER, 2017).

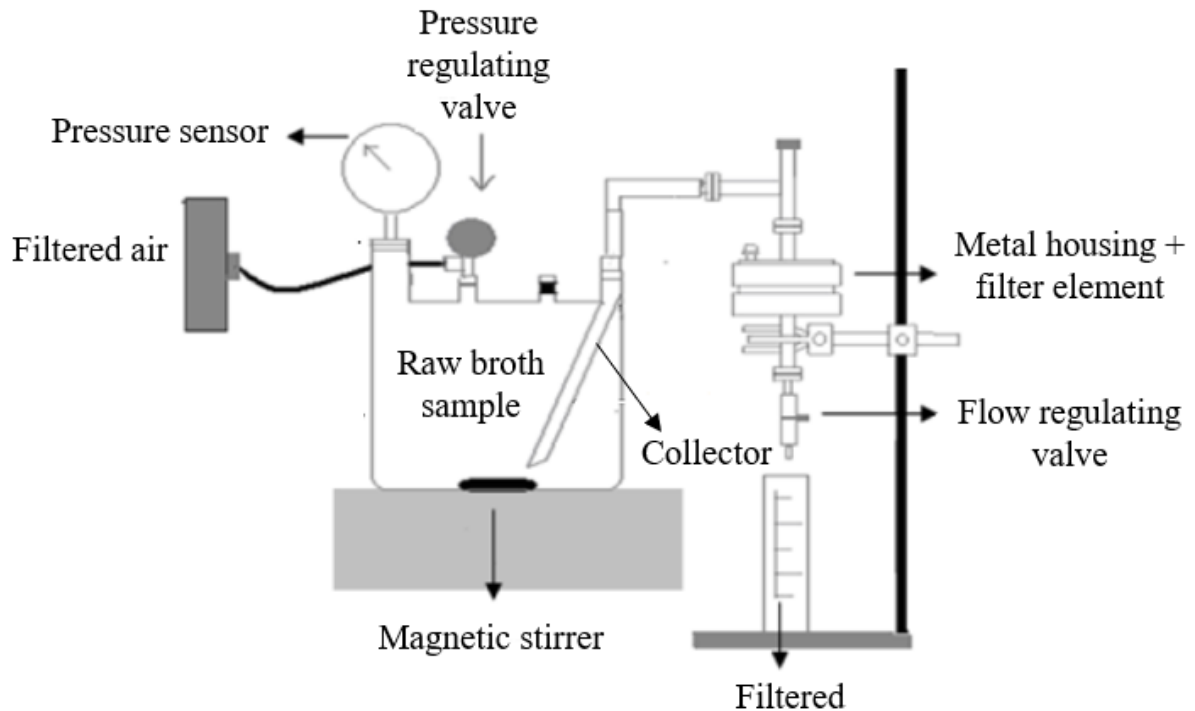


Figure 2.14 – Filtration system (CREMASCO and WENDRINER, 2015; CREMASCO and WENDRINER, 2017)

Beluci *et al.* (2018), studying the removal of the blue dye from the standard methylene, used the filtration system represented in Figure 2.15. These authors used commercial membranes of medium pore size of $0.2 \mu\text{m}$, inserted in a stainless-steel cell coupled to a pressurized air system, whose solution to be filtered was subjected to a pressure of 0.5 bar. It is important to note that, initially, the membrane was compacted with deionized water for 30 min until the flow through the membrane reached a steady state.

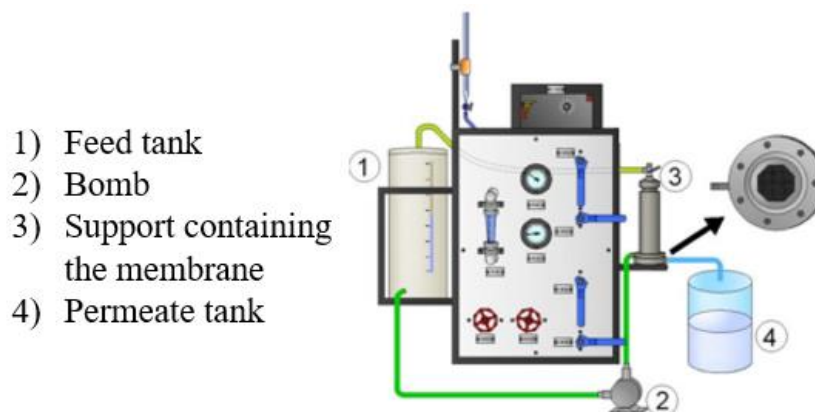


Figure 2.15 - Representation of the pressurized filtration module (BELUCI *et al.*, 2018)

2.10 Essential properties for the evaluation of microfiltration

In addition to the operational conditions of pressure and critical flow, as well as the nature of the filtering material (surface area, pore size, porosity, tortuosity), it is essential to know the temperature of the system, particularly the suspension to be processed, given its influence both on the density (ρ), and dynamic viscosity of the suspension (η). When identifying the importance of dynamic viscosity, knowledge of the suspension rheological behavior is equally important, which, in general, can be observed according to the generalized Heschel-Bulkley model as

$$\tau^n = \tau_0^n + k\gamma^m \quad (2.19)$$

being τ shear stress; τ_0 , initial shear stress; γ , fluid deformation rate; k , parameter associated with fluid consistency; m , fluid behavior index; n , coefficient associated with the residual shear effect. For the situation where $n = m = 1$ and $\tau_0 = 0$ the fluid is classified as Newtonian, or

$$\tau = \eta\gamma \quad (2.20)$$

otherwise, the fluid is said to be non-Newtonian, and there are several models to describe its rheological behavior, as shown in Table 2.6.

Tabel 2.6 – Non-Newtonian rheological models (Adapted from Steffe, 1996)

Model	n	m	Equation	
Ostwald-De-Waele	-	m	$\tau = k\gamma^m$	(2.21)
Bingham	1	1	$\tau = \tau_0 + k\gamma$	(2.22)
Heschel-Bulkley	1	m	$\tau = \tau_0 + k\gamma^m$	(2.23)
Casson	0.5	0.5	$\tau^{0.5} = \tau_0^{0.5} + k\gamma^{0.5}$	(2.24)
Mizrahi-Berk	0.5	m	$\tau^{0.5} = \tau_0^{0.5} + k\gamma^m$	(2.25)
Vocadlo	1/n	1	$\tau^{1/n} = \tau_0^{1/n} + k\gamma$	(2.26)

As for the rheological analysis of biotechnological products resulting from fermentation processes, Malinowski *et al.* (1987), from concentrated solutions in the range 0 to 345 g/L of the biomass of *Saccharomyces cerevisiae*, using a deformation rate from 0 to 1350 s⁻¹, verified non-Newtonian behavior, with a rheological description based on the

Ostwald-De-Waele, Equation 2.21. To produce xanthan gum from the fermentation of *Xanthomonas campestris*, Nery *et al.* (2008) evaluated the rheological model for an aqueous solution of xanthan gum, using for deformation rate 25 to 1000 s⁻¹, stating that the effect of the shear rate on the viscosity of xanthan gum solutions was also described by the model pointing in Equation 2.21.

Cremasco and Melo (2010) studied the rheological behavior of the suspension of *Saccharomyces cerevisiae* residues from the brewing industry, using a deformation rate from zero to 15 s⁻¹, verifying that it behaved like a Newtonian fluid between 25 °C and 50 °C. Above that last temperature and up to 75 °C, the suspension behaves like Bingham plastic, Equation 2.22. According to the authors, the increase in temperature causes an increase in the intensity of molecular agitation, which, in turn, breaks in the molecular bonds, and a change in the physical state of a situation of dispersed-unbound suspension for a paste-like suppression with scattered-linked feature (CREMASCO, MELO; 2010). Bofo (2015) studied the rheological behavior of sugar cane molasses, yeast cream, and *Saccharomyces cerevisiae* SA-1 fermentation broths, for deformation rate from zero to 250 s⁻¹, at different concentrations and temperatures. The experimental results of the molasses samples showed Newtonian behavior in the concentrations of 20 to 40 °Brix and pseudoplastic behavior in the concentrations of 50 to 70 °Brix. The experimental results obtained from the samples of yeast cream and fermented broth pointed to the best fit according to the Ostwald-De-Waele model (power-law), Equation 2.28.

CHAPTER 3

3. MATERIALS AND METHODS

This Dissertation was carried out at Mass Transfer Processes Laboratory (LPTM), Department of Process Engineering (DEPro), School of Chemical Engineering (FEQ), University of Campinas (UNICAMP). This work is in the context of development of pharmaceuticals process and product, particularly tacrolimus processing, and continues the resources of Moreira (2018), Ferrari (2018), Silva (2019). Moreira (2018), who first produced tacrolimus at LPTM/DEPro/FEQ /Unicamp, evaluated maltose and glucose as primary carbon sources, as well as soy peptone and corn liquor as nitrogen sources. Ferrari (2018) realized a robust and complete process for tacrolimus purification. This process consists, basically, of pre-purification of the fermented broth, the purification sequence with chromatographic techniques and crystallization, obtaining 99 % tacrolimus purity. Silva (2019) studied the Brazil nut oil and glucose as primary sources of carbon in the *Streptomyces tsukubaensis* fermentation to enhance tacrolimus production. This Dissertation aims to improve the tacrolimus recovery process developed at LPTM/DEPro/FEQ/Unicamp, by analysis of development of a pressurized column for microfiltration of fermented broth via *Streptomyces tsukubaensis*.

The present chapter describes the materials and methods for pre-inoculation, inoculation, fermentation, drug quantification, microfiltration, micelle counts, quantification of protein, and reducing sugars, as well as rheology study of fermented broth. Fermentation, determination of micelle concentration, quantification of proteins and reducing sugars were carried out at the Laboratory of Biochemical Engineering, Biorefining and Products of Renewable Origin (LEBBPOR/DEPro/FEQ/UNICAMP). The morphological analysis of the micelles present in the fermented broth was carried out at the Biomass Characterization, Analytical and Calibration Resources Laboratory (LRAC/FEQ/UNICAMP). The tests associated with tacrolimus quantification, microfiltration, and density were performed at LEBBPOR/DEPro/FEQ/UNICAMP. The rheology experiments were carried out at the Process Engineering Laboratory of the School of Food Engineering/UNICAMP.

3.1 Materials

3.1.1 *Streptomyces tsukubaensis* bacteria strain

Strains of bacterium *Streptomyces tsukubaensis* were used to obtain tacrolimus via fermentation. The strains were purchased from the Leibniz DSMZ Institute - German Collection of Microorganisms and Cellular Cultures (acronym DSM, 42081), and sent to the Brazilian Collection of Environment and Industry Microorganisms (CBMAI), Pluridisciplinary Center for Chemical, Biological and Agricultural Research (CPQBA/UNICAMP), identified as CBMAI – 1832 code.

3.1.2 Petri dish culture medium

The culture medium for the growth of bacteria in Petri dish has the composition recommended by the German Collection of Microorganisms and Cell Cultures GmbH (DSMZ) as shown in Table 3.1.

Table 3.1 – Composition of *GYM culture medium for the bacterium *Streptomyces tsukubaensis*

Compound	Amount (g)
Agar	12.0
CaCO ₃	2.0
Malt extract	10.0
Yeast extract	1.0
Glucose	4.0
Distilled water	1000

* GYM medium is characterized by presenting glucose, yeast extract, malt extract

3.1.3 Pre-inoculation, inoculation and fermentation

The composition of the media used for pre-inoculation, inoculation and fermentation were based on Turlo *et al.* (2012), Ferrari (2018), and Moreira (2018). Table 3.2 shows the composition of the medium for pre-inoculum and inoculum, and Table 3.3 the composition of the medium for fermentation. The fermentation using coconut oil and glucose were different, but their concentration as carbon sources (g/L) were kept the same (Table 3.3). Coconut oil is used to nationalize a Brazilian carbon source in the production of tacrolimus, in addition to providing compounds that improve the growth of bacteria for fermentation.

Table 3.2 – The composition of the medium used in pre-inoculation and inoculation

Compound	Mass / volume ratio (g/L)
Malt extract	0.60
Yeast extract	0.12
Glucose	0.60
Maltose	0.60

Source: (TURLO *et al.* 2012; FERRARI, 2018; MOREIRA, 2018)

Table 3.3 – Composition of the medium used in fermentation

Compound	Mass / volume ratio (g/L)
Coconut oil	3.00
Soy peptone	3.00
Corn liquor	0.50
MgSO ₄ ·7H ₂ O	0.05
KH ₂ PO ₄	0.20
K ₂ HPO ₄	0.40
CaCO ₃	0.30
(NH ₄) ₂ SO ₄	0.50

Source: (TURLO *et al.* 2012; FERRARI, 2018; MOREIRA, 2018)

3.1.4 Apparatus used for fermentation

The apparatus used in the fermentation operation is the same of Ferrari (2018), as shown in Figure 3.1. The system consists of a magnetic stirrer (Fisatom, model 753), Thermo Scientific Phoenix II C25P recirculating bath, 2 L Shott bottle (136x265 mm), nylon tube (4 mm internal diameter; 6 mm external diameter), triangular magnetic bar (10x10x25 mm from Fitasom brand), and silicone hose. In this Dissertation, the triangular magnetic bar was used instead of the smooth magnetic bar in order to improve agitation.

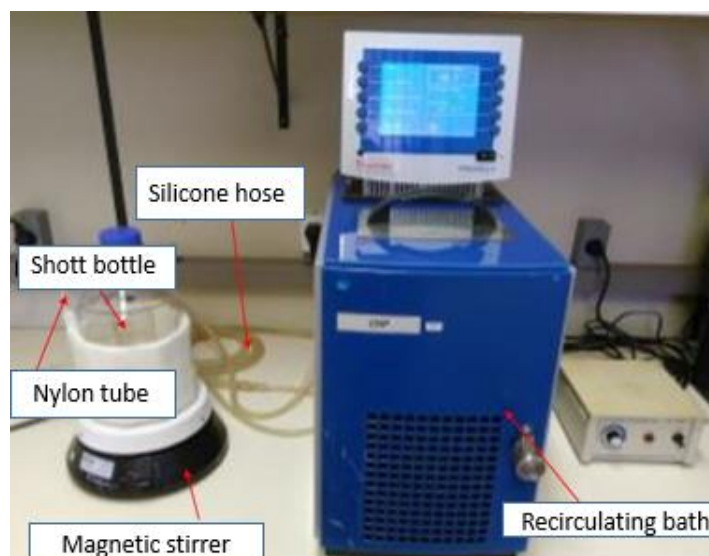


Figure 3.1 – Apparatus used in the fermentation process (FERRARI, 2018)

3.1.5 Chromatography

The High-Performance Liquid Chromatograph (HPLC) (Shimadzu) was used to separate, identify and quantify the tacrolimus produced by fermentation via *Streptomyces tsukubaensis*. The equipment has the following components: pump (LC-20AT), a UV-Vis detector (SPD-20A) and a controller board (CBM-20A). In addition, the set also has a thermostatic bath (Quimis, Q-2142M model) to maintain operation at 60 °C. The tacrolimus pattern CAS 109581-93-3, purity $\geq 98\%$, Sigma-Aldrich) was gently provided by prof. Paulo César Pires Rosa (School of Pharmaceutic Sciences/UNICAMP).

3.1.6 Protein quantification

For the quantification of proteins, the Bradford method was applied according to Kruger (2002). Reagents NaOH (1N) and Bradford were used, vortex and UV-vis spectrophotometer equipment.

3.1.7 Quantification of reducing sugars

The Somogyi-Nelson method was applied to determinate of reducing sugars (NELSON, 1944). To perform this method, Somogyi-Nelson I and II reagents (SN-I and SN-II) must be prepared. The compounds used for preparation of the reagents SN-I and SN-II and their respective concentrations are shown in (Table 3.4) and (Table 3.5).

Table 3.4 - Compounds used for the preparation of the SN-I reagent

Compound	$\text{CuSO}_4 \cdot 5\text{H}_2\text{O}$	Na_2CO_3	NaHCO_3	$\text{KNaC}_4\text{H}_4\text{O}_6 \cdot 4\text{H}_2\text{O}$	Na_2SO_4
Concentration (g/L)	4.00	24.00	16.00	12.00	4.00

Table 3.5 - Compounds used for the preparation of SN-II reagent

Compound	$(\text{NH}_4)_6\text{MO}_7\text{O}_{24}$	H_2SO_4	Na_2HAsO_4
Concentration (g/L)	50.00	42.00	6.00

3.1.8 Determination of micelle concentration

The equipment used for the visualization of the micelles was the optical microscope (of the Nikon brand and model Alphaphot-2- YS2) and the Fuchs Rosenthal grid optic counting chamber (Figure 3.2). In addition, for the sample preparation step, test tube shaker, test tube rack, and 10 μL micropipette were used.

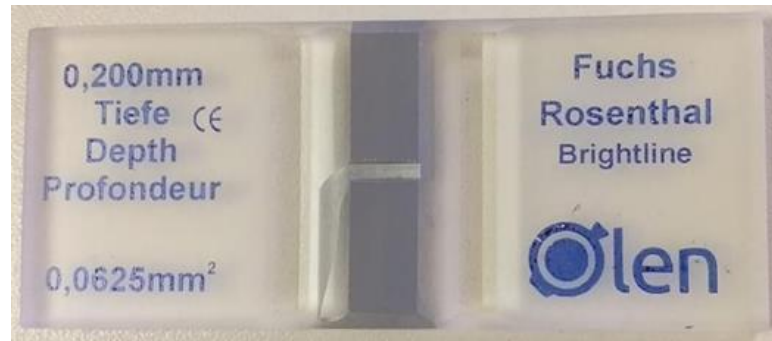


Figure 3.2 – Counting chamber Fuchs Rosenthal grid optic (Author, 2021)

The morphological analysis of the micelles in the fermented broth, with the objective of evaluating their appearance in the fermented broth, was performed by scanning electron microscopy (SEM), in the LEO 440i equipment.

3.1.9 Rheology

The samples of crude broth with acetone from the fermentation of *Streptomyces tsukubaensis* were analyzed. The equipment used was the AR 1500 ex rheometer as shown in Figure 3.3.



Figure 3.3 – AR 1500 rheometer ex. (Author, 2021).

3.1.10 Determination of density

The Dovel model pycnometer 100 mL was used to determinate the density of raw broth, while a 5 mL pycnometer was used to found the density of dried biomass (Figure 3.4).



Figure 3.4 – Pycnometer (Author, 2021).

3.2 Methods

3.2.1 Preparation of culture medium

Culture medium were prepared according to the list of components and their respective proportions shown in Table 3.1. All compounds were mixed and the pH adjusted to 7.2 with NaOH (2 mol/L) and AgCl (3 mol/L). Agar was added to this solution, heating was carried out until complete solubilization and followed by autoclaving for 20 min at 120 °C. After this period, the sterilized medium was poured into the Petri dishes until it reached 1 cm in height and the bacteria was inoculated with inoculation loop. Finally, the plates were sealed and kept for 10 days at 28 °C in an incubator for the development of microorganisms.

3.2.2 Preparation of pre-inoculum and inoculum

The compounds present in Table 3.2 in the respective proportions were solubilized in 4000 mL of distilled water and later taken for autoclaving at 120 °C for 20 min. After cooling, this solution (main solution) was used for pre-inoculation and inoculation.

To prepare the pre-inoculum, 510 mL of the main solution was transferred to three 1000 mL Erlenmeyer, one of which was used to control the process (to assess whether there is any contamination caused by other microorganisms). A bacterial loop was placed aseptically on the other two Erlenmeyer. The Erlenmeyer were placed in the orbital shaker (Shel Lab, USA) for 24 h, 110 rpm at 28 °C. After this period, 1 mL aliquot was removed

from each vial to assess bacterial growth by means of optical density (DO_{600}) in the UV-Vis Geneys-10 UV spectrophotometer, and the result should be equal to or greater than 0.6 in a length of 600 nm wave (MOREIRA, 2018). The Erlenmeyer with the highest optical density was chosen to continue the process of obtaining tacrolimus.

For the preparation of the inoculum, 810 mL of the main solution and 100 mL of the pre-inoculum were transferred to two 1000 mL Erlenmeyer and the third remained as process control without the addition of pre-inoculum. Subsequently, the Erlenmeyer were submitted to the shaker at 28 °C and 130 rpm for 24 h, and the optical density was measured keeping the same criteria described in the preparation of the pre-inoculum. The Erlenmeyer with the highest absorbance was used in the fermentation.

3.2.3 Fermentation

In this Dissertation, tacrolimus production was based on the works of Turlo *et al.* (2012), Ferrari (2018) and Moreira (2018). Fermentation was carried out for six days, 28°C and 130 rpm (MOREIRA, 2018). The compounds present in Table 3.3 and the respective proportions were solubilized in 2000 mL of distilled water and subsequently taken to the autoclaving at 120 °C for 20 min. After cooling, this solution was used as part of the fermentation liquid medium. The fermentation consisted of 1700 mL of the solution removed from autoclave and 340 mL of the inoculum. Every 24 hours, 5 mL of sample were collected from the reactor and additional 5 mL of acetone was added to interrupt the fermentation process through of bacterial cell lysis (TURLO *et al.*, 2012; MOREIRA, 2018). The collection of this sample, its processing and analysis on the HPLC were carried out to verify if the drug was being produced during fermentation. After collecting 10 mL of the culture broth, 10 mL of acetone was added to these samples in order to end the fermentation. The resulting content was filtered in pre-weighted filter paper (Whatman nº 1). The cells were washed with deionized water and kept at 80 °C for 24 h for drying.

3.2.4 Pressurized column microfiltration method

a) Description of microfiltration system

The filter built in this Dissertation consists of a pressurized stainless-steel column. Table 3.6 shows the chemical and biological information, and the average pore diameter and porosity for the different filter media used.

Table 3.6 – Technical information of the filter medium

Catalog number	Chemical information (type of material)	Biological information (wettability)	Pore size (μm)	Membrane thickness (μm)	Porosity (%)
GSWP01300 Merckmillipore	Mixed cellulose esters (MCE)	hydrophilic	0.22	150	75
SSWP02500 Merckmillipore	Mixed cellulose esters (MCE)	hydrophilic	3.00	150	83

The filtration system was pressurized with the aid of a compressor (SCHULZ[®] 7 bar capacity). The feed pressures applied during microfiltration were 1 and 2 bar, with permeate pressure equal atmospheric pressure of 0.95 bar. The simplified scheme of the operating system is shown in Figure 3.5, and Figure 3.6 shows some details of this equipment.

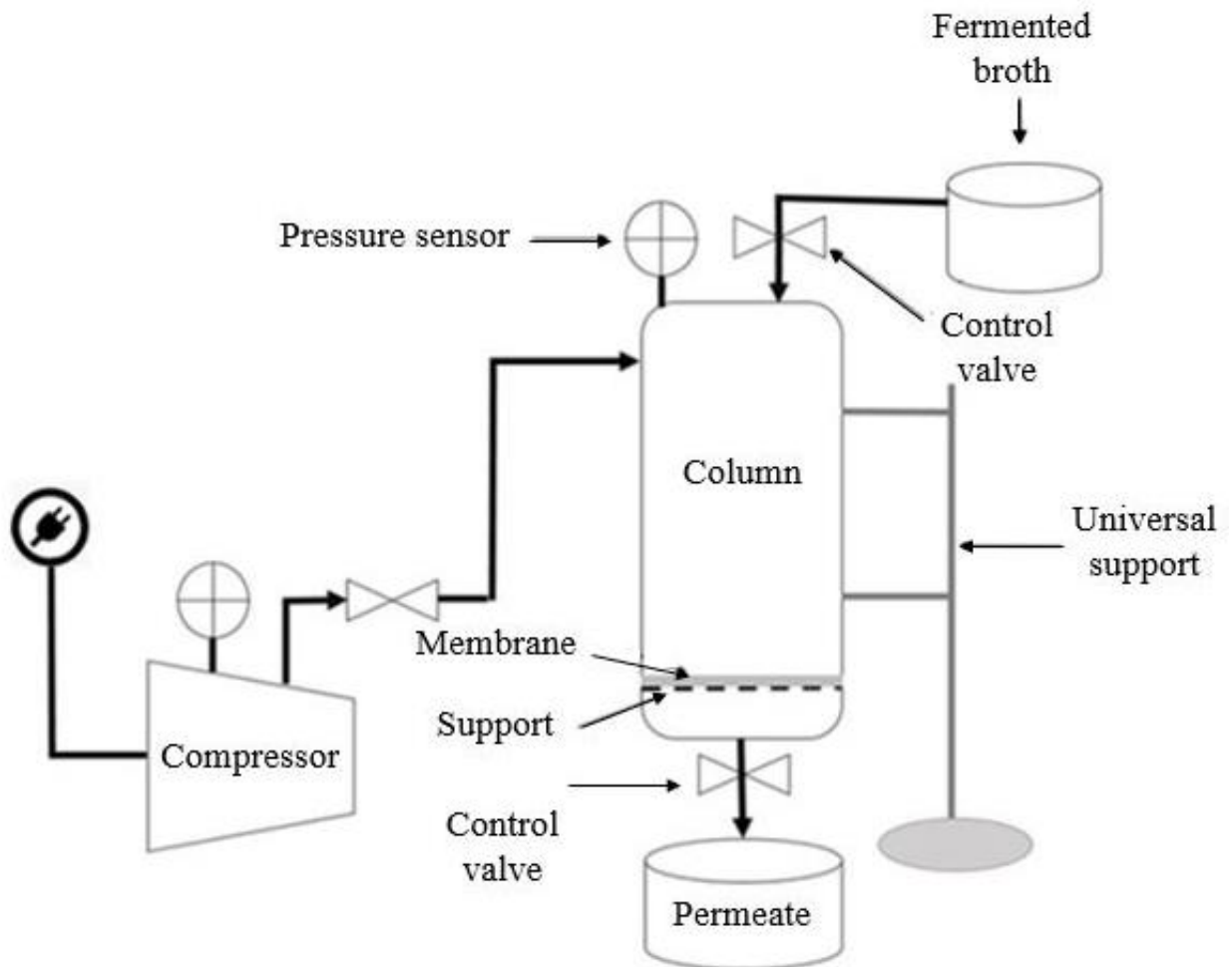


Figure 3.5 – Simplified scheme of the pressurized filter system (Author, 2021)



Figure 3.6 – Details of the filter used in microfiltration process (Author, 2021)

The pressurized filter was developed at LPTM. The filter consists of the following components: quick coupling, pressure sensor (Vika, 0 to 10 bar working pressure), sample receiving valve, pressure control valve, filtration column, permeate opening valve, and hose nozzle (Figure 3.7). The other components of filter system are: support, perforated plate, stainless-steel screen, membrane and Teflon ring. Some measurements verified with the pachymeter (DIGIMESS[®]) are shown in Table 3.7.

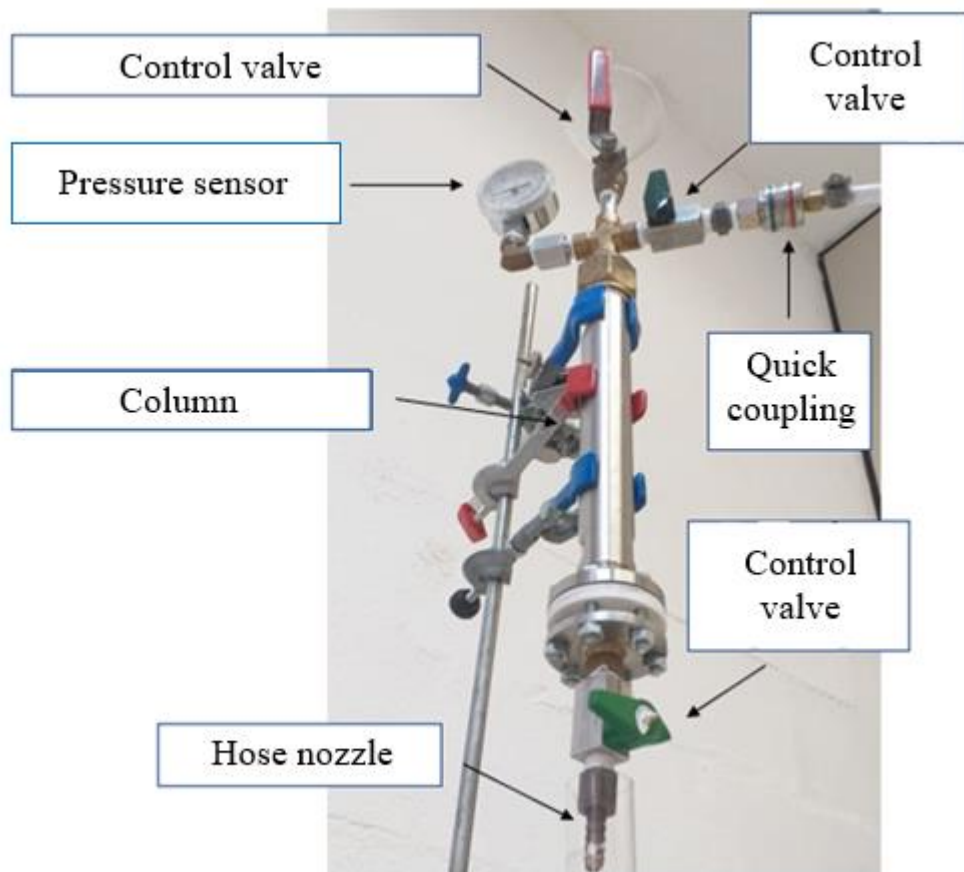


Figure 3.7 – Parts of the filtration system (Author, 2021)

Table 3.7 – Filter characteristics

Components	Measure (mm)
Filtration column outer diameter	30.5
Filtration column internal diameter	28.7
Lowered bed diameter	26.0
Perforated plate outer diameter	28.5
Perforated plate inner diameter	21.0

Source: (Author, 2021)

b) Pressurized column assembly

The procedure performed microfiltration on a pressurized column is identified in Figure 3.8. The filter set consists of adapting its components, which are: flange, perforated plate, stainless-steel screen and membrane (Figure 3.8 – 1 and 2). The filter is placed in the 45 cm clamp holder.



Figure 3.8 - Procedure applied to carry out filtration in a pressurized column (Author, 2021)

c) Air supply

The compressor was turned on to store air (Figure 3.8 – 3), then its hose was connected to the quick coupling of the filter (Figure 3.8 – 4), with all the filter valves closed to check if the filter had any air leakage. Then, the filter pressure control valve was closed (Figure 3.8 – 5), and the compressor air valve was opened (Figure 3.8 – 3). The air supply stage was performed in the presence of only the support, perforated plate, and stainless-steel screen. With the valve that controls the permeate outlet closed (Figure 3.8 – 6), 30 mL of filtered water was inserted into the top of the filter through the sample receiving valve and with the aid of a funnel (Figure 3.8 – 6). The choice of the 30 mL volume was due to the expectation of guaranteeing the Darcynian flow. The sample receiving valve was closed (Figure 3.8 – 7) and the pressure controller valve opened (Figure 3.8 – 5) allowing the microfiltration chamber to pressurize. The permeate obtaining valve was opened (Figure 3.8 – 6). Also, care was taken that at each insertion of filtered water through the upper part of the filter, the air supply valve/pressure controller closed. (Figure 3.8 – 5), preventing liquid from entering in the compressor and loss of pressure in the line. This procedure was performed several times until the pressure of the compressor hose remained constant. This can be verified when the pressure manometer needle (Figure 3.8 – 8) on the top of the filter does not vary from the desired pressure while it is occurring in the process of obtaining permeate.

d) Bifiltration of water

To carry out the compaction tests, water from the filter (IBBL[®]) was collected. The filter was assembled and the 0.22 μm pore diameter membrane was inserted in the microfiltration support and the equipment was placed on the bench again and attached to the hose. The pressure control valve (Figure 3.8 – 5) and permeate opening valve were closed (Figure 3.8 – 6), and filtered water was inserted into the top of the filter (Figure 3.8 – 7). The microfiltration column was pressurized at 1 bar and a first water pass was made. The filtrate was recirculated two more times.

e) Membrane compaction

The filter was removed from the bench, as well as the air supply hose of the compressor was disconnected (Figure 3.8 – 4), and the compressor valve turned off (Figure 3.8 – 3) in order not to depressurize the supply line. The filter was disassembled for insertion of the membrane in the microfiltration support and placed back on the bench and attached to the hose (Figure 3.8 – 4). The pressure control valve (Figure 3.8 – 5) and the permeate valve were closed (Figure 3.8 – 6), and the bifiltered water sample was inserted on top of the equipment (Figure 3.8 – 7). The microfiltration column was pressurized, and the membrane compacted, collecting water at the permeate outlet (Figure 3.8 - 6). Then, the pressure control valve (Figure 3.8 - 5) as well as the permeate valve (Figure 3.8 - 6) were closed, while the sample receiving valve (Figure 3.8 - 7) was opened. This compacting step is necessary for the thickening of the membrane and presenting less porosity and mass flow.

It is important to point that the half-valve adjustment was chosen due to previous tests, where better permeate flow controls were obtained. With the valve fully open and applying a pressure of 2 bar, it was not possible to accurately measure the change in the permeate volume over time, as the permeate reached the bottom of the beaker at high speed and completed it quickly.

f) Sample microfiltration

Microfiltration tests were carried out using the broth fermented from coconuts as carbon source at 26 °C. Before such tests, the density from the pycnometer was determined. The volume of 30 mL of broth was chosen in such a way as to verify that the flow model follows Darcy's law. The operating supply pressure (1 and 2 bar) was chosen. Microfiltration was initiated, accompanying it by filming the volume of permeate collected in

a beaker over time. After the first microfiltration, a sample of 500 μL of the permeate was collected for further analysis of the rejection. The rest of the permeate was returned to the filter (Figure 3.8 - 7). This was followed by nine more passages, totaling 10 microfiltration steps. For each step that permeate was fed, the pressure control valve was closed to prevent the broth fermented goes to compressor. Due to the medium contains tacrolimus in each run, the membranes were not reused.

g) Drying of biomass

After disassembling the filter, the screen and membrane with the biomass from the microfiltration process were weighed and taken to the drying oven at 60 $^{\circ}\text{C}$ for 24 h (MOREIRA, 2018), Figure 3.9. After drying, the screen and membrane with the biomass were weighed and the screen were placed for 20 min in HCl (1N) to clean its screen and the membrane with the heavy biomass was stored in another container.



Figure 3.9 – Drying oven utilized by biomass contend (Author, 2021)

3.2.5 Quantification of tacrolimus and its specific production

In order to obtain the tacrolimus production along the fermentative process, 10 mL of the culture broth were collected each 24h. After collecting 10 mL of the culture broth, 10 mL of acetone was added to these samples in order to end the fermentation. The resulting content was filtered in pre-weighted filter paper (Whatman n° 1) in a vacuum filter. The cells were washed with deionized water and kept at 60 °C for 24 h for drying. In this case, it was possible to know the biomass production along time, and the tacrolimus specific production is defined by the rate of its production (in mg/L) by biomass production (in g/L). The quantification of tacrolimus was done from following steps: the filtrate was evaporated (from the microfiltration process) on rotary evaporator (Fitasom, model 80) until the presence of a dark liquid. To this dark material, 5 mL of organic acetonitrile solvent and 1 mL of deionized water were added. Finally, the sample was centrifuged (Hettich, model 420 R) and 20 μ L of supernatant was injected on HPLC, to check the separation and retention time from chromatogram, such as that one presented in Figure 3.10. The mobile phase applied on the HPLC was a mixture of acetonitrile and deionized water in a ratio of 70:30 (v:v) and the stationary phase was octadecylsilane (C18), packed in a Thermo Quest Hyperbond column (300 x 3.9 mm).

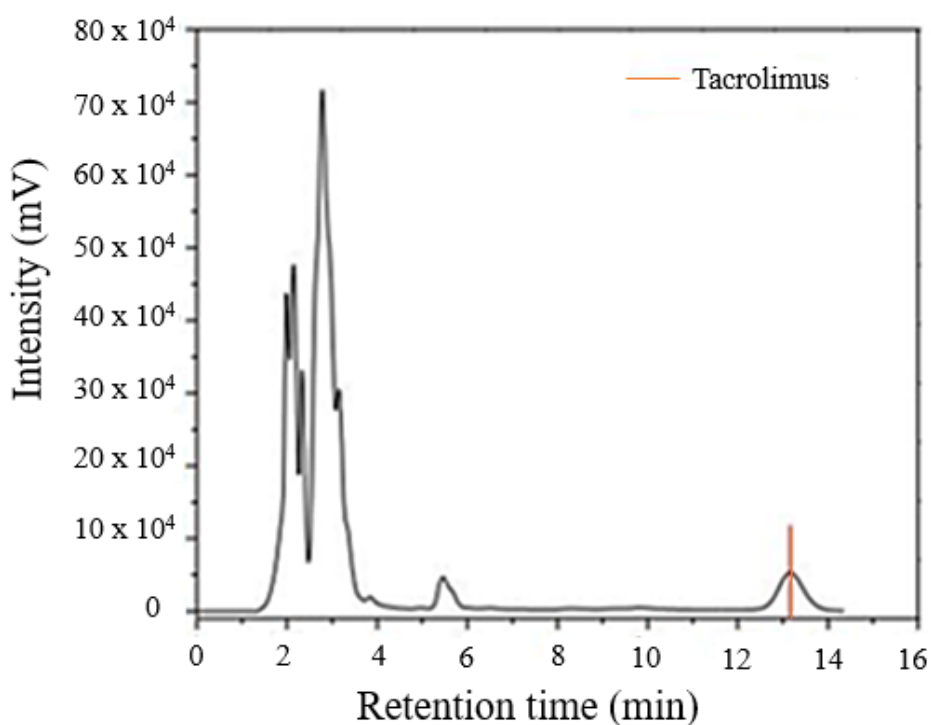


Figure 3.10 – Fermentation sample by *S. tsukubaensis* for the production of tacrolimus (Adapted from MOREIRA, 2018)

The concentration of the supernatant resulting from chromatographic analysis was converted to sample concentration according to Equation 3.1.

$$C_{\text{sample}} = \frac{C_{\text{supernatant}} \times V_{\text{supernatant}}}{V_{\text{sample}}} \quad (3.1)$$

where sample and supernatant concentrations are given in mg/L and volume in L. The calibration curve for the quantification of tacrolimus was constructed in accordance with the regulations of the Ministry of Agriculture, Livestock and Supply (MAPA). The previously defined concentrations were 30, 60, 90, 120 and 150 mg/L. The obtained curve is represented in Figure 3.11, with its determination coefficient equal 0.9999. The straight line equation for this curve was

$$y = 7.00 \times 10^{-5} x - 0.59 \quad (3.2)$$

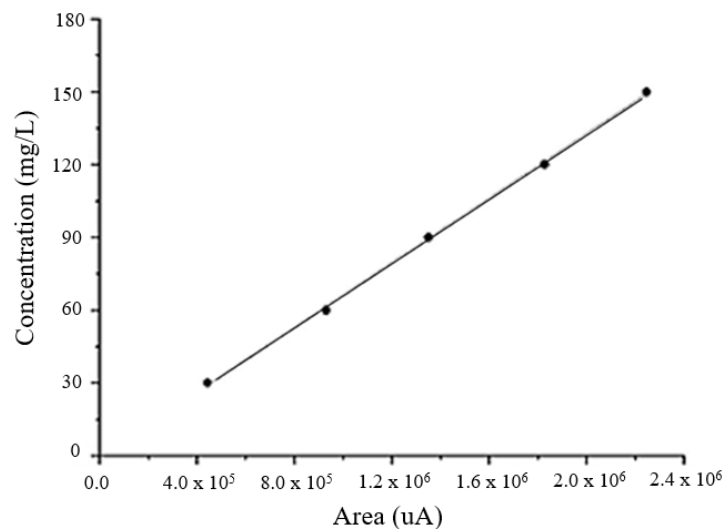


Figure 3.11 – Tacrolimus calibration curve (Author, 2021)

3.2.6 Protein quantification

For the quantification of proteins, the Bradford method was applied according to Kruger (2002). First, 100 μL of the sample was pipetted into test tubes. Subsequently, 100 μL of NaOH (1N) and 2.5 mL of Bradford's reagent were added in the samples. The mixtures were agitated in a vortex mixer during for 20 min. Finally, the absorbance of each sample were read on the UV-Vis spectrophotometer at wavelength of 595 nm. The Bradford method

calibration curve was made from standard bovine albumin solution. The previously defined concentrations were 6.25, 12.5, 25, 50 and 100 mg/L. Its determination coefficient was 0.9687 (Figure 3.12) and the resulting is given by

$$y = 591.09x + 1.74 \quad (3.3)$$

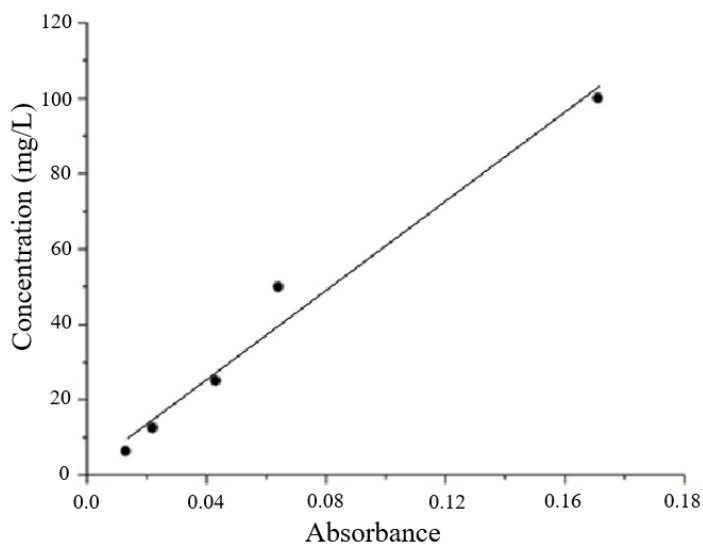


Figure 3.12 – Protein calibration curve (Author, 2021)

3.2.7 Quantification of fermentable sugars

For the preparation of the SN-I reagent (Smogyi-Nelson's reagent type I), the compounds in Table 3.4 were solubilized in 1000 mL of distilled water. This solution remained for one day at rest without light. The solution was filtered on INLAB type 10 filter paper, 3.00 μm pore diameter, with aid of a vacuum pump, and stored in amber flask. The SN-II reagent was produced by mixing solutions A and B. The preparation of solution A consists of dissolving 50 g of $(\text{NH}_4)_6\text{MO}_7\text{O}_{24}$ in 900 mL of distilled water. 42 mL concentrated H_2SO_4 was added slowly to this solution. Solution B was prepared by dissolving 6 g of Na_2HAsO_4 in 50 mL of distilled water. Finally, solutions A and B were mixed and left to stand for one day at 37°C.

With the SN-I and SN-II reagents ready, the Somogyi-Nelson method was started. First, 1 mL of the sample was collected during fermentation, and after added 2 mL of SN-I reagent. The samples were agitated in a vortex mixer laboratory, heated in water bath for 6 min and cooled in ice bath for 5 min. 2 mL of the SN-II reagent were added to each test tube, which was agitated and left to stand for 5 min. Finally, 25 mL of distilled water were added to the samples, and the absorbance were read on a UV-Vis spectrophotometer with a

wavelength of 540 nm. The test was performed in duplicate. The previously defined concentrations were 50, 100, 200, 300, 400 and 500 mg/L. The calibration curve of the Somogyi-Nelson method (Figure 3.13) was made from a standard glucose solution with a determination coefficient equal to 0.9982 and the resulting is given by

$$y = 673.17x - 0.84 \quad (3.4)$$

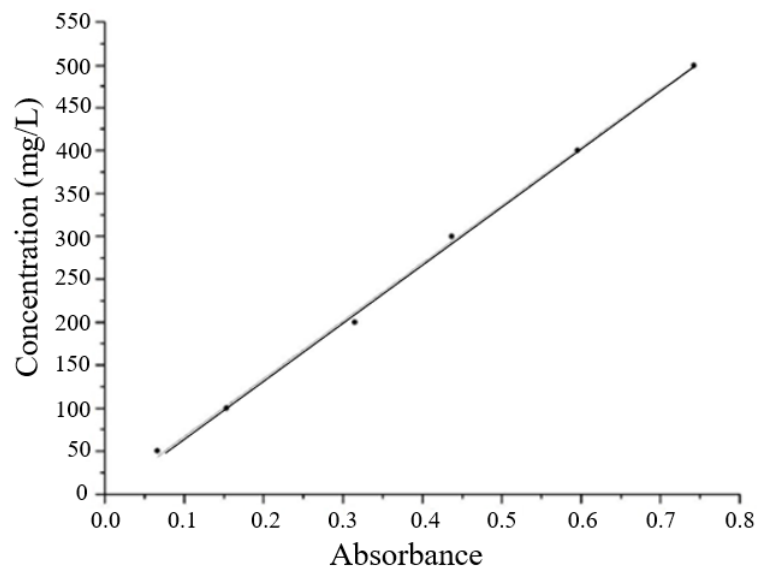


Figure 3.13 - Calibration curve for reducing sugars (Author, 2021)

3.2.8 Determination of micelle concentration

This Dissertation presents an alternative technique to obtain the concentration of micelles as number of micelles /sample volume, obtained by Fuchs Rosenthal grid optic, as function of absorbance from spectroscopy. The spectroscopic analysis was performed on a spectrophotometer (NanoPhotometer UV/VIS, IMPLEN), whose wavelength is between 200-950 nm. Four previous tests were carried out with the sample to determine the wavelength range, respecting the wavelength range of equipment, considering that the biomolecule of interest, tacrolimus, is detected at 210 nm. Also, the concentration of proteins founded in the fermented broth, form part of the micelles, corroborating the study by SILVA *et al.* (2019). In the literature, like the study by Noble (2014), the quantification of proteins is through absorption in the ultraviolet, which is based on the fact that proteins present absorption in the region of 280 nm and below 220 nm, the first due to the presence of amino acids in their constitution and the second due to the peptide bond present in them. The objective is to identify at which wavelength the maximum absorbance between 0 and 1 is obtained.

Wavelengths equal to 200, 250, 300 and 350 nm were evaluated, resulting in absorbance values equal to 0.107; 0.444; 1.207 and 1.651, respectively. The chosen wavelength range was 200 up to 300 nm, with an interval of 10 nm, the absorbance was read in this scanning range. Subsequently, sample dilutions and absorbance measurements were made for each diluted sample. The original sample of raw broth from coconuts as carbon source was diluted until the absorbance was zero, indicating the absence of micelles, thus presenting only acetone (Absorbance = 0 $\equiv \lambda_{\text{ultraviolet}} = 330 \text{ nm}$). The prepared dilutions were 10, 15, 20, 25, 30, 35, 40, 45 and 50 times. The original sample, at each dilution, was homogenized on a magnetic stirrer bar (Fisatom, model 752A) at 25 rpm. The tests were performed in triplicate. It should be noted that, for each fermented broth analyzed, it is necessary to perform a new procedure. In other words, the results to be presented here refer to specific fermentation conditions of this work.

Micelles counting was carried out with the aid of the Nikon optical microscope (Model Alphaphot - 2 - YS2) and the Fuchs Rosenthal grid optic. micelles are composed of hydrophobic and hydrophilic components. The micelles can be spherical, ellipsoid, cylindrical or unilamellar nanodimensional structures (HANAFY *et al.*, 2018). In this case, the micelles are aggregates of molecules present in the fermentation medium, such as proteins, sugars, lipids, microbial biomass etc. (SILVA *et al.*, 2019; MOREIRA *et al.*, 2020). The protocol used for counting micelles in the five grid blocks of the Fuchs Rosenthal grid optic was based on the study by Butler and Spearman (2007) with modifications. In the present study, trypan blue solution 0.4% was not used as mentioned by Butler and Spearman (2007), since the aim of the alternative technique is not to distinguish viable cells. In addition, Butler and Spearman (2007) used volume of 5 x 0.1 μL for counting, while the present technique, due to the differences in the measurements of the Fuchs Rosenthal grid optic with these researchers, it was applied 5 x 3.2 μL . Micelles were counted from broth fermented with acetone (50:50 v/v), where the acetone is placed to stop fermentation), and for each dilution prepared from this fermented broth. The crude sample aliquot was placed on the grid by touching the end of a capillary tube of the Pasteur pipet, so the sample flowed between the coverslip and the counting chamber. The chamber was positioned on the adjustable stage of the optical microscope and waited 2 min for the micelles to settle, then the microscope was focused. The procedure for handling and focusing the microscope was based on (MURPHY, 2001). The 10x objective was used to count the micelles. In addition, the micelles that were in upper and left limits were counted, unlike the micelles that touched the lower and right limits, which

were not taken into account, according to the protocol. Due to the high concentration of micelles in the original sample of the fermented broth and at low dilutions, the zigzag counting technique was adopted, avoiding errors in determining the number of micelles (BUTLER and SPEARMAN, 2007). The counting chamber of the present study has 16 squares in each grid block, each with 1 mm² of area and depth of the chamber equal 0.2 mm. Considering the transformation of the unit from mm³ to mL, and the volume of each grid block of the chamber equal 3.2 mm³, the micelles counting over each of the five grid blocks were made according to:

$$\frac{(\text{n}^{\circ} \text{ of micelles})}{\text{mL}} = \frac{(\text{n}^{\circ} \text{ of micelles counted in the mesh})}{3.2} \times 10^3 \quad (3.5)$$

Before the morphological analysis of the fermented broth micelles, the sample was preprocessed. Initially, the biomass retained in the filter papers (filter medium) with biomass were washed with deionized water and kept at 80 °C for 24 hours for drying (drying oven model 315 SE) (SILVA *et al.*, 2019). The dry biomass was inserted into the desiccator for 24 hours and taken inside a closed box for the SEM (Scanning Electron Microscopy) analysis. The first stage of the SEM consisted of cutting two regions of the filter paper with scissors, small maceration in the sample, and fixing it on the sample holder with double-sided carbon adhesive tape. Afterwards, the samples were metalized with gold and taken to SEM. The magnification performed were 20, 2000, 5000, 10000 and 20000 x. Coating samples with gold is necessary, as samples may have insulating characteristics and tend to accumulate electrical charge, causing unwanted artifacts in the image. Gold improves the emission level of electrons and ground charges (WOLLMAN *et al.*, 1993).

3.2.9 Rheology

The sample of the broth fermented from coconut oil as carbon source with acetone remained preserved in the refrigerator (temperature of 4 °C) and 25 mL were collected for rheological analysis. The sample was stirred for 1 min, at 25 rpm, to homogenize the broth and packed in a polystyrene box with ice. 12 mL of sample was placed in the rheometer for rheological testing. For this purpose, the TA Instruments AR1500ex concentric cylinder viscometer was used. The range of the deformation rate was defined from 0 to 150 s⁻¹, based on the work of Gabas *et al.* (2012), who evaluated the rheological behavior of ten solutions composed of sucrose, ethanol, yeast cells and water.

3.2.10 Density

The density of certain sample (raw broth or biomass) was calculated by

$$\rho = \frac{m_a - m_v}{V_t} \quad (3.6)$$

with

ρ is the density in g/mL.

m_a – mass of the pycnometer with the sample, g.

m_v – mass of the empty pycnometer, g.

V_t – total sample volume, mL.

CHAPTER 4

4. RESULTS AND DISCUSSION

This chapter presents the results of the microfiltration of fermented broth using glucose and coconut oil as a carbon source. In addition, the results of the concentration of micelles in raw and permeated broth, showing an alternative technique for obtaining the concentration of micelles in number of micelles/volume of sample, obtained by Fuchs Rosenthal optical grid counting chamber as function of absorbance. Finally, the contextualization of the importance of hope as an essential element in the chemical project to obtain tacrolimus is presented.

4.1 Tacrolimus, biomass and specific production

Glucose and coconut oil were tested as main sources of carbon in tacrolimus production by *S. tsukubaensis* strain. Figures 4.1 and 4.2 show the tacrolimus production, the concentration of biomass, and the specific production of the drug that is the ratio between the production of the drug (mg/L) by concentration of biomass (g/L) using the two fermentative media. The highest concentration of the drug using coconut oil as carbon source occurred at 96 hours, and presented 31.35 mg/L (Figure 4.1). In case of glucose as carbon source, the tacrolimus highest concentration occurred at 120 hours, with 22.88 mg/L (Figure 4.2). The maximum tacrolimus production from *S. tsukubaensis* fermentation, found in Literature, reports time between 96 and 192 hours (LI *et al.*, 2019; MOREIRA *et al.*, 2020). The biomass production from fermentation with coconut oil in 96 hours was equal to 18.60 g/L, while using glucose, in 120 hours, was 12.14 g/L. Figure 4.2 shows that the tacrolimus specific production was 1.69 mg/g, while in Figure 4.1, this value is 1.88 mg/g, showing the best performance of coconut oil, as carbon source, compared with glucose. Martínez-Castro *et al.* (2013), using the combination of starch and glucose as carbon source, obtained specific production of tacrolimus around 2.8 mg/g, however the C:N ratio was not disclosed. In the present study, it was not possible to determine the C:N ratio for coconut oil, because both

chemical elements are inserted in a complex medium. Mishra and Verma (2012) testing only the fermentation medium with glucose as the primary carbon source resulted in a specific production of 8.70 mg/g. However, pH and temperature conditions and pre-inoculum and inoculum medium were different from the present dissertation, as well as these authors used a *Streptomyces tsukubaensis* mutant. Moreira *et al.* (2020) showed that agitation is also an important variable in the batch fermentation process, and may be the cause of the difference between specific productivities among researchers. Martínez-Castro *et al.* (2013) used 220 rpm and Mishra and Verma (2012), 200 rpm, values different from the present Dissertation that applied 130 rpm.

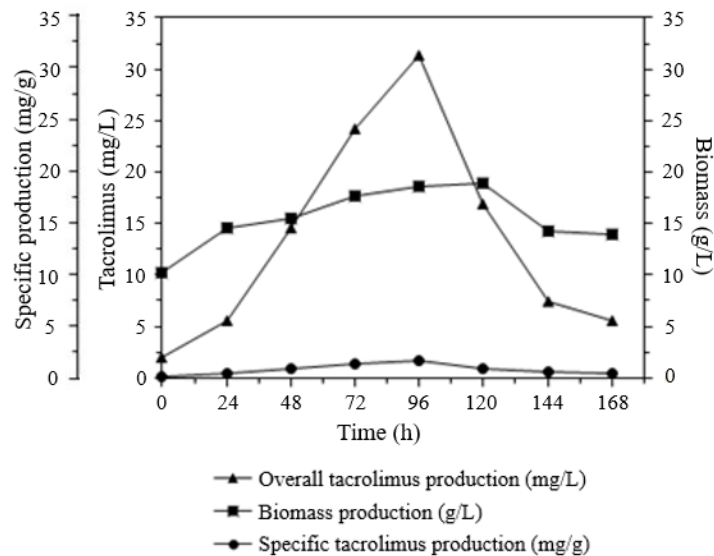


Figure 4.1 - Tacrolimus production for 168 h using coconut oil as carbon source (Author, 2021)

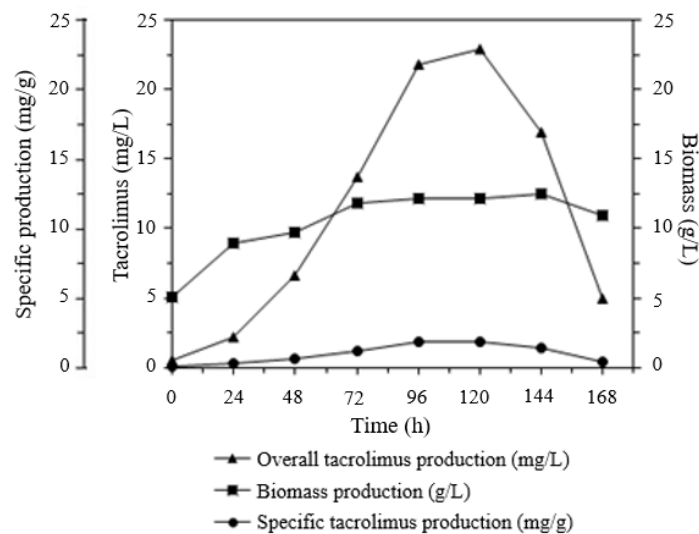


Figure 4.2 - Tacrolimus production for 168 h using glucose as carbon source (Author, 2021)

Coconut oil is mainly composed of saturated fatty acids (92 %), such as lauric acid, which about 64 % corresponding to medium chain fatty acids (MCFA) with a number of carbons ranging from 8 up to 12. MCFAs are used by cells as an energy source. The coconut oil consists in lesser amounts of monounsaturated and polyunsaturated fatty acids (LIMA and BLOCK, 2019). Glucose is a great source of carbon for bacterial growth, however, large amounts can affect negatively the production of secondary metabolites such as tacrolimus (DEMAIN, 1976; POSHEKHONTSEVA *et al.*, 2019). This effect is characteristic of mechanism known as carbon catabolic repression (CCR), that consists in systems that suppress genes involved in the use of alternative sugars, when they are in a medium that has sugars of preferential use such as glucose (LI *et al.*, 2020). According to Moreira *et al.* (2020), the increase in glucose in the fermentation media, in the C:N ratio from 3% to 4%, did not interfere greatly in the cell growth of *Streptomyces tsukubaensis*.

In addition, coconut oil also has a high concentration of bioactive compounds as vitamin E, sterols, and polyphenols (GAO *et al.*, 2020). Vitamin E comprises eight compounds found in nature, four of them are tocopherols (α -, β -, γ -, δ -tocopherol) and others, tocotrienols (α -, β -, γ -, δ -tocotrienol). The most common and biologically active of these vitamin E isomers is α -tocopherol (C₂₉H₅₀O₂). In α -tocopherol structure, there is a saturated chain, a phenol and ether group (FAIRUS *et al.*, 2019). Vitamins are one of the most important micronutrients in the biological metabolism including growth, development, and maintenance. The biological role of vitamin E is principally based on its antioxidant properties, as a prevention of lipid peroxidation. The cells are constantly exposed to free radicals that can cause oxidative stress and induce damage to biological structures (PATEL, 2020).

4.2 Fermentable sugars and proteins

The evaluation of these fermentable sugars and proteins is important since they are present in the fermented broth and influence the future purification of the drug. It is reported in the Literature that the proteins amount increases during tacrolimus biosynthesis. They are produced and consumed during fermentation (WANG *et al.*, 2017; SILVA *et al.* 2019). The concentration profile of proteins produced in the two-fermentation media is shown in Figure 4.3. In the present Dissertation, the rate of protein production was higher than the rate of its consumption. At the beginning of the fermentation with coconut oil, the protein concentration in the culture medium was 91.07 mg/L, whereas the fermentation with glucose

equal to 105.17 mg/L. This is explained by the physicochemical characteristics of the corn steep liquor used in the fermentation medium. According to Achal *et al.* (2010), corn steep liquor is composed of 24 % protein and several amino acids, such as arginine (0.4 %), cysteine (0.5 %), glycine (1.1 %), histidine (0.3 %), isoleucine (0.3 %), isoleucine (0.9 %), methionine (0.5 %) etc. In addition, these amino acids may have formed more proteins, and this explains the differences in initial protein concentrations in the two fermentations media.

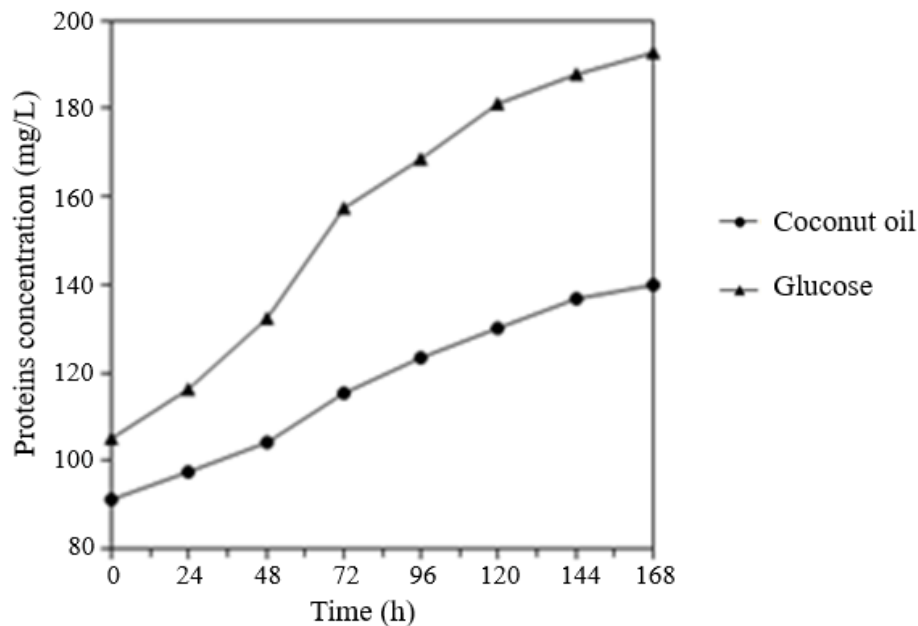


Figure 4.3 - Proteins concentration along the fermentation process using glucose and coconut oil as carbon source (Author, 2021)

Figure 4.4 shows the profile of the sugar concentration consumed in two fermentation media. The initial concentration of sugars with coconut oil and glucose, were respectively 567.59 mg/L and 507.33 mg/L. The sugar concentration in 120 hours for the medium with glucose was 181.16 mg/L, and for coconut oil in 96 hours 123.33 mg/L. The most pronounced increase in protein production in both fermentations was between 72 and 144 hours. The fermentation with glucose consumed an amount of sugar of 308.69 mg/L and with coconut oil 271.23 mg/L (Figure 4.4). Glucose was consumed more easily compared to coconut oil, because this monosaccharide is a fast source of assimilation by the bacteria and is used for the production of cells (POSHEKHONTSEVA *et al.*, 2019).

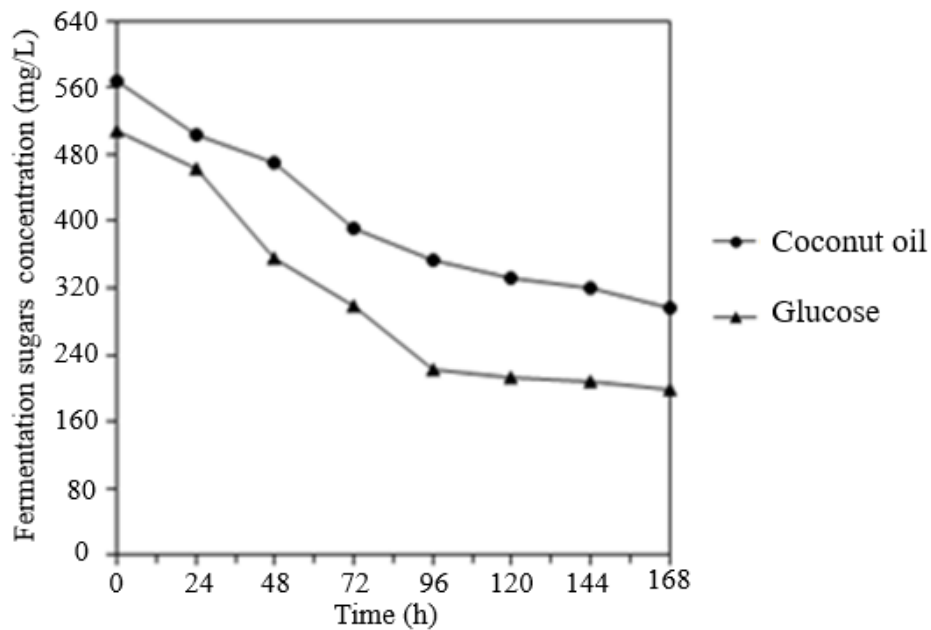


Figure 4.4 - Fermentable sugars concentration along the fermentation process using glucose and coconut oil as carbon source (Author, 2021)

The medium using coconut oil showed the highest amount of reducing sugars in 168 hours. This is due to the complexity of coconut oil, which makes it difficult for the bacteria to assimilate nutrients. In general, a large amount of sugar was consumed in the first 72 hours in both fermentation media, corresponding to the exponential phase of bacterial growth. According to Bertrand (2019), during the exponential phase all cells grow, and they are dependent on the amount of nutrients present in the medium. It is the better period for cell growth, influenced by culture conditions and genetic characteristics. According to Hwang *et al.* (2014), the production of secondary metabolites is due to the stress of the bacteria in consequence of nutrients lack.

4.3 Determination of micelles concentration

One of the results of the present Dissertation refers to proposition and performance of alternative approach to determinate the micelle concentration. As presented in Chapter 2, the first stage of processing, after fermentation, is associated with the separation of the micelles. The microfiltration was used to separate the micelles to identify the performance of the filter. The micelles concentration were determined in the broth submitted to microfiltration as well as in the permeate.

In the wavelength range determined between 200 and 300 nm, the maximum absorbance, considering it less than 1, was equal to 0.979 at 280 nm. Therefore, all dilutions were read at a wavelength of 280 nm. The graph relating the number of micelles/mL vs absorbance is shown in Figure 4.5. Thus, through the analytical curve, other samples of the same fermented broth and more diluted (due to a filtration process, for example), can be inserted in the spectrophotometer to read the absorbance, and later obtain the number of micelles /sample volume by the Equation 4.1, and without using the Fuchs Rosenthal grid optic again. The data revealed a straight line with determination coefficient of 0.995, in the form

$$y = 894.36 + 49503.00x \quad (4.1)$$

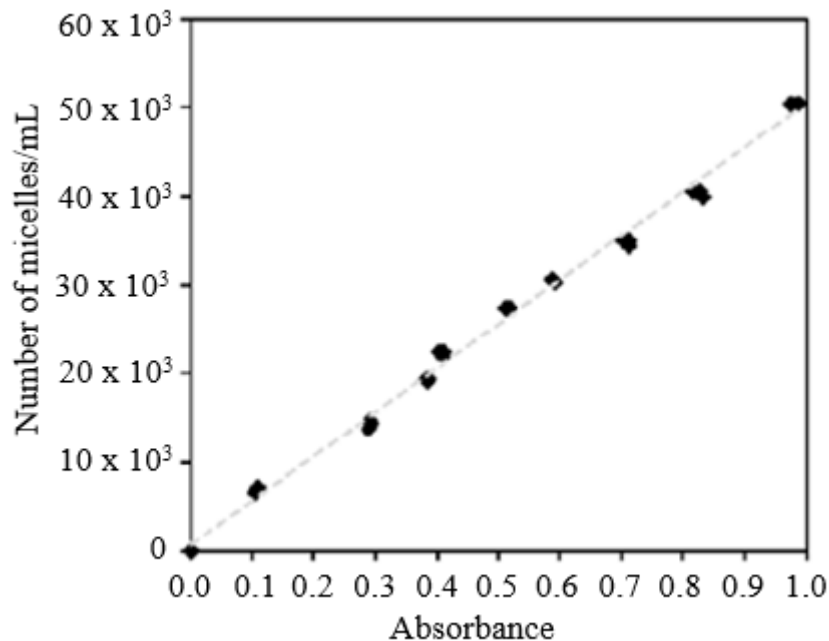


Figure 4.5 - Determination of micelles concentration from absorbance (Author, 2021)

Figure 4.6 shows the grid blocks of the Fuchs Rosenthal grid optic during focusing the microscope for reading the samples. Figures 4.6a and 4.6b show the micelles of the fermented broth (without dilution). The number of micelles were counted in the 10x objective (right column), because it is possible to visualize an entire grid block with good quality and distinguish one micelle from the other, in contrast to the 4x objective (left

column). Figures 4.6c and Figure 4.6d show the micelles of the fermented broth diluted 50 times.

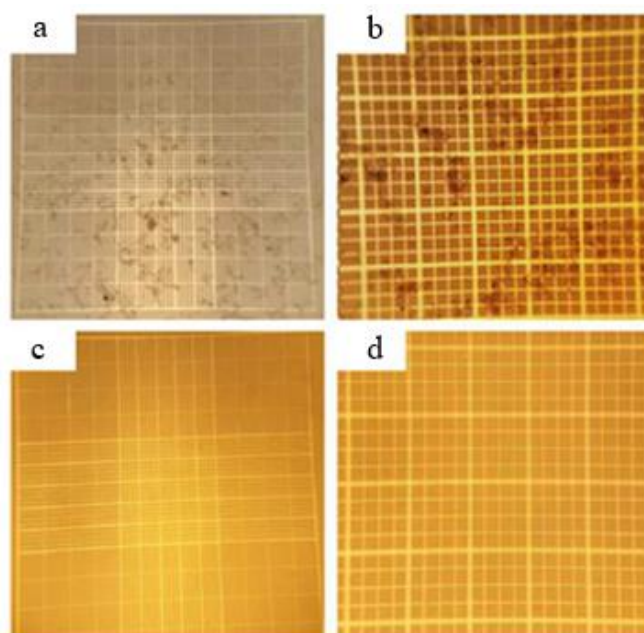


Figure 4.6 - Observation of micelles in the optical microscope (a) fermented broth: 4 x objective; (b) fermented broth:10 x objective; (c) fermented broth diluted 50 times: 4 x objective; (d) fermented broth diluted 50 times: 10 x objective (Author, 2021)

In this dilution the sample is absent from micelles. In the case of filtration, this represents total retention of micelles by the filter medium (MAO, 2016). In the analysis of the morphology of the micelles from fermented broth, via SEM, images were captured with micrometric dimensions, 1 and 3 μm , as shown in Figures 4.7 and 4.8. In Figure 4.7, the micelles are circled in red and behind, the most uniform surface, are like cellulose fibers of the filter paper. In Figure 4.7, a 5000x magnification was used. Figure 4.8 shows the aggregate of compounds that characterize the micelles at a magnification of 10000x. The microstructures around the micelle may have come from the maceration process during the analysis.

There are instruments for counting particles, however they have high cost, causing the search for cheaper alternatives, made by counting particles through the Fuchs Rosenthal grid optic. Such method, despite its low cost, proves tedious and demands time from the user, especially when used continuously. This Dissertation offers alternative technique that associates the counting of particles through the Fuchs Rosenthal grid optic with the spectroscopy technique, providing a substantial reduction in the analysis time to obtain the concentration of micelles, mainly for samples considerably more diluted than the original sample.

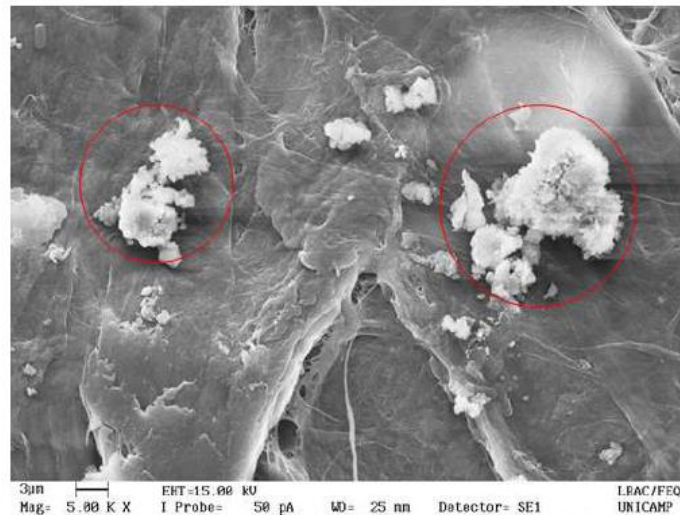


Figure 4.7 - Micelles from fermented broth with a micrometric dimension of 3 μm and a magnification of 5000x (Author, 2021)

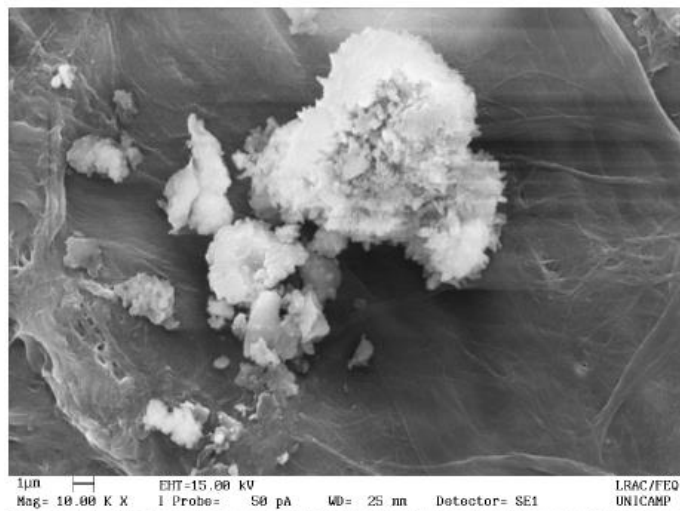


Figure 4.8 - Micelles from fermented broth with micrometric dimension of 1 μm and magnification of 10000x (Author, 2021)

To highlight the importance of this alternative technique is presented the Figure 4.9 Initially, someone chooses an appropriate wavelength for the analysis of his sample. In the second stage, there is the counting of micelles from fermented broth (without dilution), and after the dilutions from the original sample in the Fuchs Rosenthal grid optic. With the same samples, perform the absorbance reading on the spectrophotometer. With data on the number of micelles/sample volume vs absorbance, the analytical curve is constructed. From this stage, it is not necessary to use the Fuchs Rosenthal grid optic to count sample micelles from the same original broth, because the spectrophotometer is already calibrated. Therefore, in step three the researcher only reads the absorbance and obtains the number of micelles/sample volume through the equation of the straight line, already obtained.

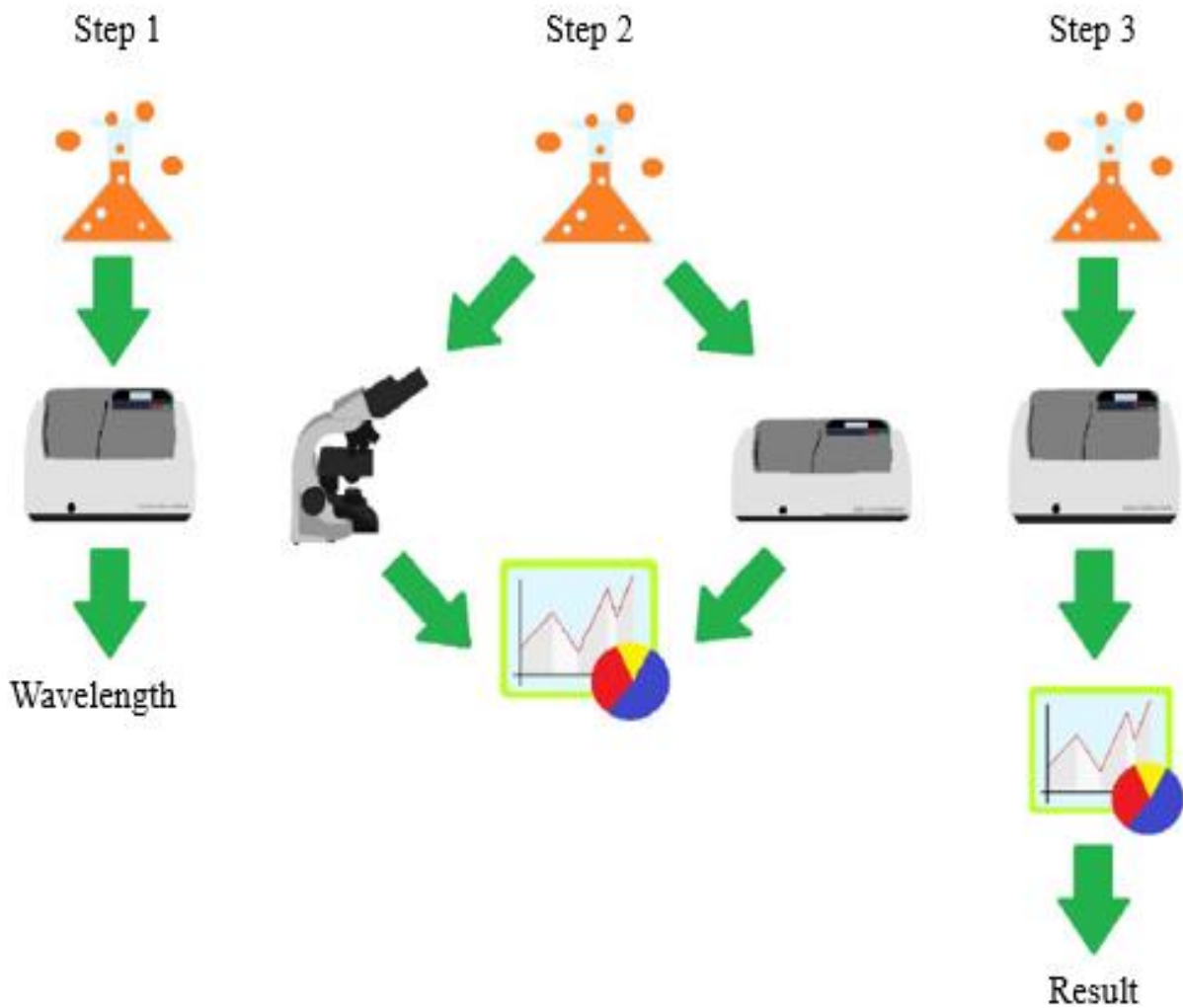


Figure 4.9 - Scheme of the proposed alternative technique (Author, 2021)

4.4 Rheology

Diluted broth samples were submitted to rheological experiments at six temperatures: $T = 20\text{ }^{\circ}\text{C}$, $T = 25\text{ }^{\circ}\text{C}$, $T = 30\text{ }^{\circ}\text{C}$, $T = 35\text{ }^{\circ}\text{C}$, $T = 40\text{ }^{\circ}\text{C}$ e $T = 50\text{ }^{\circ}\text{C}$. The rheological curves are presented in Figure 4.10, from which it was possible to evaluate the rheological models in the Table 2.4, whose results, for the rheological parameters as well as for the determination coefficient, are contained in Tables 4.1 up to 4.5. The non-Newtonian behavior was observed at temperatures studied.

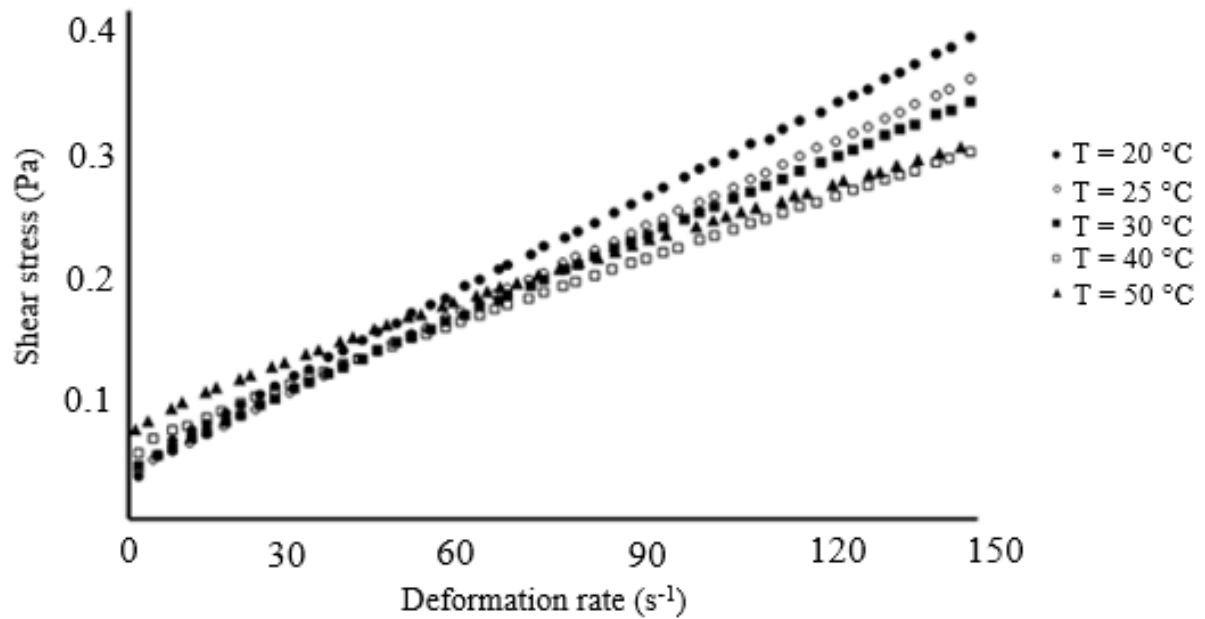


Figure 4.10 - Rheological curves of diluted fermented broth (Author, 2021)

Table 4.1 – Rheological parameters at 20 °C (Author, 2021)

Model	τ_0	K	n	m	R ²
Newtonian	0	2.694×10^{-3}	1	1	0.9509
Ostwald-De-Waele	0	1.449×10^{-2}	1	0.631	0.9812
Bingham	4.326×10^{-2}	2.263×10^{-3}	1	1	0.9990
Herschel-Bulkley	3.863×10^{-2}	2.758×10^{-3}	1	0.962	0.9995
Casson	1.371×10^{-2}	4.033×10^{-2}	0.50	0.50	0.9990
Mizrahi-Berk	2.443×10^{-2}	2.400×10^{-2}	0.50	0.590	0.9995
Vocadlo	2.619×10^{-2}	2.175×10^{-3}	1.06	1	0.9996

Table 4.2 – Rheological parameters at 25 °C (Author, 2021)

Model	τ_0	K	n	m	R ²
Newtonian	0	2.441×10^{-3}	1	1	0.9558
Ostwald-De-Waele	0	1.352×10^{-2}	1	0.624	0.9700
Bingham	3.767×10^{-2}	2.065×10^{-3}	1	1	0.9996
Herschel-Bulkley	3.079×10^{-2}	2.838×10^{-3}	1	0.939	0.9999
Casson	1.212×10^{-2}	3.845×10^{-2}	0.50	0.50	0.9980
Mizrahi-Berk	2.313×10^{-2}	2.216×10^{-2}	0.50	0.596	0.9999
Vocadlo	1.817×10^{-2}	1.942×10^{-3}	1.081	1	0.9999

Table 4.3 – Rheological parameters at 30 °C (Author, 2021)

Model	τ_0	K	n	m	R ²
Newtonian	0	2.361×10^{-3}	1	1	0.9334
Ostwald-De-Waele	0	1.209×10^{-2}	1	0.584	0.9630
Bingham	4.315×10^{-2}	1.931×10^{-3}	1	1	0.9920
Herschel-Bulkley	3.382×10^{-2}	3.382×10^{-3}	1	0.914	0.9999
Casson	1.546×10^{-2}	3.628×10^{-2}	0.50	0.50	0.9978
Mizrahi-Berk	2.625×10^{-2}	2.065×10^{-2}	0.50	0.598	0.9998
Vocadlo	1.465×10^{-2}	1.746×10^{-3}	1.126	1	0.9999

Table 4.4 – Rheological parameters at 40 °C (Author, 2021)

Model	τ_0	K	n	m	R ²
Newtonian	0	2.139x10 ⁻³	1	1	0.8140
Ostwald-De-Waele	0	2.304x10 ⁻²	1	0.408	0.9583
Bingham	5.824x10 ⁻²	1.558x10 ⁻³	1	1	0.9982
Heschel-Bulkley	4.698x10 ⁻²	2.982x10 ⁻³	1	0.876	0.9999
Casson	2.737x10 ⁻²	2.987x10 ⁻²	0.50	0.50	0.9977
Mizrahi-Berk	3.930x10 ⁻²	1.636x10 ⁻²	0.50	0.605	0.9998
Vocadlo	1.215x10 ⁻²	1.290x10 ⁻³	1.214	1	0.9999

Table 4.5 – Rheological parameters at 50 °C (Author, 2021)

Model	τ_0	K	n	m	R ²
Newtonian	0	2.293 x10 ⁻³	1	1	0.5671
Ostwald-De-Waele	0	4.143 x10 ⁻²	1	0.366	0.9286
Bingham	8.215x10 ⁻²	1.463x10 ⁻³	1	1	0.9964
Heschel-Bulkley	6.754x10 ⁻²	3.538x10 ⁻³	1	0.831	0.9999
Casson	4.743x10 ⁻²	2.616x10 ⁻²	0.50	0.50	0.9969
Mizrahi-Berk	6.141x10 ⁻²	1.349x10 ⁻²	0.50	0.617	0.9999
Vocadlo	0.833x10 ⁻²	1.090x10 ⁻³	1.350	1	0.9999

By inspection of Tables 4.1 to 4.5, it is verified that the adjustment, for the Newtonian fluid model, presented the highest value for the determination coefficient equal $R^2 = 0.9509$ at 20°C, decreasing for $T = 50$ °C whit $R^2 = 0.5671$, corroborating the non-Newtonian nature of the fluid, mainly for temperatures above 30 °C. However, for temperatures from 20 °C to $T = 30$ °C, it is reasonable possible to assume the Newtonian description, with dynamic viscosity given (with $R^2 = 0.9999$) by

$$\eta = 0.3199 - 2.096 \times 10^{-3} T + 3.460 \times 10^{-6} T^2 \quad (4.2)$$

with T in K; η in Pa.s.

On the other hand, the Ostwald-De-Waele's model presented similar performance regarding temperature influence: $R^2 = 0.9812$ for 20 °C, and $R^2 = 0.9286$ for 50°C. The other models presented $R^2 > 0.99$ for all temperatures analyzed, emphasizing the non-Newtonian nature of the solution analyzed in this work. It was possible to obtain, for each temperature and model present in Table 2.6, the values of the rheological parameters (RP = τ_0 , K, n and m), resulting in the proposition, for each RP, a correlation as function of temperature (T, in Kelvin) as

$$RP = \sum_{i=0}^{i=2} a_i T^i \quad (4.3)$$

the results of coefficients are presented in Tables 4.6 to 4.8.

Table 4.6 – Coefficients of Equation 4.3 for $RP = \tau_0$ (Pa) (Author, 2021)

Model	a_0	a_1	a_2	R^2
Bingham	5.492	-3.671×10^{-2}	6.180×10^{-5}	0.9884
Heschel-Bulkley	5.912	-3.912×10^{-2}	6.530×10^{-5}	0.9785
Casson	4.072	-2.745×10^{-2}	4.640×10^{-5}	0.9882
Mizrahi-Berk	4.535	-3.050×10^{-2}	5.154×10^{-5}	0.9976
Vocadlo	2.102	-1.303×10^{-2}	2.029×10^{-5}	0.9513

Table 4.7 – Coefficients of Equation 4.3 for $RP = K$ (Pa.s^m) (Author, 2021)

Model	a_0	a_1	a_2	R^2
Ostwald-De-Waele	4.626	-3.082×10^{-2}	5.146×10^{-5}	0.9954
Bingham	0.663×10^{-1}	-3.394×10^{-4}	5.935×10^{-7}	0.9889
Heschel-Bulkley	6.422×10^{-1}	-4.202×10^{-4}	7.189×10^{-7}	0.8819
Casson	2.490×10^{-1}	-9.057×10^{-4}	6.665×10^{-7}	0.9903
Mizrahi-Berk	2.437×10^{-1}	-11.037×10^{-4}	12.093×10^{-7}	0.9962
Vocadlo	0.671×10^{-1}	-3.882×10^{-4}	5.694×10^{-7}	0.9949

Table 4.8 – Coefficients of Equation 4.3 for $RP = n$ or m (-) (Author, 2021)

Model	a_0	a_1	a_2	R^2
Ostwald-De-Waele	3.371	-0.926×10^{-3}	0	0.9711
Heschel-Bulkley	2.225	-4.312×10^{-3}	0	0.9985
Mizrahi-Berk	0.342	-0.848×10^{-3}	0	0.9779
Vocadlo	2.953	-6.824×10^{-3}	0	0.9906

The performance of rheological models is evaluated using the absolute mean deviation (AMR), considering all the experimental values presented in Figure 4.1, according to

$$AMR(\%) = \frac{1}{N} \sum_{i=1}^{i=250} \left| \frac{\tau_{exp} - \tau_{model}}{\tau_{exp}} \right| \times 100\% \quad (4.4)$$

with $N = 250$ and the results shown in Table 4.9.

Table 4.9 – Absolute mean deviation of rheological models analysed in this work (%) (Author, 2021)

Ostwald-De-Waele	Bingham	Heschel-Bulkley	Casson	Mizrahi-Berk	Vocadlo
0.1280	5.8870	0.1350	0.0250	0.0176	0.1520

The liquid solution analyzed in the present work is highly complex as to its composition, since it contains, in addition to the original composition of the fermentative medium and the drug, bacterial biomass as well as organic materials made of reducing proteins and sugars (SILVA *et al.*, 2019). Although such medium will be diluted in 50 % of its total volume by Newtonian solvent (acetone), its rheological behavior undergoes continuous change with the increase in temperature, as can be seen with the decrease in the

value of the fluid behavior index m (Table 4.9), configuring the pseudoplastic nature of the solution. In addition, there is an influence of residual shear stress, both by the initial stress (τ_0) and by the index associated with it (n), indicating the interaction of the micelles with each other in the liquid solution, characterizing the viscoplastic nature of the solution. Such results are mirrored in the good performance of Mizhari and Berk's equation, Equation 2.25, mainly for low values of strain rate. However, Casson's equation, Equation 2.24, presents itself as an alternative for describing the rheological model of the solution evaluated in this work, since it does not need adjustments for the obtaining m .

4.5 Microfiltration

The core of this Dissertation is to analyze the rejection of micelles in the crude broth from fermentation by *Streptomyces tsukubaensis* bacteria. Here, the microfiltration is based on its permeate critical flow. It is important to note that the model to be presented is indicated for the situation in which the porous matrix is assumed as non-deformable structure, that is, in classical language, there is no cake formation. In the liquid phase processing, considered for the removal of components present in such phase, which present considerable size and high molar mass, as in the case of micelles it is possible to use microfiltration. In this situation, the porous matrix is characterized by basically presenting macropores and, therefore, the diffusive mechanism is governed by the viscous flow (or Poiseuille's diffusion), whose driving force is the pressure gradient, presenting an analogy with conventional filtration, in which the permeate volumetric flow is described by Equation 2.16, put as

$$\beta = \frac{dV}{dt} \quad (4.5)$$

If someone does a graph V vs t and observes a straight line, it is possible to say: (a) the operations occur below the critical flow; (b) there is the confirmation of Darcy's law, consequently the validity of Equation 2.10.

4.5.1 Specific resistance of filter components

Before the microfiltration study, it is essential to observe the filter characteristics, such as the constructs aspects as support for membranes or filter medium, R_{FM} , that is obtained as Equation 2.12, here rewritten as

$$R_{FM} = R_{ppsc} + R_f \quad (4.6)$$

R_f is the membrane intrinsic resistance; R_{ppsc} is perforated plate and metallic screen resistance, or

$$R_{ppsc} = R_{pp} + R_{sc} \quad (4.7)$$

The metallic screen is obtained from Equation 4.7,

$$R_{sc} = R_{ppsc} - R_{pp} \quad (4.8)$$

Figure 4.11 presents the V vs t results for the situation in which the filter assembly consisting only of perforated plate and another set of perforated plate and metallic screen, both situation at 1 bar and 2 bar feed pressures.

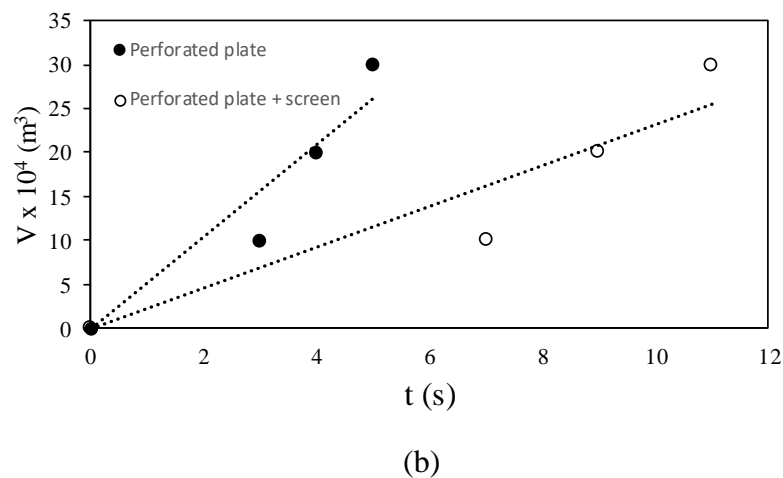
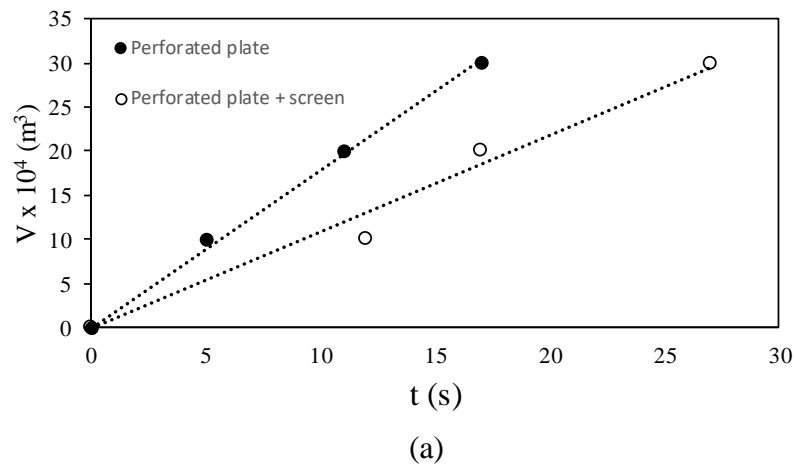


Figure 4.11 – Microfiltration with water to obtain the specific resistance of filter components: (a) 1 bar; (b) 2 bar (Author, 2021)

The values of determination coefficient, R^2 , of lines and the values of the resistances, from the angular coefficient of these lines, β , are presented in Table 4.10.

Table 4.10 – Specific resistance of filter components (Author, 2021)

p_F (bar)	R^2 (-)	$R_{pp} \times 10^{-7}$ (m^2/kg)	R^2 (-)	$R_{ppsc} \times 10^{-7}$ (m^2/kg)	$R_{sc} \times 10^{-7}$ (m^2/kg)
1	0.9972	0.56	0.9680	0.91	0.36
2	0.9040	4.03	0.8805	5.02	0.99

The stainless-steel presents a fine screen and when subjected to 2 bar, it penetrated into pore of the perforated plate. At this pressure, water may also have circulated through the bottom of the filter, in a random movement, interfering in the measure of the permeate flow rate. This can be verified by the low values of the determination coefficient for 2 bar operational pressure in Table 4.10.

Bifiltered water was used at 26 °C for experimental tests. To obtain the dynamic viscosity value of the water, the following correlation was used, valid for 0 °C to 40 °C (KESTIN *et al.*, 1978)

$$\log\left(\frac{\eta}{\eta|_{T=20^\circ\text{C}}}\right) = \left(\frac{20-T}{T+96}\right) [1.2364 - 1.37 \times 10^{-3}(20-T) + 5.7 \times 10^{-6}(20-T)^2] \quad (4.9)$$

with T in °C; η in $\mu\text{Pa}\cdot\text{s}$; $\eta|_{T=20^\circ\text{C}} = 1.002 \mu\text{Pa}\cdot\text{s}$. In this Dissertation, $\eta = 8.703 \times 10^{-4} \text{ Pa}\cdot\text{s}$. The value of the water density was obtained from Equation 4.10, valid for the range from 5 °C to 40 °C (JONES and HARRIS, 1992),

$$\rho = \sum_{i=0}^{i=4} a_i T^i \quad (4.10)$$

with

$a_0 = 999.85308$; $a_1 = 6.32693 \times 10^{-2}$; $a_2 = -8.523829 \times 10^{-3}$; $a_3 = 6.943248 \times 10^{-5}$; $a_4 = -3.821216 \times 10^{-7}$;
T in °C; ρ in kg/m^3 ; at 26 °C, $\rho = 996.78 \text{ kg}/\text{m}^3$.

The intrinsic resistances of 0.22 μm and 3.00 μm membranes are obtained in same way. From Equation 4.6,

$$R_f = R_{FM} - R_{ppsc} \quad (4.11)$$

The values of R_{ppsc} are in Table 4.10, while R_{FM} comes from Equation 4.6, by V vs t graph, as that on in Figure 4.12. Table 4.11 shows R_{FM} e R_f results.

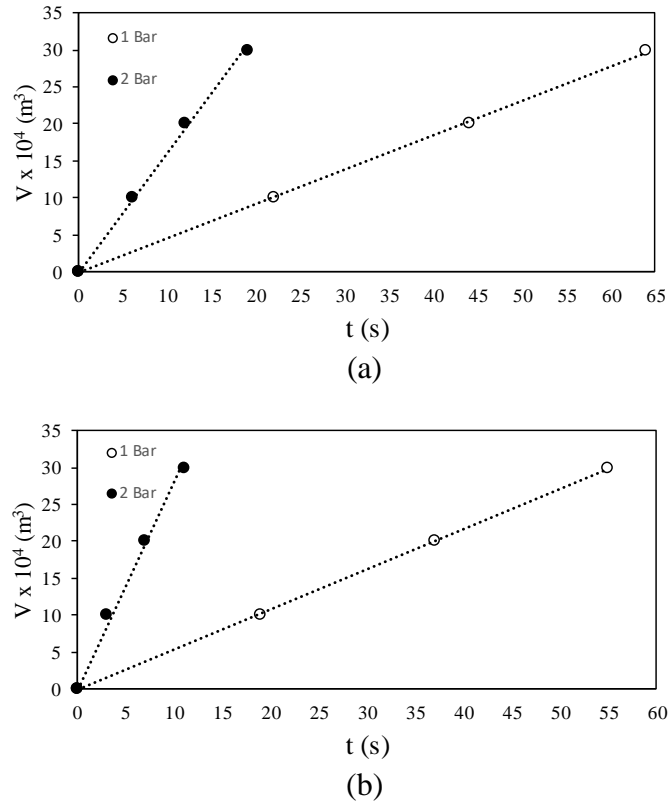


Figure 4.12 – Microfiltration with water to obtain the specific resistance of filter medium and membrane: (a) 0.22 μm ; (b) 3.00 μm (Author, 2021).

Table 4.11 – Specific resistance of filter medium and membrane (Author, 2021)

p_F (bar)	σ_p (μm)	R^2 (-)	$R_{FM} \times 10^{-7}$ (m^2/kg)	$R_f \times 10^{-7}$ (m^2/kg)
1	0.22	0.9994	2.15	1.24
1	3.00	0.9998	1.84	0.93
2	0.22	0.9982	13.0	7.98
2	3.00	0.9933	7.50	2.48

When the membranes were subjected at to 2 bar, they were compacted on the stainless-steel screen. These membranes occupied pores of the screen and practically fused with them, as shown in Figure 4.13, causing folding or destruction of the membrane. This may explain why the intrinsic resistances of the membranes, in Table 4.11, showed different values in the two operational pressures.



Figure 4.13 – Membrane appearance at 2 bar:
 (a) original membrane; (b) folded membrane; (c) partially destroyed membrane
 (Author, 2021)

4.5.2 Microfiltration process

The microfiltration study of the fermented broth derived from fermentation by *Streptomyces tsukubaensis*, in which equal acetone volume was added to the broth, to stop fermentation. From this feed solution at 26 °C, the density was $\rho = 1114.93 \text{ kg/m}^3$, while the dynamic viscosity of the solution, considering Newtonian fluid, was obtained from the Equation 4.2 or $\eta = 25.195 \times 10^{-4} \text{ Pa.s}$.

4.5.3 Single step

In single step microfiltration, 30 mL of fermented broth with acetone or feed solution was processed just once time. Total resistance comes from Equation 4.4, rewritten as

$$R_T = \frac{(\text{Area})\Delta p}{\eta\beta} \quad (4.12)$$

The V vs t graph is in Figure 4.14, with determination coefficient, $R^2 = 0.9985$, and total resistance, $R_T = 7.087 \times 10^7 \text{ m}^2/\text{kg}$.

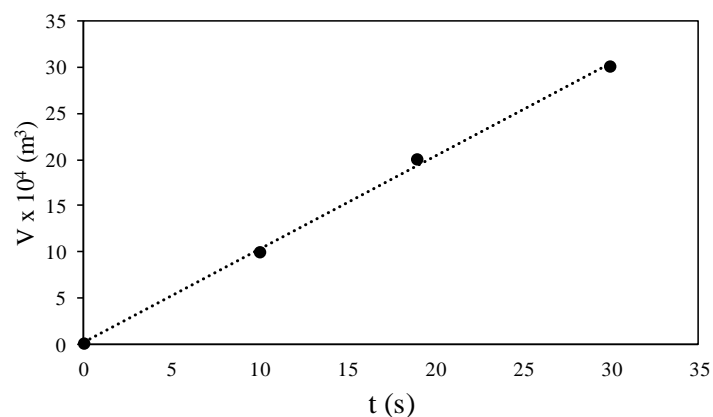


Figure 4.14 –Single microfiltration test: 3.00 μm and 1 bar (Author, 2021)

From Equation 4.1 with $x = \text{Absorbance}$ and $y = \text{number of micelles/mL}$, it is possible to know the rejection performance. The results for particle count analysis of feed solution and permeate, obtained by single microfiltration are presented in Table 4.12, verifying the average rejection equal $R = 35.99 \%$, and it was decided for microfiltration steps. The analysis of the quality of the permeate and the efficiency of the microfiltration process with the fermented broth and acetone are associated closely with rejection which is the percentage of micelles removed by the membrane. This rejection, in other words, is related with microfiltration efficiency.

Table 4.12 – Rejection results of single microfiltration test: $3.00 \mu\text{m}$ and 1 bar (Author, 2021)

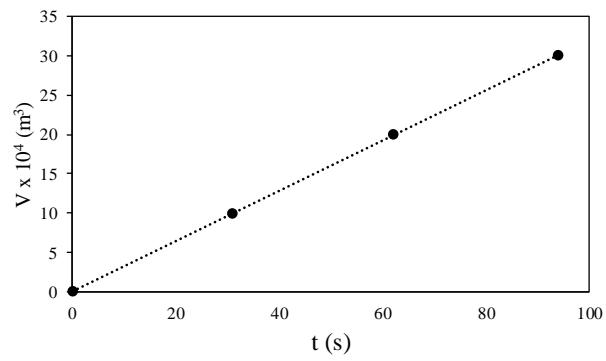
	Feed (duplicate)	Permeate (duplicate)
Absorbance	0.998	0.632
Number of micelles/mL	50274	32180

4.5.4 Multiple steps: preliminary study

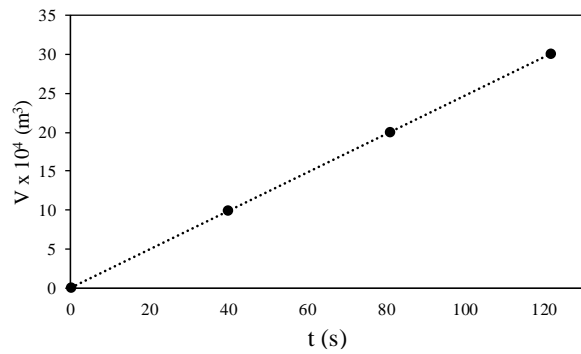
The goal of this Dissertation was to obtain 95 % rejection at least. In this case, it was chosen four steps using operational pressure of 1 bar and 0.22 membrane pore diameter. In other hand, after the solution feed had been filtrated for the first time, the permeate was recirculated for more three times. In this case, there are four microfiltration or four steps. At each step there is a new suspension feed, different from the previous one, just as the filter medium is different. This causes different resistance values for each step. For each step it was obtained a V vs t figures, presented in Figure 4.15. The values of rejection are in Table 4.13. It is noticed that maximum value of rejection was 87.5 %.

Table 4.13 – Rejection results of multiple microfiltration tests: $0.22 \mu\text{m}$ and 1 bar (Author, 2021)

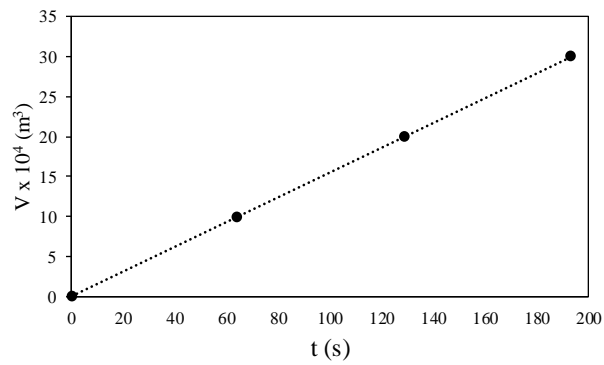
	Feed (duplicate)	Permeate (duplicate)	R (%)
Step #1	0.998	0.632	
Number of micelles/mL	50274	32156	36.04
Step #2	0.998	0.321	
Number of micelles/mL	50274	16785	66.61
Step #3	0.998	0.109	
Number of micelles/mL	50274	6290	87.49
Step #4	0.998	0.107	
Number of micelles/mL	50274	6265	87.54



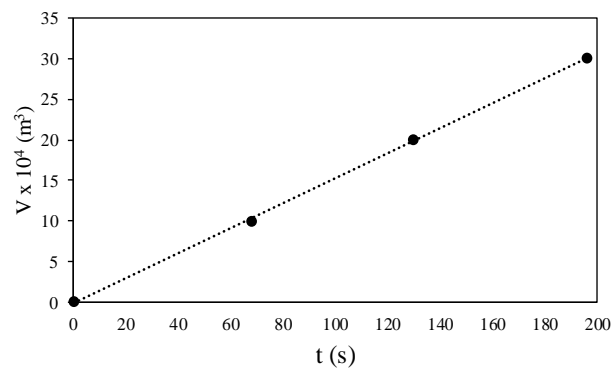
(a)



(b)



(c)



(d)

Figure 4.15 – Preliminary study of microfiltration test – 0.22 μm and 1 bar:

(a) Step #1 ($R^2 = 0.99993$); (b) Step #2 ($R^2 = 0.99995$);

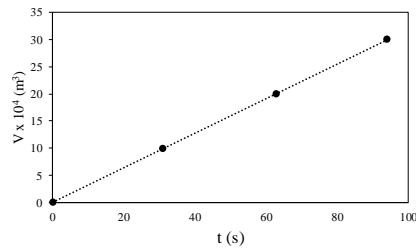
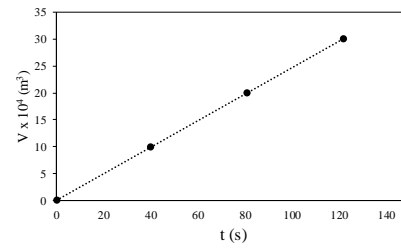
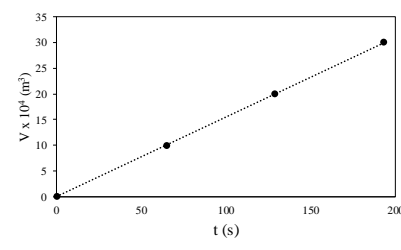
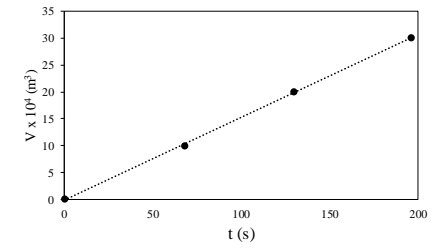
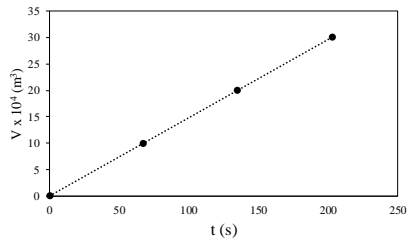
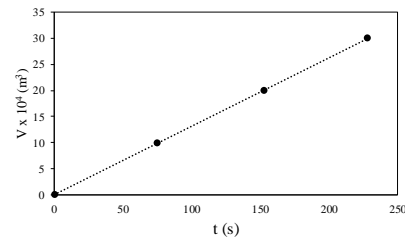
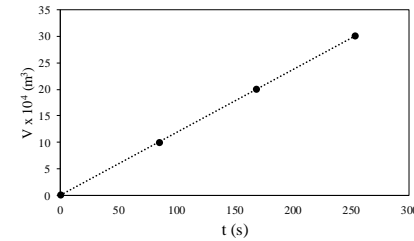
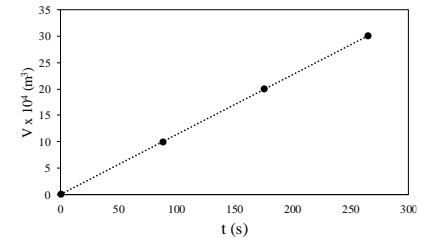
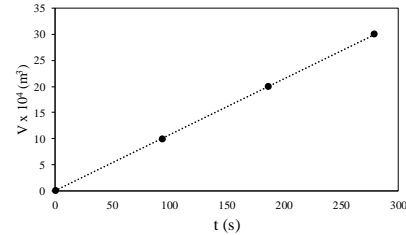
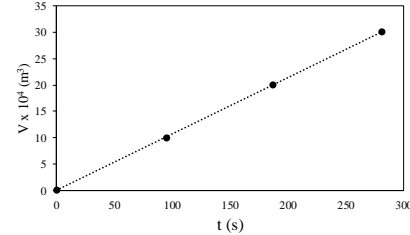
(c) Step #3 ($R^2 = 0.99999$); (d) Step #4 ($R^2 = 0.99965$) (Author, 2021)

4.5.5 Microfiltration in multiple steps

The microfiltration in multiple steps works, but with four steps the rejection obtained was 87.5 %. In the present section, the microfiltration operational condition is 1 bar and 2 bar, using 0.22 μm and 3.00 μm pore membrane with ten steps of operation. After 30 mL solution feed to be filtrated in first time, the permeate was recirculated more nine times, configuring ten microfiltration or ten steps. In each step it was obtained a V vs t figures, that are presented in Figure 4.16 for 0.22 μm and 1 bar condition; Figure 4.17 for 0.22 μm and 2 bar condition; Figure 4.18 for 3.00 μm and 1 bar condition; Figure 4.19 for 3.00 μm and 2 bar condition, with determination coefficient pointed in each step. In this case, in all runs and steps it was observed $R^2 > 0.996$, implying the correct application of Darcy's law or the validity of Equation 2.10, as well as the process operates below the critical flow. The duplicates relating to the multiple stages of microfiltration processes are listed in Appendix A.

During microfiltration in several stages, a decline in the permeate volumetric flow (β), as presented in Figures 4.20 and 4.21, is observed over time, due to a series of phenomena that provide favorable conditions for membrane encrustation. As the membrane is selective, that is, it allows only a few solutes to pass through, there is an accumulation of solutes that are rejected by the membrane. In this way, a concentrated layer of micelles is formed at the membrane interface that offers additional resistance. The interaction between the solute and the membrane, the size and the morphology of the pores also help in the appearance of additional resistances, particularly due to fouling formation.

Figure 4.20 shows that, for 1 bar operation pressure and 3.00 μm membrane, that permeate volumetric flow starts around 10 m^3/s reducing it up to 4 m^3/s in step #10. On the other hand, for 0.22 μm membrane at 2 bar, its permeate volumetric flow did not vary considerably from step #4. In addition, for high Δp values, it is observed that the flow no longer depends on the pressure due to fouling phenomena that altering the internal membrane characteristics, such as its porosity. Figure 4.21 shows that the difference in volumetric flow at 1 and 2 bar is more significant in the 0.22 μm membrane (Figure 4.21a) than in the 3.00 μm membrane (figure 4.21b). For both operational pressure and both membranes, mass flow tends to remain constant in step #7. With the 3.00 μm to 1 bar membrane (Figure 4.21b) the volumetric flow in steps 1 and 2 is less than 2 bar runs, but at 1 bar in step #3 it becomes higher and the flow volumetric practically remains constant at step #6 up to 10.

(a) Step #1 ($R^2=0.99993$)(b) Step #2 ($R^2=0.99995$)(c) Step #3 ($R^2=0.99999$)(d) Step #4 ($R^2=0.99999$)(d) Step #5 ($R^2=0.99965$)(e) Step #6 ($R^2=0.99998$)(f) Step #7 ($R^2=0.99993$)(g) Step #8 ($R^2=0.99999$)(h) Step #9 ($R^2=0.99998$)(i) Step #10 ($R^2=0.99996$)Figure 4.16– Microfiltration in multiple steps: 0.22 μm and 1 bar (Author, 2021)

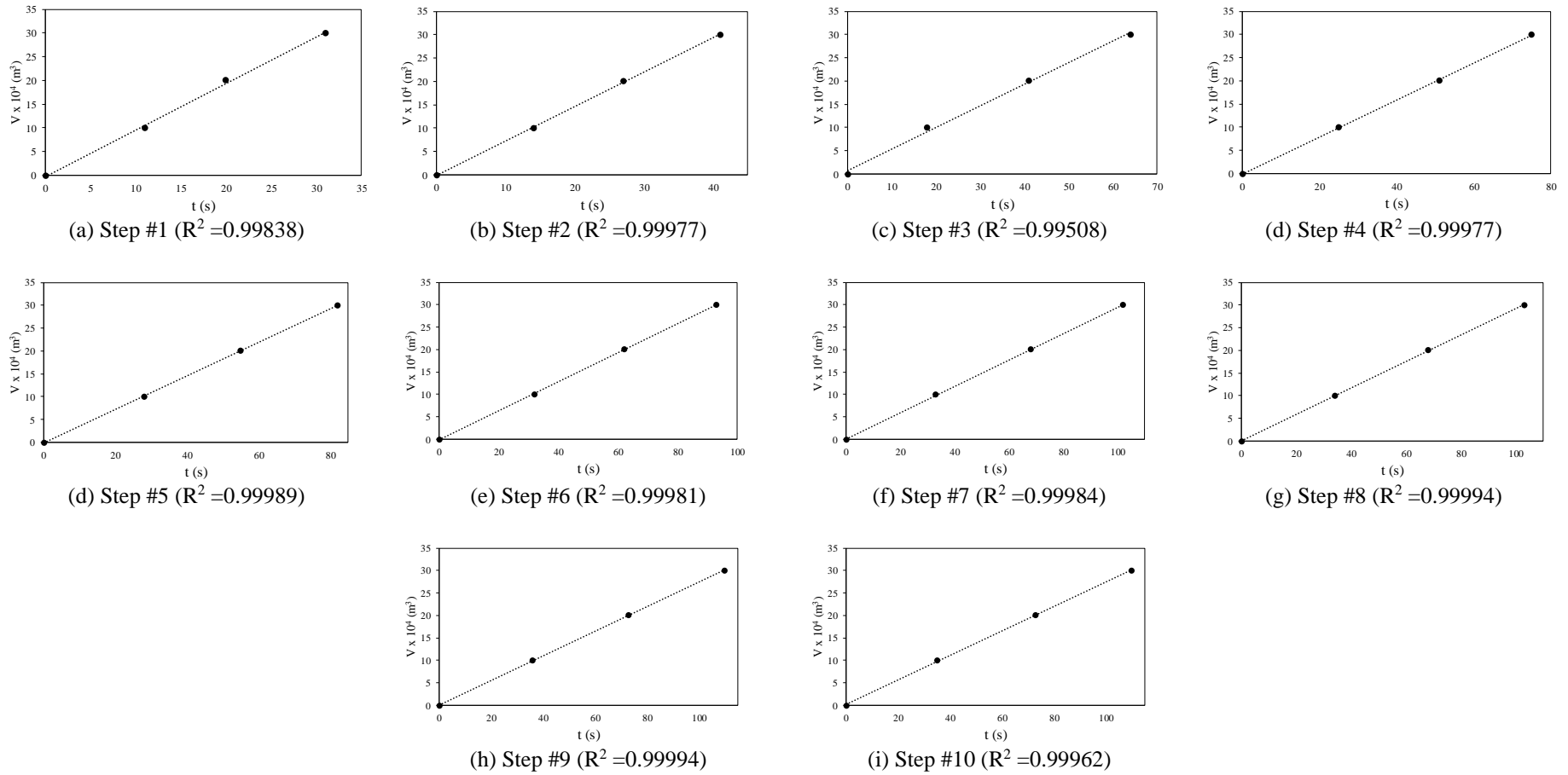


Figure 4.17 – Microfiltration in multiple steps: 0.22 μm and 2 bar (Author, 2021).

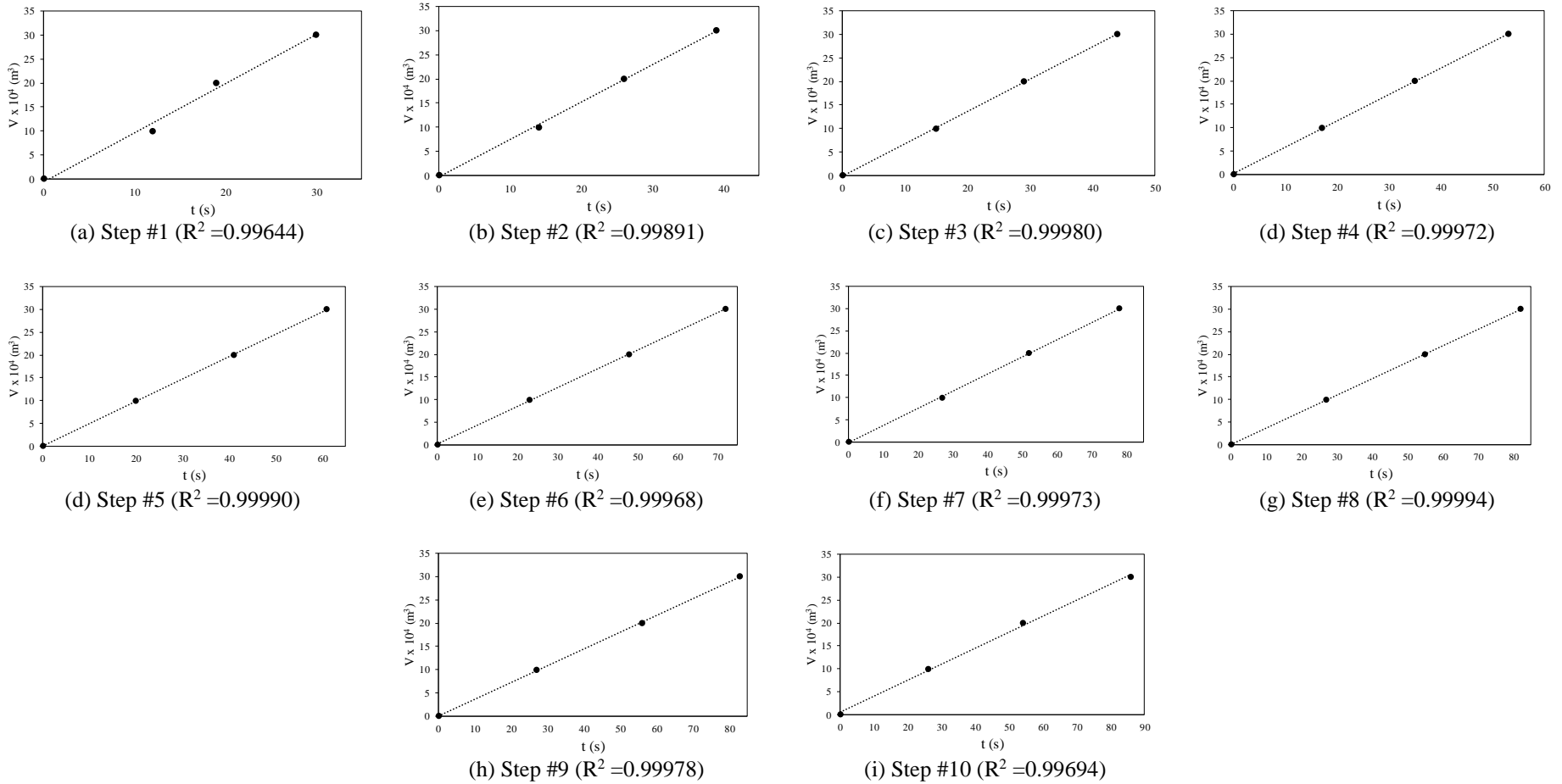
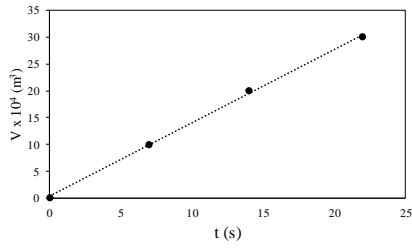
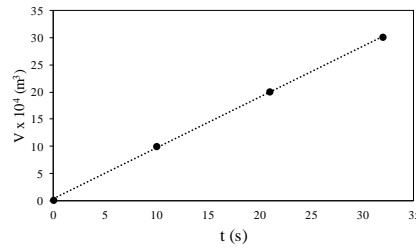


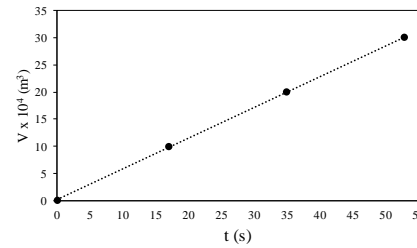
Figure 4.18 – Microfiltration in multiple steps: 3.00 μm and 1 bar (Author, 2021)



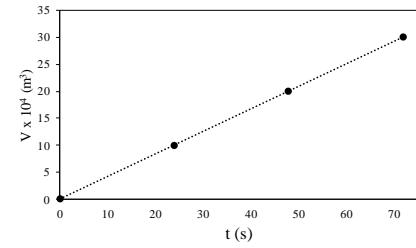
(a) Step #1 ($R^2=0.99863$)



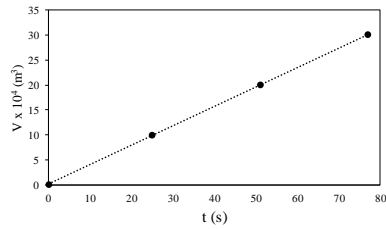
(b) Step #2 ($R^2=0.99923$)



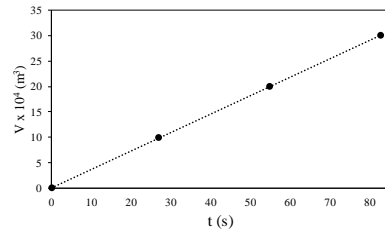
(c) Step #3 ($R^2=0.99972$)



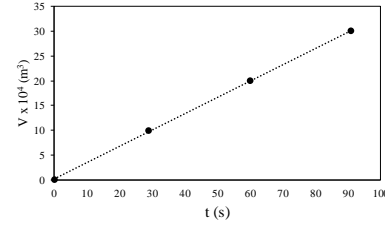
(d) Step #4 ($R^2=0.99999$)



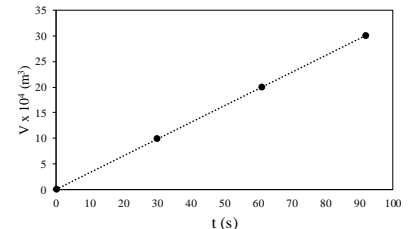
(d) Step #5 ($R^2=0.99987$)



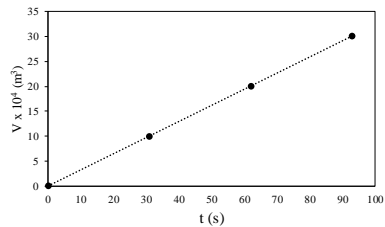
(e) Step #6 ($R^2=0.99989$)



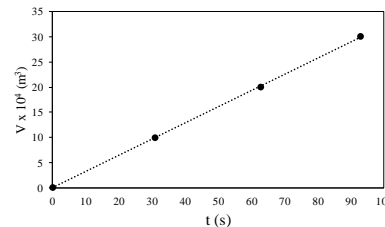
(f) Step #7 ($R^2=0.99962$)



(g) Step #8 ($R^2=0.99991$)

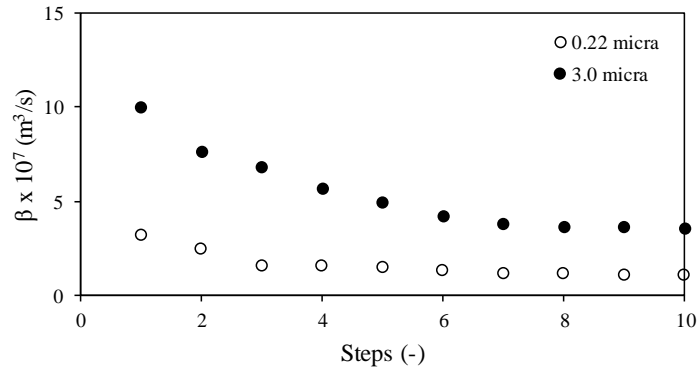


(h) Step #9 ($R^2=0.99999$)

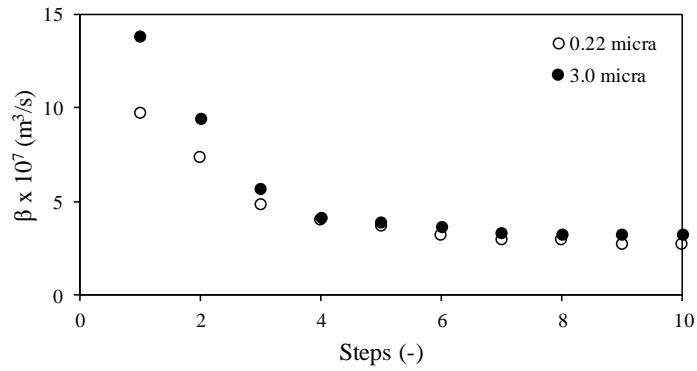


(i) Step #10 ($R^2=0.99985$)

Figure 4.19 – Microfiltration in multiple steps: 3.00 μm and 2 bar (Author, 2021)

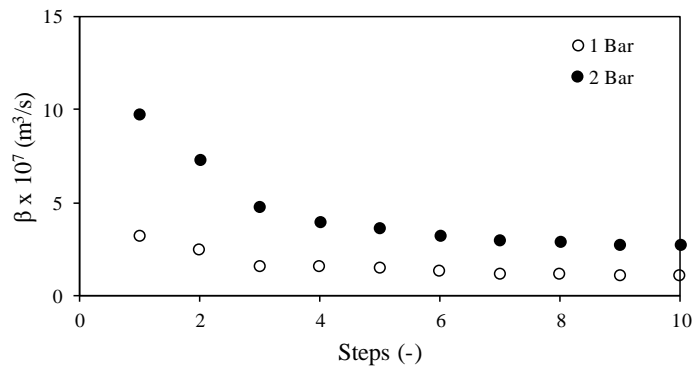


(a)

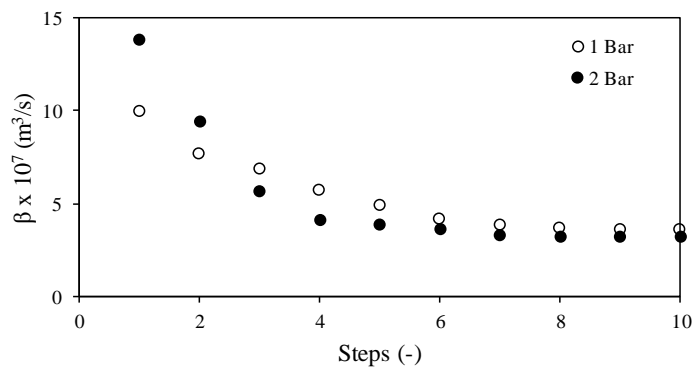


(b)

Figure 4.20 – Influence of multiple microfiltration in volumetric flow: (a) 1 bar; (b) 2 bar



(a)



(b)

Figure 4.21 – Influence of multiple microfiltration in volumetric flow: (a) 0.22 μm ; (b) 3.00 μm (Author, 2021).

As the process progresses, the fouling phenomenon occurs, as previously mentioned. These encrustations grow over time into membranes and they become a new filter medium in each new step. However, after several steps, the fouling becomes compact causing increased resistance and microfiltration time with each new passage. In this case, it is noticed that the membrane with smaller pore diameter has greater influence on the resistance and increases the step time during the multiple stages, corroborating with Figure 4.22a. Figure 4.22a shows that at 1 bar the microfiltration time in step #10 with the 0.22 μm membrane is about 300s, while for the 3.00 μm membrane it is close to 100 s. The microfiltration profile time at 2bar along the steps (Figure 4.22b), did not vary considerably between the two membranes when compared with Figure 4.22a. This is due to the fragmentation of the micelles from fermented broth.

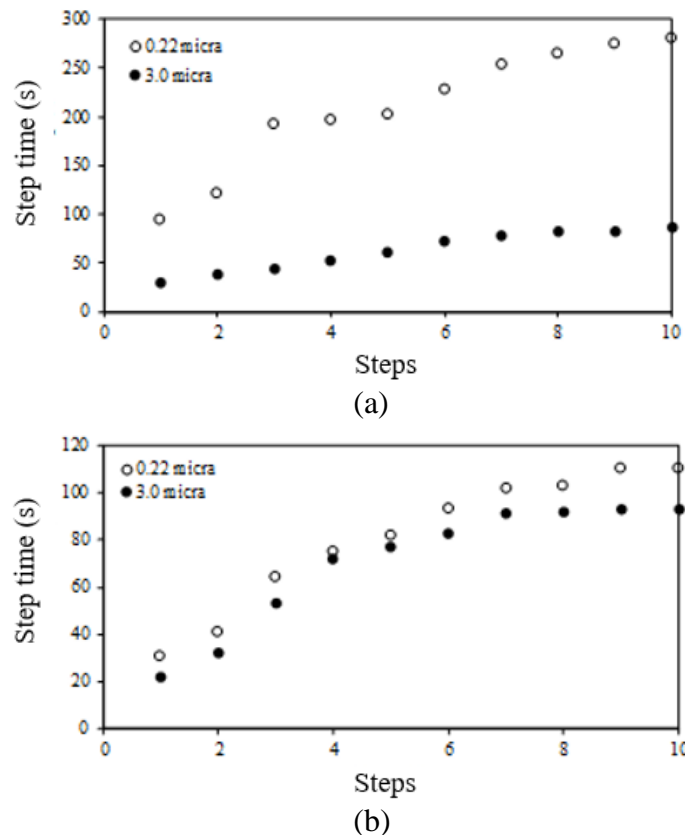


Figure 4.22 – Influence of multiple microfiltration in step time:
(a) 1 bar; (b) 2 bar (Author, 2021)

Figure 4.23a shows that the 0.22 μm membrane subjected to the pressure of 1 bar takes longer to stabilize than 2 bar. For 1 bar pressure, the step #10 arrives at around 300 s, while 1 bar, around 100 s. While the 3.00 μm membrane (Figure 4.23b), independently of pressure, the step time starts to stabilize in run #7 at around 100 s and remains basically the same up to step#10.

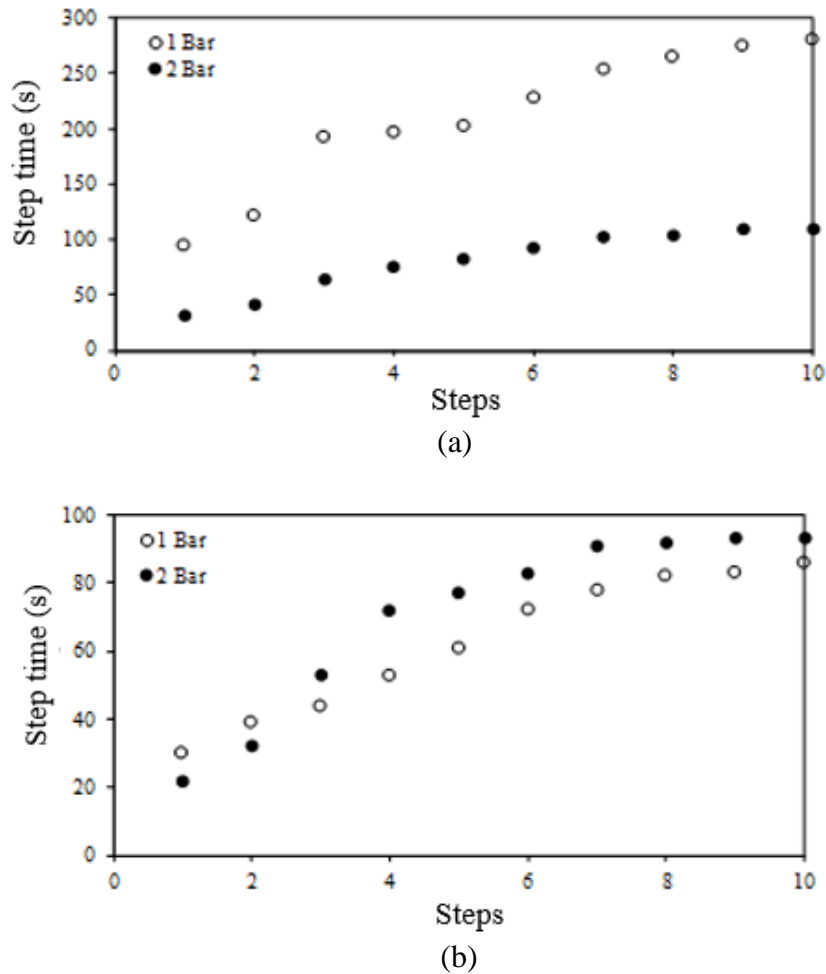
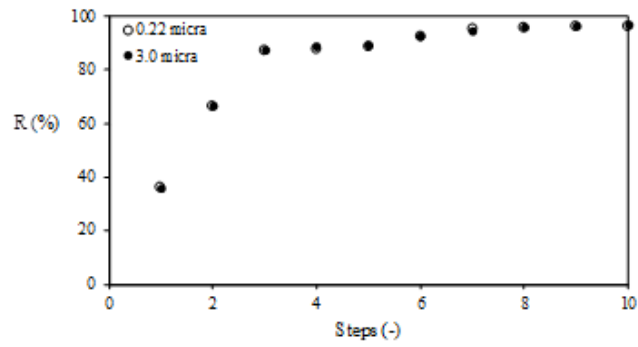
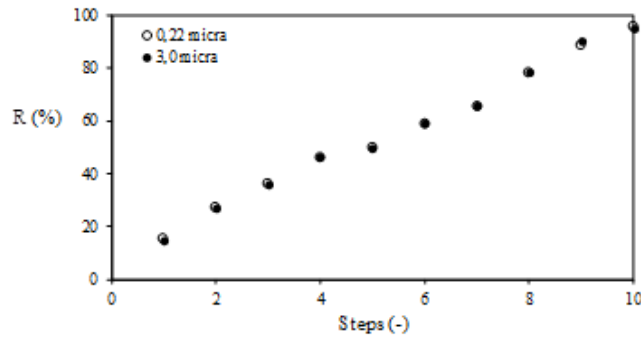


Figure 4.23 – Influence of multiple microfiltration in step time:
(a) 0.22 μm ; (b) 3.00 μm (Author, 2021)

Figure 4.24 shows that at 1 and 2 bar the rejection for the 0.22 μm and 3.00 μm membranes was approximately the same. At 2 bar, the rejection always is in an increasing mode, while at 1 bar it increases until step #3 and there is a slowly increasing until became constant. In addition, at 1 bar, around step #7, it already reaches 95%: reaching a maximum rejection of 97% in the step #10. Figure 4.25 corroborates that both membranes have similar rejection behavior in the two pressures, presenting the same rejection profile versus steps. The operational pressure and membrane pore dimension influence in the microfiltration performance, due to several aspects, including the resistances offer for microfiltration medium.

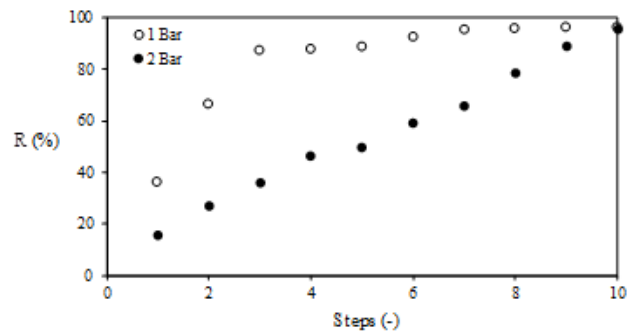


(a)

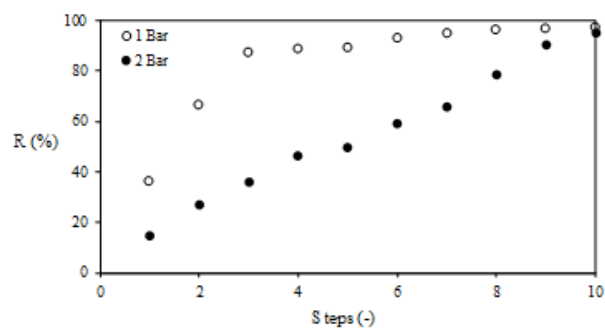


(b)

Figure 4.24 – Influence of multiple microfiltration in micelles rejection:
(a) 1 bar; (b) 2 bar (Author, 2021)



(a)



(b)

Figure 4.25 – Influence of multiple microfiltration in micelles rejection:
(a) 0.22 μm ; (b) 3.00 μm (Author, 2021)

In the present Dissertation it is not analyzed the rheological behavior of permeate, whose experimental dynamic viscosity could be considered in Equation 4.12, for instance. However, to consider this influence, it is possible to do a brief approach for that. In this case, someone assumes that permeate solution can be describe as kind of slurry, where its dynamic viscosity can be express as (COULSON and RICHARDSON, 1993)

$$\eta = \eta_0 \exp\left(\frac{2.5\phi}{1-0.609\phi}\right) \quad (4.13)$$

where ϕ is the volumetric fraction of solids. But, in this Dissertation, this value refers to the micelles volumetric concentration, given by

$$\phi = \frac{V_{\text{micelle}}}{V_{\text{solution}}} \quad (4.14)$$

The volume of solution, in this work, is 30 mL, but the micelle volume is unknown. But here, it is necessary to assume another hypothesis, which it is associated with biomass produced from fermentation process. In this case, the micelle volume is approximated by

$$V_{\text{micelle}} = \frac{m_p}{\rho_p} \quad (4.15)$$

with m_p the biomass in the feed solution at each feed step, and ρ_p the density of biomass (Figure 4.26). Its value found by picnometry (see section 3.2.10) is equal $\rho_p = 0.7865 \text{ g/cm}^3$.



Figure 4.26 – Biomass of the fermentation broth (Author, 2021)

The value of m_p is that one from retentate, obtained from section 2.3.4 (biomass quantification). The micelles concentration in feed and permeate are known (see section 3.28) in terms of number of micelles/mL (N_p) In this case, it is possible to obtain the retentate N_{pR} , as

$$N_{pR} = N_{pF} - N_{pP} \quad (4.16)$$

where N_{pF} is the number of micelles in the feed/mL and N_{pP} is the number of micelles in the permeate/mL. These values were determined for rejection analysis. Then, it was possible to associate the m_p in retentate phase with respective particle number/mL, as presented in Figure 4.27, that gives the following correlation ($R^2 = 0.9919$)

$$m_p = 2.885 \times 10^{-2} \exp(7.642 \times 10^{-5} N_p) \quad (4.17)$$

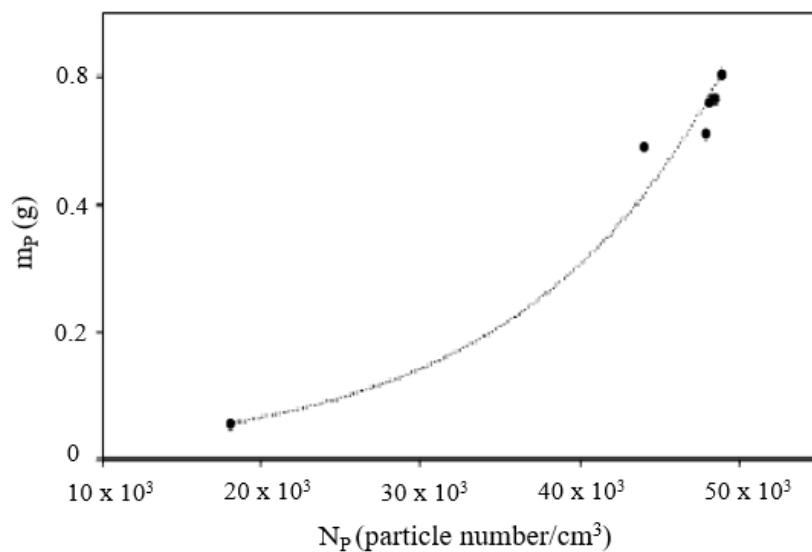


Figure 4.27 – Calibration curve for mass of biomass (Author, 2021)

For instance: at first step, the feed particle number/cm³ was 50274, that amounts, from Equation 4.18, $m_p = 1.345$ g. If someone considers $\rho_p = 0.7865$ g/cm³, that results (by Equation 4.15), $\phi = 0.057$. This value, in its turns, is related with its dynamic viscosity, that at 26°C, by Equation 4.2, is $\eta = 25.195 \times 10^{-4}$ Pa.s. With this value and $\phi = 0.055$, the value of η_0 , by Equation 4.14, is $\eta_0 = 21.74 \times 10^{-4}$ Pa.s, or from Equation 4.14

$$\eta = 21.74 \times 10^{-4} \exp\left(\frac{2.5\phi}{1 - 0.609\phi}\right) \quad (4.18)$$

This correction was considered in Equation 4.12 for each run and step. The values of total resistance are presented in Figures 4.28 and 4.29. Figures 4.28a and 4.28b, for instance, show that as microfiltration steps increase, the total resistance also increases. The effect is most significant with 2 bar pressure for both membranes. At 2 bar, the total resistance does not show marked variation when compared to 1 bar due to the micelles fragmentation effect. In the case of the 0.22 μm membrane, the stability of the total resistance occurs around step #9, while at 3.00 μm in step #7. Figures 4.29a and 4.29b show that, regardless of the pore size of the membrane, the total resistance of the microfiltration process at 2 bar increases considerably over the multiple steps, while at 1 bar it varies little. The R_T profile versus steps at 1 and 2 bar for the 0.22 μm and 3.00 μm membranes were similar. In addition, the 0.22 μm membrane in step #3 showed a resistance significative increasing in relation with previous steps. It is can be explained by accommodation of the micelles into filtered medium due to the fouling effects, or by the folding of the membrane that was verified at the end of the process as shown in Figure 4.30.

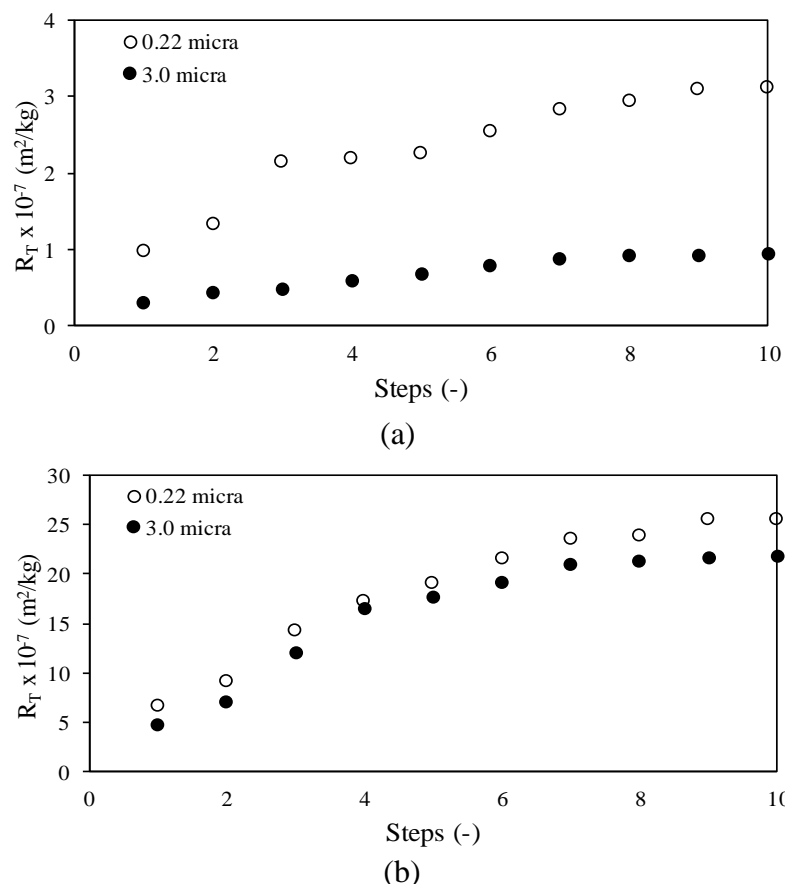


Figure 4.28 – Influence of multiple microfiltration in total resistance: (a) 1 bar; (b) 2 bar (Author, 2021)

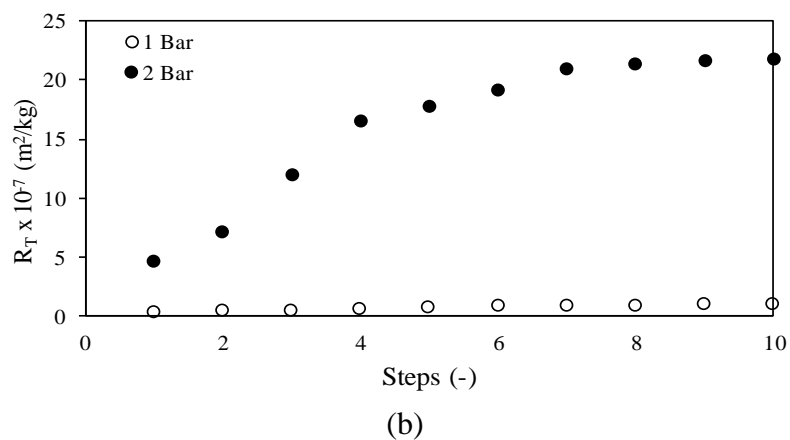
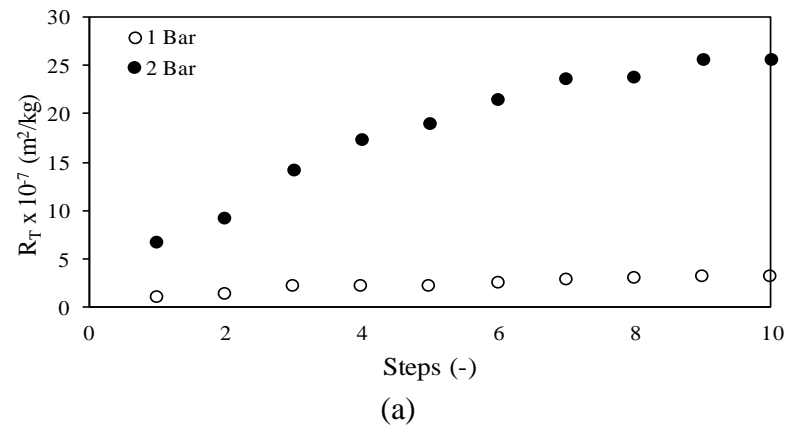


Figure 4.29 – Influence of multiple microfiltration in total resistance: (a) 0.22 μm ; (b) 3.00 μm (Author, 2021)

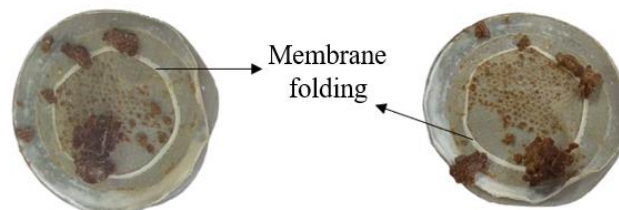


Figure 4.30 – Membrane 0.22 μm folding verified after the multiple steps microfiltration (Author, 2021)

4.6 Tacrolimus and hope in the scientific and social context

This Dissertation, in its technical aspect, is inserted in tacrolimus processing, and continues the resources of Moreira (2018), Ferrari (2018), and Silva (2019), with goals in micelles removal from fermented broth. There is another aspect as important as technological contribution: how this study can contribute to population, particularly that one dependent on tacrolimus, an essential immunosuppressant to maintain lives of anonymous people, whose dream is just to dream with ordinary existence.

Fifty years ago, there was the generation of "peace and love". In the current generation, some young people keep "love" in their speeches, however instead of "peace", prefer

"guns", without realizing, by fun or frivolous posture, they make apology against the life preservation. It is urgent to humanize the technological vision to train professionals who respect the other, and, consequently, have the sensitivity and courage to make decisions that contribute to a more conscious, just, and responsible society. The future of technology professionals does not only point to technical competence, but also to a critical awareness, capable of acting in social transformation. And this is possible, by instilling in the formation of these people that technical knowledge can and should be directed to the common good, such as drug processing, which includes, besides scientific and technological basis, a noble objective that, in addition to being able to save lives, makes it possible to bring hope to those who suffer in the expectation of maintaining their own lives. However, in view of covid-19 pandemic in 2020, there was a new situation in people's lives and profound impact for the current generation. The humanity has had historic moment of extreme exceptionality. Ordinary situations and demands would be assessed, circumvented, digested in such a way as to proceed with daily activities. It is not the case, because one lives in a universe that approaches science fiction, apocalyptic, but deeply real.

The coronavirus pandemic has altered the life of the population affected, for example, by chronic kidney disease, whose prospect of survival is a transplant. In addition to physical pain, the patient lives from the expectation of improvement, or in other words, from hope. When a kidney disease is detected, the patient has hope of quick cure, however he suffers when he finds out that his life will be governed by a treatment, such as dialysis. During dialysis, the patient has the hope of a kidney transplant, participating in an endless wait for a compatible organ. Upon finding such an organ and performing the surgery of his graft, the patient has the hope that his organism will receive the new organ as his own and, for that, he starts administering immunosuppressive that, at the time of adapting the organism for the graft, exposes to the most diverse types of infection. The patient starts to have the double hope that the organism will adapt to the immunosuppressive, as well as to avoid exposures that could make him lose this organ. In addition, the patient has the hope of having the immunosuppressive at his disposal, so that he can start to sow the hope of living. This cycle continues even after the end of the covid-19 pandemic.

The production and purification of tacrolimus have been developed at Mass Transfer Process Laboratory (LPTM), School of Chemical Engineering (FEQ), University of Campinas (UNICAMP), resulting in diversified results, Figure 4.31, such as patent deposited at INPI (CREMASCO and FERRARI, 2018). Scientific articles were writing from this technological knowledge (SILVA *et al.*, 2019; MOREIRA *et al.*, 2020; BERTAN; CREMASCO, 2020a); formation of human resources with two Doctoral Thesis (FERRARI,

2018; MOREIRA, 2018) and a Master Dissertation (SILVA, 2019). In addition, these results were presented in the classroom in undergraduate and graduate levels, contributing on the formation of professionals with social conscience. Appendix B presents tests for undergraduate students in Chemical Engineering at FEQ/Unicamp as results from this Dissertation.

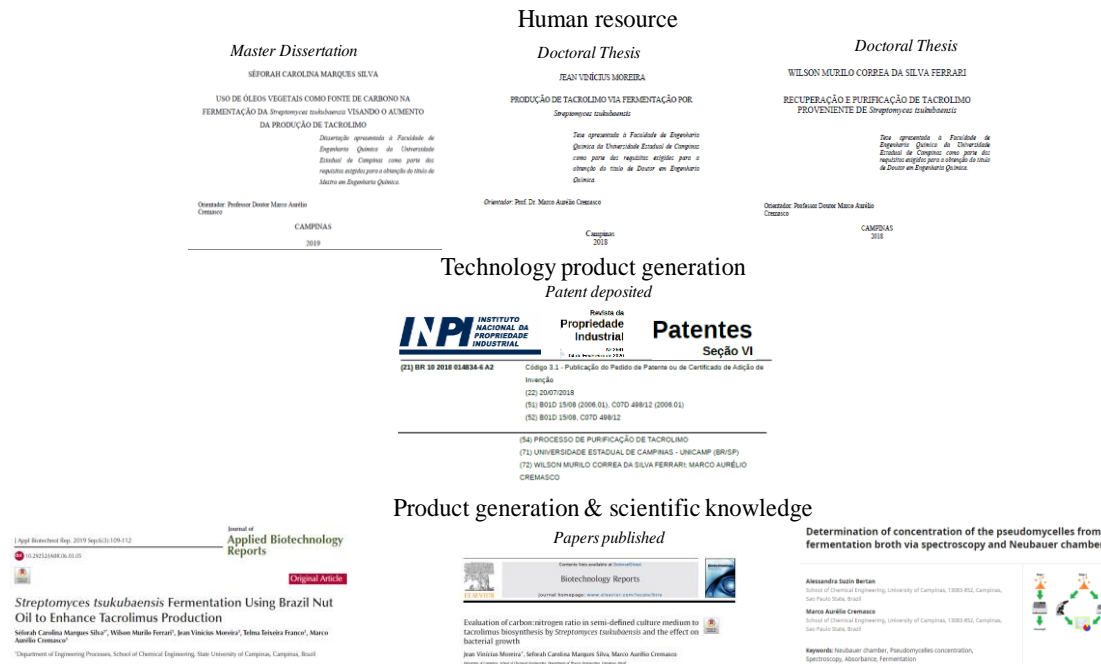


Figure 4.31- Diversified results from tacrolimus processing at LPTM/DEPro/FEQ/UNICAMP (Author, 2021)

It is clearly shows the importance of technical vision, economic opportunities necessarily linked to the social context. In addition to the technical and scientific feasibility of processing tacrolimus, it was an important impact on society. The interview by LPTM/FEQ/UNICAMP research group, published in the “Jornal da Unicamp” on 03 March 2020 had national repercussion. This newspaper article was divulgated in several sources, including TV Record's report, news on the websites of the Brazilian Chemical Society, Brazilian Society of Immunology, Brazilian Association of Intellectual Property, Transplant Center - RN, Government of the State of São Paulo, SP SAÚDE, SBT Interior, INVEST SP, News in FOCO MS, Innovare, among others (Figure 4.32). This repercussion demonstrates that the population needs hope, and that the academic community provides it with scientific, technical, and social commitment by spread of communication of its scientific and technological production. The access to information, principally for simple people, can be identify as fundamental Human Right and this is recognized by international community, such as the United Nations (UN) and the Organization of American States (OAS). According to article 19 of the UDHR, every human being has the right to freedom, without interference, to have opinions and to search, receive and

transmit information and ideas by any means and independent of borders (UN, 2016). In this case, the academy opens and amplifies the dialogue with society and brings hope to the less favored and invisible people.

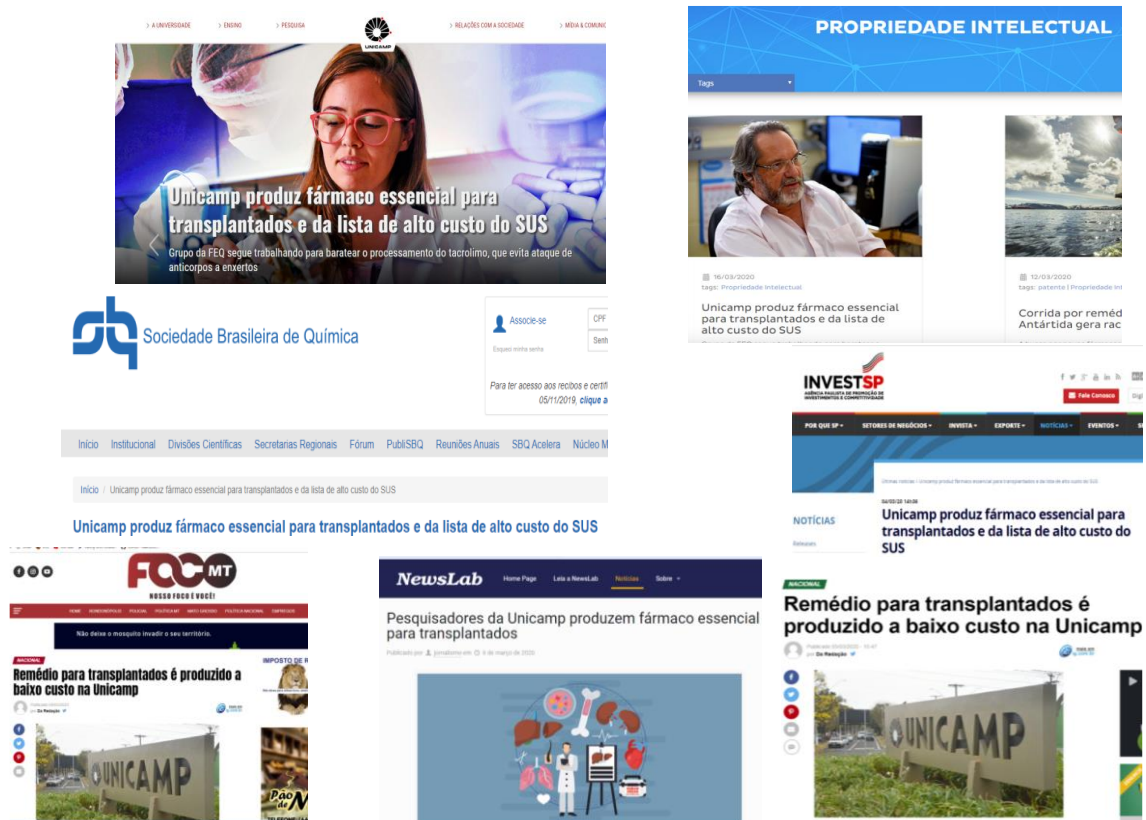


Figure 4.32 – Repercussion of tacrolimus production at LPTM/DEPro/FEQ/UNICAMP (Author, 2021)

Another social indicator in consequence from media divulgation was repercussion in social media, the feeling of hope was common, and the repercussions were even greater (Figure 4.33). Not only patients, but also the general population leave their opinion, showing the importance of the drug. A transplanted patient with recent A.D.S wrote in the report published on TVB Record “*My God, who would say that after months without delivery we would be having a new medication problem and no expected return*”. Another follower of this same page, G.C, also left her feeling of hope “*Thanks God, may everything be alright for improving distribution*”. On the page of University of Campinas on Facebook, followers highlighted the importance of research, L.M. wrote, “*Congratulations to the Unicamp team, the family of transplant recipients are so grateful*”, and L.E. J said, “*My son uses this medicine. I know the importance of this study.*”

Once the health is intrinsically associate with Human Rights, the article 25 (§ 1) of the Universal Declaration of Human Rights (UDHR) lays down the basis for international

legal framework ensuring the right to health. The article 12 of the International Covenant on Economic, Social and Cultural Rights requires states parties to adopt measures in at least four separate areas, one of which is disease prevention, treatment, and control, including access to basic medicines and medical services. The UDHR calls on states to ensure that people living in poverty have access to essential health services and medicines (UN, 2016). It is notable that the population living in poverty does not have the minimum conditions of healthy life, besides does not access to full information about public policies. According to Marks (2014), it is necessary to involve scientists and engineers in partnership with Human Rights specialists to plan public policies that improve quality health, including access to medicines.

The social impact of the study such as that one developed in the present work, increases the scientific and technical challenge for researchers. This present Dissertation shows the microfiltration of micelles from fermented broth. In this case, it appears a new hope associated with the scale-up of tacrolimus production. It is manifested in the opinion of a person, that said: “I hope that partnerships will appear to produce on a large scale” (Figure 4.33). Thus, customers in the biopharmaceutical industry usually require upscaling trials with a minimum amount of the formulation, as the respective formulations are quite expensive. Therefore, small-scale trials must be reliable, because they are used to evaluate the impact on product quality and the basics for the large-scale filtration process. In literature, scale-up experiments are performed by determination of the filter capacity (HAINDL *et al.*, 2020). Then, this Dissertation opens the opportunity to explore scale-up using the microfiltration results to remove the micelles from fermentation broth. Then, to increase to production of tacrolimus and to offer this product with no costs for poverty people, by SUS, as presented in the article 25 (§ 1) of the UDHR.



Figure 4.33 – The social impact of hope from technological study (Author, 2021)

The engineering scale-up approach gives a new hope: the possibility of transference of this technology to industry, and, here, another hope emerges: to offer the medicine for people, with low cost for government and ease access for patients. All this hope is summarized by symbol of LPTM's research line, as presented as green ribbon in Figure 4.33.

In the Brazil, green is the color of hope, and the ribbon represents the donation organ campaign. When associated with laboratory name (LPTM) and “Esperança” (hope), this symbol demonstrates the social commitment of the researchers with people that have ordinary hope in their lives since to drink a little more water or a glass of wine (due to limitation of the liquid injection during dialysis treatment) to dream with the end of their uncertainties. Hope wins uncertainty. This symbol summarizes the empathy of science and technology with social commitment.

The approach presented in this section was submitted in the I Brazilian Interdisciplinary Congress of Science and Technology (BERTAN and CREMASCO, 2020b), obtained the first place in the Science and Technology Extension (Figure 4.34), showing the importance to contextualize the technological studies with social and urgent needs.



Figure 4.34 – Best work at I Congresso Brasileiro Interdisciplinar de Ciência e Tecnologia (31/08/2020 – 04/09/2020)

CHAPTER 5

5. CONCLUSION AND SUGGESTIONS

A pressurized column was developed and applied in this Dissertation for microfiltration of broth fermented from *Streptomyces tsukubaensis*, presenting good performance. With 30 mL feed volume, it was notice that a single passage was not enough to achieve the Dissertation goal which was 95 % micelle rejection at least. It was necessary to recirculate the permeate. The objective was achieved with seven steps, but the maximum micelle rejection, 97 %, was achieved with ten steps, using 1 bar pressure operation and 3.00 μm pore membrane, as shown in Figure 5.1.

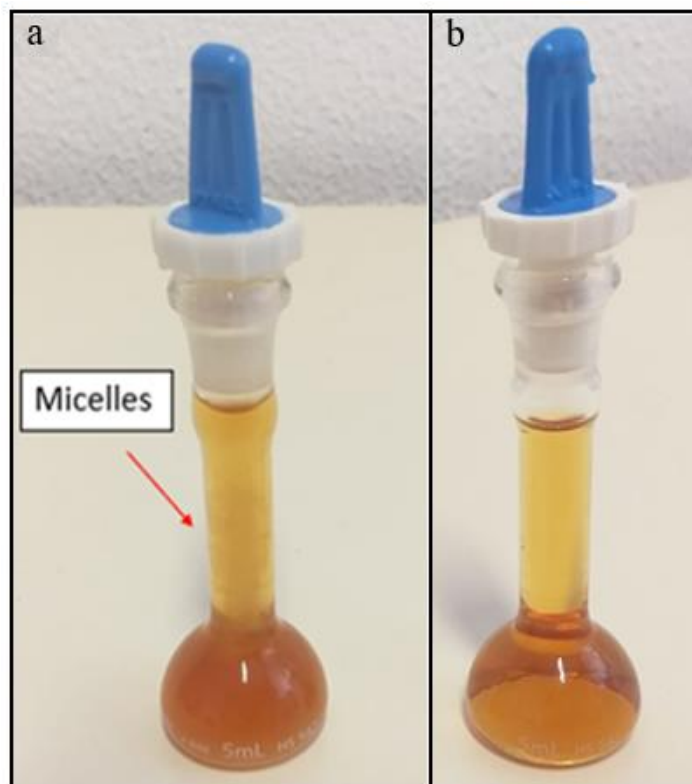


Figure 5.1 – (a) raw broth with acetone; (b) permeated from step 10 of the microfiltration conducted on the column pressurized at 1 bar with 3.00 μm membrane (Author, 2021)

The micelle rejection results were independent of the pore size, that is, values close to 3.00 μm and 0.22 μm were found for the pressures of 1 and 2 bar. In general, the volumetric flow decreases with increasing of steps number and then reaches a constant value.

This behavior is observed with total resistance, that keeps constant after certain step, but, before it, the total resistance increases with steps number. The 3.00 μm pore membrane has the advantage of performing microfiltration in less time than the 0.22 μm pore membrane. And a screen with greater mechanical resistance and less fouling along the steps. It is economical since it has a purchase value of U\$ 87 for 3.00 μm and U\$ 148 for 0.22 μm (100 unities, Merck Millipore MF-Millipore™), pointing another important factor favorable to use 3.00 μm pore membrane.

A study of fermentation was carried out using coconut oil and glucose as carbon sources, to identify and quantify tacrolimus and to quantify biomass, sugars, and proteins. The use of coconut oil as carbon source in fermentation via *Streptomyces tsukubaensis* increased the production of tacrolimus (31.35 mg/L in 96 hours) compared to the use of glucose (22.88 mg/L in 120 hours). In addition, the specific tacrolimus production using coconut oil was superior to the fermentation using glucose, being equal respectively to 1.88 mg/g and 1.69 mg/g. Thus, coconut oil is an option to replace the traditional carbon source: glucose. This fact can be explained, because glucose is a fast source of carbon, that is, the bacteria use this compound for its growth during exponential phase. However, in high concentrations, it acts as inhibitor of secondary metabolites such as tacrolimus. On the other hand, coconut oil has saturated and unsaturated fatty acids in its composition. It is reported in the Literature (MISHRA and VERMA, 2012; ÓRDÓNES-ROBLES *et al.*, 2018; POSHEKHONTSEVA *et al.*, 2019) that vegetable oils that own unsaturated fatty acids increase the production of tacrolimus. Another factor that contributes to this are the unsaturation in the structure molecule of the medicine.

As expected throughout the batch fermentation process, sugars were consumed, proteins were produced. In the present study, the rate of protein production was higher than the rate of consumption. Part of bacteria secreted proteins in the fermented broth interfere in the purification process, as well as bacterial cells and polysaccharide (QI *et al.*, 2019), included microfiltration step. These results are interesting, especially for countries with tropical and subtropical climate, where coconut oil is widely produced.

For the separation of the micelles from the fermentation broth aiming at the subsequent purification of the desired component, an alternative technique was developed that associates the particle counting by the Neubauer chamber with the spectroscopy technique, providing a substantial reduction in the analysis time to obtain the micelle concentration, mainly for samples considerably more diluted than the original sample. There are systems for this purpose, however of high cost, causing the search for cheaper alternatives, made by counting

particles by the Neubauer chamber. While HIAC 9703⁺ particle counter has purchase price around US\$ 40,000, while the mirrored Fuchs Rosenthal chamber cost was close US\$ 80.

The broth fermented from *Streptomyces tsukubaensis* with equal acetone volume was analyzed considering its rheological behavior. The liquid solution presented high complexity, since it contains, in addition to the original composition of the fermentative medium and the drug, bacterial biomass as well as organic materials made of proteins and reducing sugars. Although such medium will be diluted in 50 % of its total volume by Newtonian solvent (acetone), its rheological behavior undergoes continuous change with the increase in temperature, as can be seen with the decrease in the value of the fluid behavior index, m , configuring the pseudoplastic nature of the solution. In the other hand, for operation temperature up to 30 °C it was possible to assume Newtonian behavior, whose hypothesis was considered in this Dissertation.

From the results of this Dissertation and in view of the possibility of its continuity, it is can be offered the following suggestions:

a) To increase the broth volume to be processed to, for example, 90 mL, and from this, to study the influence of steps number in microfiltration performance.

b) To improve the filtration system with the inclusion of a pump for the permeate recirculation.

c) To perform the rheological analysis of the permeate after the passages through the filter.

d) To do the physical characterization of the retentate (dried biomass) to obtain its granulometric distribution and porosity.

e) To do a prior analysis of the technical feasibility of retentate liquid extraction for possible recovery of tacrolimus.

f) Characterize the permeate to identify ascomycin, proteins and lipids.

g) Use a fiber optic probe for continuous measurement over time of the concentration of micelles in the permeate.

h) Once tacrolimus is recommended for the treatment of rheumatoid arthritis, lichen planus, bronchial asthma, vitiligo, psoriasis, atopic dermatitis, uveitis, nephropathy, to do bibliographic study of the people who can benefit from obtaining this important drug.

The last suggestion is closely associated with the social commitment in which this Dissertation is inserted. The year 2020 enters to history of humanity, exposing its fragility due to a virus, which affects from prime ministers to people that remain invisible to public policies, among these, those ones that maintain their lives with use of immunosuppressive, such as

tacrolimus. Humanity's hope lies in science quick response to beat the coronavirus, but the hope of those that need tacrolimus remain, because they depend on medicine at their disposal. Technology professionals have the differentiating role of proposing, developing chemical design to production of tacrolimus. Such professionals can be adding human value to their *modus operandi*. In other words, it is possible to do science and develop innovative technology with strong social commitment based on the hope. It is important to mention that hope is associated to believe in the realization of what one desires. It must always be greater than uncertainty. And the role of researchers is to minimize this uncertainty by applying their scientific and technical knowledge, in view of their social commitment and, mainly, exercising empathy during their studies, understanding the situation of patients waiting for transplant and those that need tacrolimus for their survival. Hope harbors the heart of every person who depends on medication, that is, is the meaning of life for them, as well as for researchers that found more meaning for their work. However, the patients cannot live only with hope, but with science, technology and social commitment, the hope can become itself in reality, and showing that life is a gift for all. This philosophy can be summarized by symbol of this Dissertation and the LPTM research line, as presented in Figure 5.3.



Hope wins uncertainty

Figure 5.2 – LPTM laboratory symbol (Author, 2021)

6. REFERENCES

- ABSHER, M. Evaluation of culture dynamics. Massachusetts: Academic Press, 1973, 896p.
- ACHAL, V., MUKHERJEE, A., REDDY, M. S. Biocalcification by *Sporosarcina pasteurii* using corn steep liquor as nutrient source. *Industrial Biotechnology*, v. 6, n. 3, p. 170-174, June 2010.
- AHARONOWITZ, Y. Nitrogen metabolite regulation of antibiotic biosynthesis. *Annual Review of Microbiology*, v. 34, p. 209-233, 1980.
- ANTUNES, V.C . Use of microfiltration to improve the quality and extend the shelf life of pasteurized milk. *Brazilian Journal of Food Tecnology*, v. 17, n. 1, p. 75 -86, Jan/Mar 2014.
- AQUINO, A. D. As diferenças entre nanofiltração, ultrafiltração, microfiltração e osmose reversa. *Revista e Portal Meio Filtrante*, November/December 2011. Available in: <<https://www.meiofiltrante.com.br/Artigo/649/asdiferencasentrenanofiltracao-ultrafiltracao-microfiltracao-e-osmose-reversa>>. Accessed on: 20 dez 2020.
- BELUCI, N.; HOMEM, N.; AMORIM, M. T et al. Modificação de membrana de microfiltração comercial pelo método de filtração utilizando óxido de grafeno. In: PROCEEDINGS OF THE 14th WATER CONGRESS, 2018, Évora, Anais eletrônicos... Available in: <https://www.researchgate.net/publication/330669218_modificacao_de_membrana_de_micro_filtracao_comercial_pelo_metodo_de_filtração_sob_pressao_utilizando_oxido_de_grafeno> Accessed on: 20 dez 2020.
- BERTAN. Emprego da microfiltração em coluna pressurizada de caldo oriundo da fermentação via *Streptomyces tsukubaensis* para a obtenção de tacrolimo. Campinas: School of Chemical Engineering, University of Campinas, 2019. 62 p. Qualification (Master).
- BERTAN, A. S., CREMASCO, M. A. Determination of concentration of the pseudomyces from fermentation broth via spectroscopy and Neubauer chamber. *European Journal of Biological Research*, v.10, n. 3, July-September 2020a.
- BERTAN, A.S, CREMASCO, M.A. The hope as social commitment in the processing of tacrolimus. In: ANAIS DO I CONGRESSO BRASILEIRO INTERDISCIPLINAR EM CIÊNCIA E TECNOLOGIA, 2020, Online. Anais eletrônicos... Available in: <<https://www.even3.com.br/anais/icobicet2020/257014-the-hope-as-social-commitment-in-the-processing-of-tacrolimus/>> Accessed on: 20 dez 2020b.
- BERTRAND, R. L. Lag phase – a dynamic, organized, adaptive, and evolvable period that prepares bacteria for cell division. *Journal of Bacteriology*, v. 201, n. 7, p. 1-21, April 2019.
- BOFO, D. C. Reologia de fluidos envolvidos no processo de obtenção de bioetanol. São José do Rio Preto: Institute of Biosciences, Letters and Exact Sciences, Universidade Estadual Paulista “Júlio de Mesquita Filho”, 2015, 168 p. Dissertation (Master).
- BUTLER, M., SPEARMAN, M. *Methods in biotechnology: animal cell biotechnology*. Edited by: Pörtner R, 2007. Cell counting and viability measurements, p. 205-222.

CENTRAL DE TRANSPLANTES DO RN. Unicamp produz fármaco essencial para transplantados e da lista de alto custo do SUS, March 2020. Available in: <<https://www.facebook.com/CentralDeTransplantesDoRn/>>. Accessed on: 20 dez 2020.

CHEN, D., ZHANG, Q.I., ZHANG, Q et al. Improvement of FK506 production in *Streptomyces tsukubaensis* by genetic enhancement of the supply of unusual polyketide extender units via utilization of two distinct site-specific recombination system. Applied and Environmental Microbiology, v. 78, n. 15, p. 5093 – 5103, August 2012.

CHOI, B-T., HAM, Y-B., YU S-S et al. United States, Method for refining of high purity of tacrolimus. US 8.362.238B2. January. 29, 2013.

CONITEC – COMISSÃO NACIONAL DE INCORPORAÇÃO DE TECNOLOGIA NO SUS. Everolimo, sirolimo e tacrolimo para imunossupressão em transplante cardíaco. Relatório de Recomendação, São Paulo, n. 175, September 2015a. Available in: <http://conitec.gov.br/images/Relatorios/2015/Imunossupressores_TransplanteCardiaco_final.pdf>. Accessed on: 20 December 2020.

CONITEC – COMISSÃO NACIONAL DE INCORPORAÇÃO DE TECNOLOGIA NO SUS. Uso de imunossupressores (everolimo, sirolimo e tacrolimo) em transplantes pulmonares. Relatório de Recomendação, São Paulo, n. 200, August 2015b. Available in: <http://conitec.gov.br/images/Consultas/Relatorios/2015/Relatorio_Imunossupressores_TransplantePulmonar_CP.pdf>. Accessed on: 20 December 2020.

CONITEC – COMISSÃO NACIONAL DE INCORPORAÇÃO DE TECNOLOGIA NO SUS. Imunossupressores pós-transplante de pâncreas. Relatório de Recomendação, São Paulo, October 2016a. Available in: <http://conitec.gov.br/images/Consultas/Relatorios/2016/Relatorio_Imunossupressao_TransplantePancreas_CP2016.pdf>. Accessed on: 20 December 2020.

CONITEC – COMISSÃO NACIONAL DE INCORPORAÇÃO DE TECNOLOGIA NO SUS. Protocolo clínico e diretrizes terapêuticas imunossupressão no transplante hepático em adultos. Relatório de Recomendação, São Paulo, n. 236, August 2016b. Available in: <http://conitec.gov.br/images/Consultas/Relatorios/2016/Relatorio_PCDT_ImunossupressaoTransplanteHepatico_CP_2016_v2.pdf>. Accessed on: 20 December 2020.

COSTA, D. C., CASTRO, R. S. D., CAMARGO, M. S. F. D et al. Rejeição de transplantes de córnea: tratamento tópico vs. pulsoterapia-resultados de 10 anos. Arquivos Brasileiros de Oftalmologia, v. 71, n.1, p. 57-61, 2008.

COULSON, J. M., RICHARDSON, J. F. Chemical Engineering. Vol.2. Oxford: Pergamon Press, 1993. 954 p.

CREMASCO M. A., WENDRINER, E. Avaliação de meios filtrantes a serem empregados na filtração lenticular de vinho tinto considerando-se o nível de turbidez do filtrado. In: BLUCHER CHEMICAL ENGINEERING PROCEEDINGS, XXXVII, 2015, São Carlos. v. 2, n. 1, p. 1–6. Available in: <<http://www.proceedings.blucher.com.br/article-details/avaliacao-de-meios-filtrantes-a-serem-empregados-na-filtracao-lenticular-de-vinho-tinto-considerando-se-o-nivel-de-turbidez-do-filtrado-20581>>. Accessed on: 20 Dec. 2020.

CREMASCO, M. A. Difusão mássica. São Paulo: Editora Blucher, 2019, 284 p.

CREMASCO, M. A. Operações unitárias em sistema particulados e fluidomecânicos. 3. Ed.. São Paulo: Blucher, 2018, 423 p.

CREMASCO, M. A., FERRARI, W. M. C. S. Processo de purificação de tacrolimo. Campinas, Brazil. BR10201801483, July. 20, 2018.

CREMASCO, M. A.; MELO, K. P. Rheological characterization of recovery yeast (*Saccharomyces cerevisiae*) cream from brewing process. Chemical Engineering Transactions, v. 21, p. 763 – 768, 2010.

CREMASCO, M.A., WENDRINER, E. Emprego da teoria simplificada da filtração na obtenção de parâmetros operacionais destinados à filtração lenticular. In: ANAIS DO CONGRESSO BRASILEIRO DE SISTEMAS PARTICULADOS, 2017, Maringá. Anais eletrônicos... Campinas, Galoá, 2017. Available in: <<https://proceedings.science/enemp/papers/emprego-da-teoria-simplificada-da-filtracao-na-obtencao-de-parametros-operacionais-destinados-a-filtracao-lenticular>> Accessed on: 20 dez 2020.

CRISTOFOLI, K. Clarificação de vinho branco por microfiltração utilizando diferentes membranas cerâmicas e compósitas. Caxias do Sul: Post-Graduation in Engineering and Materials Science, University of Caxias do Sul, 2016. 121 p. Thesis (Doctorate).

CUI, W et al. Therapy of tacrolimus combined with corticosteroids in idiopathic membranous nephropathy. Brazilian Journal of Medical and Biological Research, v.50, n. 4, p. 1-7, March 2017.

DÄHNHARDT, D., BASTIAN, M., DÄHNHARDT-PFEIFFER, S et al. Comparative the effects of proactive treatment with tacrolimus ointment and mometasone furoate on the epidermal barrier structure and ceramide levels of patients with atopic dermatitis. Journal of Dermatological Treatment, p. 1-30, 2019.

DEMAIN, A. L. Genetic regulation of fermentation organisms: fermentation, regulation, antibiotics. Stadler Genetics Symposia Series, v. 8, p. 41-55, 1976.

DHALIWAL, J. S., MASON, B. F., KAUFMAN, S. C. Long-term use of topical tacrolimus (FK506) in high-risk penetrating keratoplasty. Cornea, v.27, n. 4, p. 488-493, May 2008.

DORAN, P. M. Bioprocess engineering principles. San Diego: Academic Press, 1997, 439 p.

DUMONT, F., GARRITY, G. M.; FERNANDEZ, I. M et al, United States. Process for producing FK-506. US 5.116.756, May. 26, 1992.

DUONG, H. C., NGUYEN, N. C. Membrane processes and their potential applications for fresh water provision in Vietnam. Vietnam Journal of Chemistry, v. 55, n. 5, p. 533-544, January 2017.

ERDINEST, N.; BEN-ELI, H.; SOLOMON, A. Topical tacrolimus for allergic eye diseases. Current Opinion in Allergy and Clinical Immunology, v. 19, n.5, p.535-543, 2019.

FAIRUS, S., MING, C. H., SUNDRAM, K. Antioxidant status following postprandial challenge of two different doses of tocopherols and tocotrienols. *Journal of Integrative Medicine*, v. 18, n.1, p. 68-79, January 2019.

FERRARI, W. M. C. D. S. Recuperação e purificação de tacrolimo proveniente de *Streptomyces tsucubaensis*. Campinas: School of Chemical Engineering, University of Campinas, 2018. 134 p. Thesis (Doctorate).

FREIRE, M. Mortes de pacientes na fila do transplante saltam 44% na pandemia. Folha de São Paulo. Available in: <<https://www1.folha.uol.com.br/cotidiano/2020/09/mortes-de-pacientes-na-fila-do-transplante-saltam-44-na-pandemia.shtml>>. Accessed on: 20 dez 2020.

GABAS, A.L., MENEZES, R.S., TELIS-ROMERO, J. Reologia na indústria de biocombustíveis. Lavras: INDI, 2012, 156 p.

GAJZLERSKA, W., KURKOWIAK, J., TURLO, J. Use of three-carbon chain compounds as biosynthesis precursors to enhance tacrolimus production in *Streptomyces tsukubaensis*, *New Biotechnology*, v. 32, n. 1, p. 32. 39, January 2015.

GAO, W., JIANG, Z., DU, X et al. Impact of surfactants on nanoemulsions based on fractionated coconut oil: emulsification stability and *in vitro* digestion. *Journal of Oleo Science*, v. 69, n.3, p. 227-239, February 2020.

GÖRÖG, S. Ultraviolet-visible spectrophotometry in pharmaceutical analysis. United States: CRC Press, 2017, 405 p.

GOVERNO DO ESTADO DE SÃO PAULO. Unicamp produz remédio essencial para transplantados e da lista de alto custo do SUS, March 2020. Available at: <<https://www.saopaulo.sp.gov.br/ultimas-noticias/unicamp-produz-remedio-essencial-para-transplantados-e-da-lista-de-alto-custo-do-sus/>>. Accessed on: 20 dez 2020.

HAASE, R., RICHTER, J. Phänomenologische Koeffizienten für Elektrizitätsleitung und Diffusion in konzentrierten Elektrolytlösungen. *Zeitschrift für Naturforschung A*, v.22, n.11 n.22, p. 1761- 1770, June 1967.

HABERT, A.C., BORGES, C. P., NOBREGA, R. Processos de separação de membranas. Rio de Janeiro: E-papers, 2006, 180 p.

HAINDL, S., STARK, J., DIPPEL, J et al. Scale-up of Microfiltration Processes. *Chemie Ingenieur Technik*, v. 92, n.6, p.746 – 758, 2020.

HANAFY, N. A. N., EL-KEMARY, M., LEPORATTI et al. Micelles structure development as a strategy to improve smart cancer therapy. *Cancers*, v. 10, n.7, p. 2-14, July 2018.

HOGAN, A. C., MCAVOY, C. E., DICK, A. D et al. Long-term efficacy and tolerance of tacrolimus for the treatment of uveitis. *Ophthalmology*, v. 114, n.5. p. 1000-1006, 2007.

HU, K., DICKSON, J.M. Membrane processing for dairy ingredient separation. Edited by Kang Hu, 2015. Cap. I: Microfiltration for casein and serum protein separation, p. 1-34.

HUMAN RIGHTS HANDBOOK FOR PARLIAMENTARIANS. 2016. Available at: <<https://www.ohchr.org/Documents/Publications/HandbookParliamentarians.pdf>>. Accessed on: 07 fev 2021.

HUANG, D.; XIA, M.; LI, S et al. Enhancement of FK506 production by engineering secondary pathways of *Streptomyces tsukubaensis* and exogenous feeding strategies. *Journal of Industrial Microbiology & Biotechnology*, v. 40, n. 9, p. 1023-1037, June 2013.

HWANG, K. S., KIM, H. U., CHARUSANTI, P., et al. Systems biology and biotechnology of *Streptomyces* species for the production of secondary metabolites. *Biotechnology advances*, v. 32, n.2, p. 255-268, March-April 2014.

INNOVAGRO. Unicamp, Brasil produce medicamentos esenciales para pacientes de trasplantes y la lista de altos costos del SUS, March 2020. Available at: <https://www.redinnovagro.in/noticia.php?idenNoticia=4611>>. Accessed on: 20 dez 2020.

INVESTSP. AGÊNCIA PAULISTA DE PROMOÇÃO DE INVESTIMENTOS E COMPETITIVIDADE, March 2020. Available at: <<https://www.investe.sp.gov.br/noticia/unicamp-produz-farmaco-essencial-para-transplantados-e-da-lista-de-alto-custo-do-sus/>>. Accessed on: 20 dez 2020.

JAUREGI, P., COUTTE, F., CATIAU, L et al. Micelle size characterization of lipopeptides produced by *B. subtilis* and their recovery by the two-step ultrafiltration process. *Separation and purification Technology*, v. 104, p. 175-182, November 2013.

JONES, F. E., HARRIS, G. L. Its-90 density of water formulation for volumetric standards calibration. *Journal of Research of the National Institute of Standards and Technology*, v. 97, n. 3, p. 335-340, May-June 1992.

JORNAL DA UNICAMP. Unicamp produz fármaco essencial para transplantados e da lista de alto custo do SUS, March 2020. Available in : <<https://www.unicamp.br/unicamp/ju/noticias/2020/03/03/unicamp-produz-farmaco-essencial-para-transplantados-e-da-lista-de-alto>> Accessed on: 20 dez 2020.

JORNAL HOJE EM DIA. Falta de medicamentos prejudica transplantados em Minas, espera dua até seis meses, June 2019. Available in : <https://www.hojeemdia.com.br/horizontes/cidades/falta-de-medicamentos-prejudicatransplantados-em-minas-espera-dura-at%C3%A9-seis-meses-1.721728>>. Accessed on: 20 dez 2020.

JUANG, R-S., CHEN, H-L., CHEN, Y-S. Membrane fouling and resistance analysis in dead-end ultrafiltration of *Bacillus subtilis* fermentation broths. *Separation and Purification Technology*, v.63, n. 3, p. 531-538, November 2008.

JUNG, S., LEE, K., PARK, Y-J et al. Process development for purifying tacrolimus from *Streptomyces* sp. Using Adsorption. *Biotechnology and Bioprocess Engineering*, v. 16, p. 1208 - 1213, July 2011.

GUERRA JR, A. A. G., SILVA, G. D., ANDRADE, E. I. G et al. Cyclosporine versus tacrolimus: cost-effectiveness analysis for renal transplantation in Brazil. *Cadernos de Saúde Pública*, v. 26, p. 163-174, February 2015.

KERI, V., CSORVASI, A., MELCZER, I et al. Method of purifying tacrolimus. United States, US 2006/0142565 A1. June. 29, 2006.

KESTIN, J., SOKOLOV, M., WAKEHAM, W. A. Viscosity of liquid water in the range - 8 °C to 150 °C . *The Journal of Physical Chemistry*, v. 7, n. 3, p.941-948, 1978.

KINO T., HATANAKA H., HASHIMOTO, M. et al. FK-506, a novel immunosuppressant isolated from a *Streptomyces*. I. Fermentation, isolation, and physicochemical and biological characteristics. *Journal of Antibiotics*. v. 40, n. 9, p. 1249 - 1255, 1987.

KOVARIK, B. K., HOYER, P. F., ETTENGER, R et al. Cyclosporine absorption profiles in pediatric kidney and liver transplant patients. *Pediatric Nephrology*, v. 18, n. 12, p. 1275 - 1279, 2003.

KRUGER, N. J. *The Protein Protocols Handbook*. 2 ed. Edited by: John M.Walker, 2002. Chapter IV: The Bradford Method for Protein quantification, p. 15-22.

KULKARNI, M., PRABHU, S. K., SHIVAKUMAR, M. C et al. Canada, Process for the production of macrolides using a novel strains, *Streptomyces* sp. BICC 7522, US 7.704.725B2. October, 20. 2005.

LI, Y., SHAHBAZI, A., KADZERE, C. T. Separation of cells and proteins from fermentation broth using ultrafiltration. *Journal of Food Engineering*, v. 75, n. 4, p. 574-580, August 2006.

LI, C., CHEN, X., WEN, L et al. An enhancement strategy for the biodegradation of high-concentration aliphatic nitriles: Utilizing the glucose-mediated carbon catabolite repression mechanism. *Environmental Pollution*, v. 55, n. 5, p. 534-543, October 2020.

LI, Y., SHAOXIONG, L., WANG, J., MA, D., WEN, J. Enhancing the production of tacrolimus by engineering target genes identified in important primary and secondary metabolic pathways and feeding exogenous precursors. *Bioprocess and Biosystems Engineering*, v.42, p. 1081-1098, March 2019.

LIMA, R. D. S., BLOCK, J. M. Coconut oil: what do we really know about it so far? *Food Quality and Safety*, v. 3, n.2, p. 61-72, February 2019.

MALINOWSKI, J. J., LAFFORGUE, C., GOMA, G. Rheological behaviour of high density continuous cultures of *Saccharomyces cerevisiae*. *Journal of Fermentation Technology*, v. 65, n. 3, p. 319-323, 1987.

MAO N. *Advances in Technical Nonwovens*. Edited by: George Kellie, 2016. Chapter X: Nonwoven, p. 273-310.

MARKS, S. P. *Human Rights and the Challenges of Science and Technology*. *Science and Engineering Ethics*. Available in: <<https://dash.harvard.edu/handle/1/12561403>>. Accessed on February 8, 2014.

MARTELLI, A. Redução das concentrações de cloreto de sódio na alimentação visando a homeostase da pressão arterial. *Revista Eletrônica em Gestão, Educação e Tecnologia Digital*, v. 18, p. 428-436, Abril 2014.

MARTINEZ-CASTRO, M., SALEHI-NAJAFABADI, Z., ROMERO, F et al. Taxonomy and chemically semi-defined media for the analysis of the tacrolimus producer '*Streptomyces tsukubaensis*'. *Applied Microbiology and Biotechnology*, v. 95, n.2, p. 2139-2152, September 2012.

MASSARANI, G. *Fluidodinâmica em sistemas particulados*. Rio de Janeiro: Editora UFRJ, 1997, 147 p.

MELO, K. Pandemia de covid-19 diminui quantidade de transplantes no Brasil. Agência Brasil. Available in: <<https://agenciabrasil.ebc.com.br/saude/noticia/2020-05/pandemia-de-covid-19-diminui-quantidade-de-transplantes-no-brasil>>. Accessed on December 21, 2020.

MISHRA, A., VERMA, S. Optimization of process parameters for tacrolimus (FK506) production by new isolate of *Streptomyces* sp. using response surface methodology (RSM). *Journal of Biochemical Technology*, v. 3, n. 4, p. 419-425, January 2012.

MO, S., YANG, H. S. Development of FK506-hyperproducing strain and optimization of culture conditions in solid-state fermentation for the hyper-production of FK506. *Journal of Applied Biological Chemistry*, v. 59, n.4, p 289–298, December 2016.

MOREIRA, J. V. Produção de tacrolimo via fermentação de *Streptomyces tsukubaensis*. Campinas: School of Chemical Engineering, University of Campinas, 2018, 117 p. Thesis (Doctorate).

MOREIRA, J. V., SILVA., S. C.M., CREMASCO, M. A. Evaluation of carbon:nitrogen ratio in semi-defined culture medium to tacrolimus biosynthesis by *Streptomyces tsukubaensis* and the effect on bacterial growth. *Biotechnology Reports*, v. 26, n. e00440, p. 1-6, February 2020.

MOREIRA, M. Estudo da ação do imunossupressor tacrolimus na pancreatite aguda experimental induzida pela arginina. Curitiba: Postgraduate Program in Surgical Clinic of the Health Sciences Sector, Federal University of Paraná, 2008, 36 p. Dissertation (Master).

MORETTI, L. B. Transplantes no HC aumentam quase 40 % no último ano. *Jornal da Unicamp*. Available in:<<https://www.unicamp.br/unicamp/noticias/2018/06/20/transplantes-no-hc-aumentam-quase-40-no-ultimo-ano>>. Accessed on December 21, 2020.

MURAMATSU, H., NAGAI, K. *Streptomyces tsukubaensis* sp. Nov., a producer of the immunosuppressant tacrolimus. *The Journal of antibiotics*, v. 66, p. 251-254, January 2013.

NELSON, N. A. photometric adaptation of the Somogyi method for the determination of glucose. *Journal of Biological Chemistry*, v.153, n. 2, p. 375-380, February 1944.

NERY, T. B. R., BRANDÃO, L. V., ESPIRIDIANO, M. C. A et al. Biossíntese de goma xantana a partir da fermentação de soro de leite: rendimento e viscosidade. *Química Nova*, v.. 31, n. 8, p. 1937-1941, November 2008.

NISHIARA, T., HONDA, K., MUKAI, K et al. Japan, Method for separating analogous organic compounds. US 6.492.513B1. December. 10, 2002.

NOBLE, J. E. Quantification of protein concentration using UV absorbance and Coomassie dyes. *Methods in Enzymology*, v. 536, p. 17-26, 2014.

NOTÍCIA EM FOCO MT. Remédio para transplantados é produzido a baixo custo na Unicamp, March 2020. Available at:< <https://noticiaemfocomt.com.br/remedio-para-transplantados-e-produzido-a-baixo-custo-na-unicamp/>>. Accessed on: 20 dez 2020.

OKUHARA, M., TANAKA, H., GOTO, T et al, United States, Process for production of tricyclo compounds with *Streptomyces*. US 5.830.71. Nov. 03, 1998.

OKUHARA, M., TANAKA, H., GOTO, T. Strain of *Streptomyces* for the production of tricyclo compounds. Japan. US005624842A, April. 29, 1997.

OKUHARA, M., TANAKA, H.; GOTO T.; et al. Japan, Tricyclo compounds, a process for their production and a pharmaceutical composition containing the same. US 4.956.352. January. 11, 1990.

OLIVEIRA, P. C., PAGLIONE H. B., SILVA V et al. Mensuração da não-adesão aos medicamentos imunossupressores em receptores de transplante de fígado. *Acta Paulista de Enfermagem*, v. 32, n.3, p. 319-326, April 2019.

ÓRDÓÑEZ-ROBLES, M., SANTOS-BENEIT, F., MARTÍN, J. F. Unraveling nutritional regulation of tacrolimus biosynthesis in *Streptomyces tsukubaensis* through omic. *Approaches. Antibiotics*, v. 7, n. 2, p. 1-19, May 2018.

PATEL, V. *Molecular nutrition vitamins*. Massachusetts: Academic Press, 2020, 792 p.

PATIL, N. S., MENDHE, R., KHEDKAR, A. P et al. Process for the purification of macrolides. United States, US 7.473.366. January. 6, 2009.

POSHEKHONTSEVA, V. Y., FOKINA, V. V., SUKHODOLSKAYA, G. V., et al. Effect of starch composition on the biosynthesis of immunosuppressant tacrolimus (fk-506) by *Streptomyces tsukubaensis* vkm ac-2618d strain. *Applied Biochemistry and Microbiology*, v. 55, n. 5, p. 534-543, September 2019.

QI, L., HU, Y., CHAI, Q et al. Enhanced filtration performance and antibiofouling properties of antibacterial polyethersulfone membrane for fermentation broth concentration. *Journal of Industrial and Engineering Chemistry*, v. 72, n.25. p. 346-353. April 2019.

RUIZ, B., CHÁVEZ, A., FORERO, A et al. Production of microbial secondary metabolites: regulation by the carbon source. *Critical Reviews in Microbiology*, v. 36, n. 2, p. 146-167, March 2010.

RUSHTON, A., WARD, A. S., HOLDICH, R. G. *Solid-liquid filtration and separation technology*. New York: VCH Publishers, 1996, 551 p.

SÁNCHEZ, A. R., SHERIDAN, P. J., ROGERS, R. S. Successful treatment of oral lichen planus-like chronic graft-versus-host disease with topical tacrolimus: a case report. *Journal of Periodontology*, v. 75, n.4, p. 613-619, 2004.

SÁNCHEZ, S.; CHÁVEZ, A.; FORERO, A et al. Carbon source regulation of antibiotic production. *The Journal of Antibiotics*, v. 63, p. 442-459, July 2010.

SBT INTERIOR. Unicamp produz remédio essencial para transplantados, March 2020. Available in: <https://sbtinterior.com/noticia/unicampproduzremedioessencialparatransplantados,2571633455675.html>>. Accessed on: 20 Dec. 2020.

SHERWOOD, T. K. Projeto de processos da indústria química. São Paulo: Editora Edgard Blucher Ltda, 1972, 190 p.

SILVA, S. C. M. S. Uso de óleos vegetais como fonte de carbono na fermentação da *Streptomyces tsukubaensis* visando o aumento da produção de tacrolimo. Campinas: School of Chemical Engineering, University of Campinas, 2019. 63 p. Dissertation (Master).

SILVA, S. C. M., FERRARI, W. M., MOREIRA, J. V et al. *Streptomyces tsukubaensis* fermentation using Brazil nut oil to enhance tacrolimus production. *Applied Biotechnology Reports*, v. 6, n.3, p. 109 – 112, September 2019.

SILVA, V. R. D., SCHEER, A. D. P. Estudo do processamento por microfiltração de soluções aquosas de pectina em membranas cerâmicas. *Acta Scientiarum. Technology*, v. 33, n.2, p. 215-220, February 2011.

SILVESTRE, M. C. Sistemas de filtragem aplicados em processos fabris automotivos. Trabalho de Graduação. Guaratinguetá: School of Mechanical Engineering, Paulista State University, 2014, 110 p.

SINGH, B. P., KUMAR, P., HAQUE, S et al. Improving production of tacrolimus In *Streptomyces tacrolimicus* (ATCC 55098) through development of novel mutant by dual mutagenesis. *Brazilian Archives of Biology and Technology*, v. 60, n. e17160366, Jan/Dec 2017.

SOARES, J. Como Fazer hemodiálise pode afetar a felicidade de um paciente idoso, December 2019. Available in : < <https://jornal.usp.br/ciencias/ciencias-da-saude/como-fazer-hemodialise-pode-afetar-a-felicidade-de-um-paciente-idoso/>>. Accessed on: 30 Dec. 2020.

SOBRINHO, W. P. Transplantados são infectados por Covid – 19 no HC de SP, que interdita setor. UOL. Available in:<<https://noticias.uol.com.br/saude/ultimas-noticias/redacao/2020/05/11/hc-suspeita-que-profissionais-infectem-pacientes-eparatransplantes-em-sp.htm>>. Accessed on May 11, 2020.

SP SAÚDE. Unicamp produz remédio essencial para transplantados e da lista de alto custo do SUS, March 2020. Available in : <<http://portaldenoticias.saude.sp.gov.br/unicamp-produz-remedio-essencial-para-transplantados-e-da-lista-de-alto-custo-do-sus/>>. Accessed on: 20 Dec. 2020.

STEFFE, J. F. Rheological method in food process engineering. East Lansing: Freeman Press, 1996, 428 p.

TRIPATHI, A. R., SINGH, N. K., IUHTRA, U. Optimization of nutrient components for tacrolimus production by *Streptomyces tsukubaensis* using Plackett-Burman followed by response surface methodology, IOSR Journal of Pharmacy, v 4, n. 7, p. 66-75, July 2014.

TURŁO, J., GAJZLERSKA, W., KLIMASZEWSKA, M et al. Enhancement of tacrolimus productivity in *Streptomyces tsukubaensis* by the use of novel precursors for biosynthesis. Enzyme Microbial Technology, v. 51, n. 6-7, p. 388-395, December 2012.

UMEBARA, T. Microfiltração de caldo de cana: caracterização do caldo permeado e retentado. Curitiba: Food Technology, Federal University of Paraná, 2010. 100 p. Dissertation (Master).

VAID, S. Process for producing tacrolimus using vegetable oil as sole source of carbon. United States, US 2007/0142424 A1. June. 21, 2007.

VIEIRA, E. Tempo de criar. Brasília : Confederação Nacional da Indústria, 2006, 21 p.

WANG, J., LIU, H., HUANG, D et al. Comparative proteomic and metabolomic analysis of *Streptomyces tsukubaensis* reveals the metabolic mechanism of FK506 overproduction by feeding soybean oil. Applied Microbiology and Biotechnology, v. 101, n. 6, p. 2447-2465, March 2017.

WHITE, D., LAWSON, N., MASTERS, P et al. Clinical Chemistry. New York: Garland Science, 2016, 608 p.

WOLLMAN, E. W., FRISBIE, C. D., WRIGHTON, M. S. Scanning electron microscopy for imaging photopatterned self-assembled monolayers on gold. Langmuir, v.9, p.1517-1520, 1993.

ZHANG, M., GU, L., ZHENG, P et al. Improvement of cell counting method for Neubauer counting chamber. Journal of Clinical Laboratory Analysis, v. 34, n. e23024, p. 1-6, August 2019.

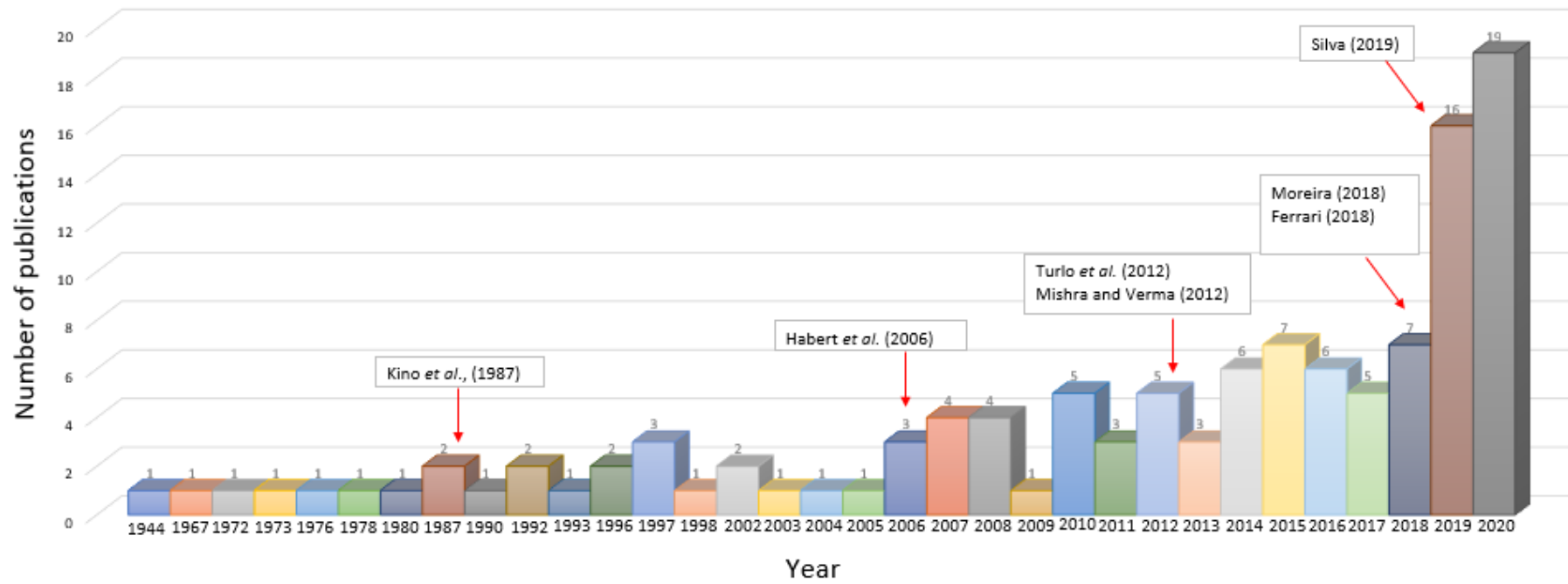


Figure 6.1 – Number of publications/years used in the Dissertation. The authors highlighted are central in this work (Author, 2021)

Table A.1 - Duplicate test 0.22 μm and pressure 1 bar (Author, 2021)

Steps	$R_T \times 10^{-7} \text{ (m}^2/\text{kg)}$	% Rejection
1	8.97	35.99
2	9.25	66.56
3	9.98	87.39
4	10.01	87.59
5	10.08	88.87
6	11.34	92.31
7	11.61	95.27
8	15.72	95.76
9	19.87	96.25
10	25.89	96.25

Table A.2 - Duplicate test 0.22 μm and pressure 2 bar (Author, 2021)

Steps	$R_T \times 10^{-7} \text{ (m}^2/\text{kg)}$	% Rejection
1	6.66	15.41
2	8.82	27.18
3	13.51	35.99
4	16.26	46.33
5	18.23	49.92
6	20.09	58.93
7	21.94	65.78
8	22.13	78.48
9	23.65	88.87
10	24.61	95.76

Table A.3 - Duplicate test 3.00 μm and pressure 1 bar (Author, 2021)

Steps	$R_T \times 10^{-7} \text{ (m}^2/\text{kg)}$	% Rejection
1	7.09	35.99
2	7.41	66.61
3	7.46	87.88
4	7.54	89.36
5	7.63	90.34
6	7.74	93.30
7	7.81	94.77
8	7.84	96.25
9	7.86	97.24
10	7.86	97.24

Table A.4 - Duplicate test 3.00 μm and pressure 2 bar (Author, 2021)

Steps	$R_T \times 10^{-7}$ (m²/kg)	% Rejection
1	2.66	14.77
2	2.98	27.03
3	3.46	36.14
4	3.57	46.33
5	3.68	49.58
6	3.92	59.52
7	4.54	66.07
8	4.82	78.53
9	5.19	90.84
10	5.28	95.76

UNIVERSITY OF CAMPINAS
SCHOOL OF CHEMICAL ENGINEERING
EQ 741 - TRANSPORT PHENOMENA III

PED. Alessandra Suzin Bertan
Prof. Marco Aurélio Cremasco
Subject: 4th Evaluation of EQ 741: List # 3.
Deadline: 10 October 2020 until 7 p.m (via Moodle).

Upon detecting a kidney problem, the patient has the hope of a quick cure, although he may discover that his life will be governed by medical treatment, such as hemodialysis. During hemodialysis, the patient has the hope of a kidney transplant, participating in an endless wait for a compatible organ. Finding such organ and performing the graft surgery, the patient has the hope that his organism will receive the new organ and starts to use immunosuppressant that, at the time of adapting the organism to the graft, it exposes to the diverse types of infection. The patient starts to have a double hope that the organism adapts to the immunosuppressant as well as to avoid detecting that he can lose this graft (BERTAN and CREMASCO, 2020b). According to Soares (2019), the hemodialysis filters the blood, that is, it does the part of the work that would be destined for the kidney. It starts with the blood pumped from the patient's arteriovenous fistula, it goes through a pump. The isotonic saline solution and heparin (to prevent blood clots) are added. The blood passes through a pressure monitor and enters the dialyzer, which removes waste products from the blood through its semipermeable membrane. The blood flows in a dialyzer compartment, while the dialysate (water filtered with the dialysis solution) flows in opposite direction. The semipermeable membrane allows blood cells, proteins, and other important substances to remain in that patient's blood. Finally, the blood passes through the last pressure monitor and air trap detector, returning to the organism by venous access (Figure B.1).

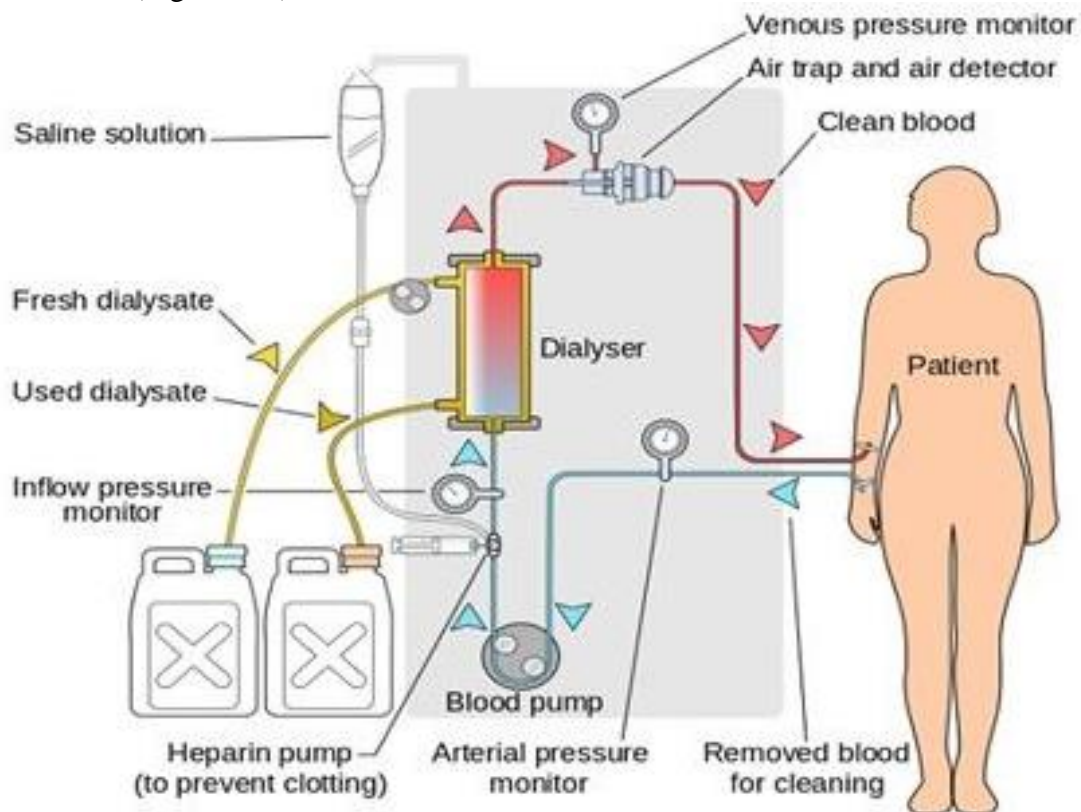


Figure B.1 – Hemodialysis procedure (adapted from Soares, 2019)

The isotonic saline solution is essential for the hemodialysis procedure, since the chlorine present in this salt is essential in maintaining body homeostasis, controlling the fluids that enter and leave the body tissues. In addition, sodium is responsible for regulating blood pressure and volume, assisting in the transmission of nerve impulses and muscle contraction, regulating the acid-base and hydro-electrolyte balance (MARTELLI, 2014). The isotonic solution occurs when the solute concentration and osmotic pressure are equal. Given the importance of the social conscience in the scope of Chemical Engineering, consider the follow application for hemodialysis: there is a solution that contains 0.9 g NaCl in 100 mL of distilled water necessary to be administered during the process of hemodialysis. Based on Table B.1, which contains the values of the experimental diffusion coefficient of NaCl in water at 25 °C, calculate the values of the thermodynamic diffusion coefficients for each molality and give a graph comparing with the experimental values. Identify, in your results, the value of the thermodynamic diffusion coefficient of NaCl in water used in hemodialysis.

Table B.1 - Diffusion coefficient of NaCl at 25 °C in aqueous solution for different molalities (HAASE and RICHTER, 1967)

m (mol of salt/kg of water)	0.1	0.2	0.3	0.4	0.5	0.6	0.7	0.8	0.9	1.0
$D_A \times 10^{-5}$ cm ² /s (experimental)	1.483	1.477	1.475	1.474	1.473	1.474	1.475	1.477	1.478	1.480

Data: $\rho_{H_2O} = 997$ kg/m³, Molar mass NaCl = 23 g/mol, $\lambda_1 = 50,10$ ohm/eq. e $\lambda_2 = 76,35$ ohm/eq at 25°C.

UNIVERSITY OF CAMPINAS
SCHOOL OF CHEMICAL ENGINEERING
EQ 741 - TRANSPORT PHENOMENA III

PED. Alessandra Suzin Bertan
Prof. Marco Aurélio Cremasco
Subject: 5th Evaluation of EQ 741: List # 2.
Deadline: 17 November 2020 until 7 p.m (via Moodle).

Bertan (2019) used the perpendicular microfiltration system (dead-end), illustrated in Figure B.2, intended for the separation of micelles from fermented broth of *Streptomyces tsukubaensis* aiming at the production of tacrolimus, an important immunosuppressant used in the maintenance of transplanted organs. Before, however, the author carried out compaction studies of the filter medium using water at 28 °C. Using perforated stainless-steel plate and steel wire screen as supports for a membrane made of mixed cellulose esters. Applying operation pressure at the filter inlet equal to 1.0 bar and the permeate pressure at 0.95 bar, Bertan (2019) obtained the permeate collected volumes over time as shown in Table B.2.

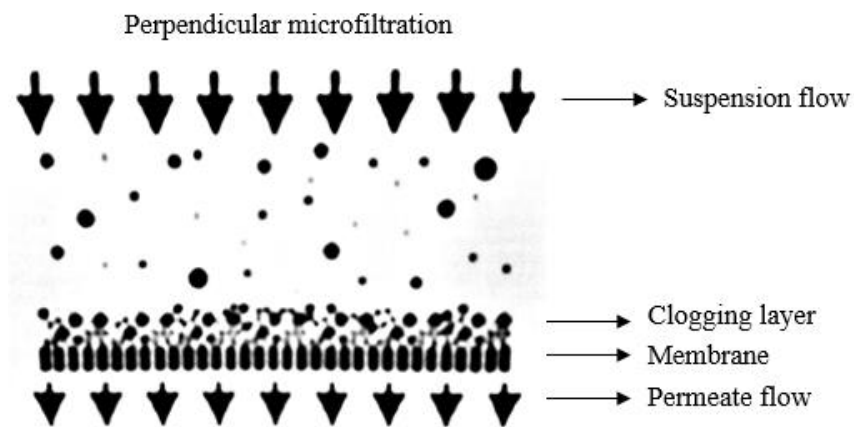


Figure B.2 - Perpendicular feeding

Table B.2 - Evaluation of permeate flow in different particulate media (BERTAN, 2019)

V (cm ³)	Perforated plate, time (s)	Wire screen and perforated plate, time (s)	Wire screen, perforated plate and membrane time (s)
0	0	0	0
10	1	1	12
20	2	2	23
30	3	4	30

Given the importance of the engineering that involves the microfiltration in question and knowing that the area used for filtration is equal to 17.30 cm², obtain:

- (a) the total resistance of the filtering set as well as that of each element that comprises it;
- (b) the permeate mass flow;
- (c) the value of the capillary diffusion coefficient of water in the membrane, that presents pore diameter equal $\sigma_p = 0.22 \mu\text{m}$ and porosity $\varepsilon_p = 0.75$.

The permeate mass flow is defined as

$$j_m = \frac{m}{(\text{Area})t} \quad (1)$$

or, in terms of volume,

$$j_m = \frac{\rho V}{(\text{Area})t} \quad (2)$$

where ρ the density of the permeate; Area, filtration area; t, time. The permeate mass flow can also be expressed in terms of Darcy's law pressure

$$j_m = \frac{\Delta p}{\eta R_T} \quad (3)$$

The term Δp in Equation 3, refers to the differential pressure; η , the dynamic viscosity of the processed solution; R_T , the overall resistance offered by membrane,

$$R_T = R_f + R_G + R_p + R_s \quad (4)$$

with R_f the intrinsic resistance of the membrane, R_G , refers to the resistance resulting from the fouling effects, which can be defined as the irreversible deposition of retained particles, colloids, emulsions, suspensions, macromolecules, salts etc. R_p , resistance due to polarization because of solute concentration; R_s , concerns resistance due to membrane support on the filter. Diffusivity capillary or viscous diffusivity is defined as

$$D_{V,ef} = \frac{k\bar{P}}{\eta\varepsilon_p} \quad (5)$$

P_{abs} , average from feed and permeate pressure; η , dynamic viscosity of the medium that permeates the matrix; ε_p , its porosity; k is the permeability comes from the Kozeny-Carman equation in the form

$$k = \frac{\sigma_p^2}{180} \left[\frac{\varepsilon_p^3}{(1 - \varepsilon_p)^2} \right] \quad (6)$$

The capillary (or viscous) diffusion coefficient, D_V , associating it to effective diffusivity, $D_{V,ef}$, according

$$D_V = D_{V,ef} \times \varepsilon_p \quad (7)$$

To obtain the dynamic water viscosity value, the following correlation can be used, valid for the range of 0 °C to 40 °C (KESTIN *et al.*, 1978)

$$\log\left(\frac{\eta}{\eta|_{T=20^{\circ}\text{C}}}\right) = \left(\frac{20 - T}{T + 96}\right) [1.2364 - 1.37 \times 10^{-3}(20 - T) + 5.7 \times 10^{-6}(20 - T)^2] \quad (8)$$

where T is used in °C; the result of η in $\mu\text{Pa}\cdot\text{s}$ and $\eta|_{T=20^{\circ}\text{C}} = 1,002 \mu\text{Pa}\cdot\text{s}$

The value of water density can be determined from the following correlation, valid for the range of 5 °C to 40 °C (JONES and HARRIS, 1992)

$$\rho = \sum_{i=0}^{i=4} a_i T^i \quad (9)$$

with $a_0=999.85308$; $a_1=6.32693 \times 10^{-2}$; $a_2=-8.523829 \times 10^{-3}$; $a_3 = 6.943248 \times 10^{-5}$; $a_4=-3.821216 \times 10^{-7}$; where is used T in °C, and the result of ρ in kg/m^3 .

Additional information:

1 bar = 1×10^5 Pa; $1 \mu\text{Pa}\cdot\text{s} = 1 \times 10^{-3}$ Pa.s; $1 \mu\text{m} = 1 \times 10^{-6}$ m; $1 \text{ m}^3 / \text{s} = 1 \times 10^6 \text{ cm}^3 / \text{s}$.

UNIVERSITY OF CAMPINAS
SCHOOL OF CHEMICAL ENGINEERING
EQ 741 - TRANSPORT PHENOMENA III

PED. Alessandra Suzin Bertan
Prof. Marco Aurélio Cremasco
Subject: 10th Evaluation of EQ 741: List # 1.
Deadline: 10 December 2020 until 7 p.m (via Moodle).

1. Tacrolimus is a medicine used in immunosuppressive therapeutic protocols, mainly in liver and kidney transplants, as also recommended for the treatment of diseases autoimmune diseases, such as rheumatoid arthritis, bronchial asthma, and various dermatological disorders, such as vitiligo and demartitis. In 2019, Brazilian press reported the lack of tacrolimus in several units of the Unified Health System (SUS) in our country, greatly compromising the life of people who depend on the drug. The intensification, therefore, of the production of medicines must be the focus of public policies and research centers, committed to the issue of technological production, which goes beyond the economic to also be directed to the social good. In this context, there is hope, which seeks shelter in the heart of those who depend on the medicine, to strengthen the meaning of life for both the patient and researchers, who end up identify a more sublime meaning for your work. However, patients cannot live just with hope. With science, technology, and social commitment, hope it can materialize and show that life is a gift for everyone (BERTAN and CREMASCO, 2020b). Guided by this philosophy, work carried out at the Laboratory of Process of Mass Transfer, Department of Process Engineering, School of Chemical Engineering at State University of Campinas (LPMP/DEPro/FEQ/Unicamp) directed to the tacrolimus production from fermentation of *Streptomyces tsukubaensis*. After obtaining the tacrolimus in the fermentation stage, the resulting broth passes through microfiltration steps to separate the micelles, followed by liquid-liquid extraction and ultrafiltration. The resulting solution is subjected to adsorption, configuring the pre-purification step. Consider the hypothetical situation of the adsorption of tacrolimus, diluted in organic solvent ($v = 0.28 \text{ cm}^2/\text{min}$) in fixed bed ($D = 1.0 \text{ cm}$; $L = 25 \text{ cm}$; $\epsilon = 0.45$), using appropriate adsorbent ($d_p = 20 \text{ }\mu\text{m}$; $\epsilon_p = 0.36$) as stationary phase. Knowing the initial concentration, c_0 , of tacrolimus in the mobile phase is $57,41 \text{ mg/L}$, it was found, after 16 min, that its concentration at the exit of the column, c_f , was 8.11 mg/L , using volumetric flow of the mobile phase, Q , equal to 5 mL/min . The values of the convective mass transfer coefficient of tacrolimus in the solvent, the free diffusion coefficient of tacrolimus in the solvent and its diffusivity in the adsorbent are equal, respectively, to 2.0 cm/min , $6.0 \times 10^{-4} \text{ cm}^2/\text{min}$, and $2.9 \times 10^{-4} \text{ cm}^2/\text{min}$, estimate the value of adsorption equilibrium constant (k_p) assuming linear isotherm. Consider that adsorption can be described by global linear model of mass transfer and *plug-flow* flow with axial dispersion.